Biochemical and Mechanistic Studies of the Interactions Between Vitamin K Antagonists and Vitamin K Epoxide Reductase

Clara K. Hsia

A dissertation
submitted in partial fulfillment of the
requirements for the degree of

Doctor of Philosophy

University of Washington
2012

Reading Committee:
Allan E. Rettie, Chair
Kent L. Kunze
William M. Atkins

Program Authorized to Offer Degree:
Medicinal Chemistry

University of Washington

Abstract

Biochemical and Mechanistic Studies of the Interactions Between Vitamin K Antagonists and Vitamin K Epoxide Reductase

Clara K. Hsia

Chair of the Supervisory Committee:
Professor Allan E. Rettie
Department of Medicinal Chemistry

The studies that are presented in this dissertation have; (i) established a mechanism by which warfarin dose response is modulated by *VKORC1* genotype under optimized conditions for kinetic analysis of human vitamin K epoxide reductase (VKOR) catalytic activity, (ii) evaluated previously suggested irreversible and reversible mechanisms of VKOR inhibition by vitamin K antagonists (VKAs), and (iii) elucidated the role of tyrosine 139 in the catalytic center and inhibitor binding site of VKOR.

Firstly, observation of VKOR activity in human liver microsomes (HLMs) under varied experimental conditions demonstrated that human VKOR is a highly labile enzyme. Under optimal conditions, evaluation of genotyped HLMs for downstream effects of altered *VKORC1* mRNA expression revealed a relationship between the *VKORC1* B haplotype and increased the catalytic activity and protein expression of VKOR. This demonstrates that warfarin dose is regulated through a transcriptional mechanism wherein higher levels of *VKORC1* mRNA

translate to increased protein expression and associated enzymatic activity of VKOR, thus requiring a higher dose of warfarin to maintain the same target level of anticoagulation.

Secondly, the co-existence of irreversible and reversible modes of VKOR inhibition was re-investigated by the dilution method with the addition of two treatments, 20 mM DTT and 4% BSA, aimed specifically at stringent removal of inhibitor from microsomes. A post-dilution evaluation of VKOR activity in bovine liver microsomes that had been treated with 4-hydroxycoumarin and 1,3-indanedione VKAs demonstrated that they are not irreversible inhibitors, but appear to be tight-binding compounds that exhibit non-competitive type reversible kinetics with respect to vitamin K epoxide (KO).

Finally, recombinantly expressed VKOR carrying a tyrosine→phenylalanine mutation, which was made to test the importance of Y139 as a base or proton donor in the mechanism of KO reduction, had no effect on steady-state kinetic parameters for the formation of vitamin K_1 or 3-hydroxyvitamin K (a putative side-product). Any mutation of Y139, however, generated a warfarin-resistant enzyme. Therefore, although this residue is located proximally to the catalytic site of VKOR, we conclude that Y139 is not directly involved in the mechanism of substrate turnover, but has a pivotal role in warfarin binding and inhibition.

TABLE OF CONTENTS

LIST OF FIGURES

LIST OF TABLES

LIST OF ABBREVIATIONS

3-OH VK_1	3-hydroxyvitamin K
18S	18S ribosomal RNA
BCA	bicinchoninic acid
BLM	bovine liver microsome
BSA	bovine serum albumin
cDNA	complementary DNA
CHAPS	3-[(3-Cholamidopropyl)dimethylammonio]-1-propanesulfonate
C_T	threshold cycle
CYP	cytochrome P450
DMF	dimethylformamide
DMSO	dimethyl sulfoxide
DTT	dithiothreitol
EDTA	ethylenediaminetetraacetic acid
GAPDH	glyceraldehyde 3-phosphate dehydrogenase
GGCX	gamma-glutamyl carboxylase
GusB	beta-glucuronidase
HEPES	4-(2-hydroxyethyl)-1-piperazineethanesulfonic acid)
HLM	human liver microsome
HPLC	high-pressure liquid chromatography
hVKOR	human recombinant VKOR
KO	vitamin K epoxide
LC/APCI-MS-MS	liquid chromatography atmospheric chemical ionization-tandem mass spectrometry
MK	menaquinone
MRM	multiple reaction monitoring
mRNA	messenger RNA
MS	mass spectrometry
NADPH	nicotinamide adenine dinucleotide phosphate

NMR	nuclear magnetic resonance spectroscopy
NQO1	NAD(P)H-dependent quinone oxidoreductase
PCR	polymerase chain reaction
RNA	ribonucleic acid
RNase	ribonuclease
SDS-PAGE	sodium dodecyl sulfate-polyacrylamide gel electrophoresis
TMD	transmembrane domain
TYA	threonine tyrosine alanine
UDP	uridine diphosphate
UGT	UDP-glucuronosyltransferase
UTR	untranslated region
UV	ultraviolet
VKA	vitamin K antagonist
VK_1	vitamin K_1 , vitamin K quinone, phylloquinone
VK_2	vitamin K_2, menaquinone-4
VKH_2	vitamin K hydroquinone
VKOR	vitamin K epoxide reductase
VKORC1	vitamin K epoxided reductase complex subunit 1
WT	wild-type

ACKNOWLEDGMENTS

The author wishes to express sincere appreciation to those individuals who have helped make this effort possible though their contributions:

To Dr. Allan E. Rettie, who patiently guided and graciously cared for me throughout this project;

To Drs. Kent L. Kunze and William M. Atkins who served on the reading and supervisory committees;

To Drs. Gail D. Anderson, David R. Goodlett, Edward J. Kelly, and Mark J. Rieder, who served on the supervisory committee;

To Mr. Dale Wittington and Dr. Ross Lawrence, who trained and guided me in the mass spectrometry facility;

To Drs. Matthew McDonald, Cathy Yeung, Guoying Tai, and Matt Cheesman, who trained me in the laboratory.

To Drs. Matthew McDonald and Wenjin Guo, who contributed to this work;

To Laura Shireman, Kevin Coe, Peng Hsiao, Matt McDonald, Jed Lampe, Larissa Balogh, Mariko Nakano, Caleb Woods, Oliver Parkinson, Kayte Edson, Amanda Johnson, and Jamil Haque for their support and friendship during graduate school;

To the Department of Medicinal Chemistry for their financial support;

To Naomi Choi, Jenny Mayhew, Caleb Woods, and Mike Guttman, for their support especially during the past year.

Finally, to my parents Quincy and Margaret, and my brother Glen for their love, support, and encouragement.

DEDICATION

To my mom and dad,
who still tell me that I can be and do anything I put my mind to.

Chapter 1

Vitamin K, Vitamin K Epoxide Reductase, and Vitamin K Antagonists

1.1 Vitamin K

Discovery of Vitamin K

The discovery of vitamin K was made some eighty years ago by Henrik Dam (who named it after the German word 'Koagulation') [1-3]. Dam observed that when chickens were fed a cholesterol-free diet, they developed a hemorrhaging condition that could not be reversed by adding cholesterol back into their diet. He concluded that, an anti-hemorrhagic fat-soluble micronutrient had also been removed during the extraction of cholesterol from the feed. Twenty years later, Quick and Stefanini noted that the hemorrhagic disease Dam had observed was caused by a deficiency of active prothrombin [4,5]. Stenflo et al. and Nelsesuen et al. reported in 1974, that the synthesis of active prothrombin depends on a vitamin K-dependent (VKD) post-translational modification [2,3,6,7]. Structural characterization of prothrombin that was isolated from normal and vitamin K antagonist-treated cows revealed that the prothrombin of treated cows lacked a novel amino acid (now known as a γ-carboxyglutamic acid or Gla) on the amino-terminus of active prothrombin from "normal" cows. Further studies demonstrated that prothrombin had multiple sites at which the modified glutamic acid was present. The discovery that several other coagulation factors, for example, factors VII [8], X [9], and IX [10] [10-12] (Figure 1.1) were vitamin K-dependent proteins established vitamin K as an absolute necessity for active coagulation factor synthesis. In 1943, Dam and Edward Doisy shared the Nobel Prize in Physiology and Medicine for the discovery (Dam), and the purification, characterization, and synthesis (Doisy) of vitamin K [13].

Sources of Vitamin K

'Vitamin K' is a broad term for all 2-methyl-1,4-naphthoquinone derivatives that are critical for protein post-translational modification. Physiologically active vitamin K exists in two forms (Figure 1.2) : phylloquinone (VK_1) and a series of menaquinones (MK-n) where n is the number of isoprenoid units that make up the side chain. Dietary VK_1 comes primarily from green leafy vegetables [14,15], while menaquinones are obtained by eating animal (MK-4) and soy products (MK-7) [16]. The major forms of menaquinones have 4 to 10 repeating units (MK-4 to MK-10). A dietary source of MK-4 is poultry [17] as it is synthesized from VK_1 in various tissues of the body . Other menaquinones, for example MK-10 and MK-11, are also synthesized by intestinal bacteria [18,19].

Physiological Roles of Vitamin K-dependent Proteins

Other than coagulation, physiological functions of vitamin K-dependent proteins include bone metabolism (osteocalcin), intracellular signaling (tyrosine kinase), and cell growth (Gas6) [20,21] [22]. The most significant vitamin K-dependent proteins, however, are coagulation factors, namely II (prothrombin), VII, IX and X, protein Z, protein S, and protein C.

Glutamic acids of vitamin K-dependent proteins undergo γ-carboxylation to γ-carboxyglutamic acids (Gla), catalyzed by γ-glutamyl carboxylase (GGCX) (Figure 1.3). Most VKD proteins have an N-terminal propeptide, which is recognized by GGCX and tethers the VKD protein to the carboxylase as it carboxylates 3-14 glutamic acids in one binding event. The 45-amino acid domain that is adjacent to the propeptide and houses 9-11 Glu residues, is a highly conserved region among VKD proteins that is known as the Gla domain. A second carboxyl group on the

glutamic acid greatly increases its affinity for Ca^{2+}. Full carboxylation is required for the activation of clotting proteins. For coagulation factors, calcium-binding induces a conformational change that exposes the phospholipid-binding site of the Gla domain. Thus, fully carboxylated coagulation factors can form a tight complex at the membrane surface of platelets (where coagulation occurs) [23].

Vitamin K Cycle (Figure 1.4)

The carboxylation of glutamic acids is performed by the enzyme, γ-glutamyl carboxylase (GGCX), which requires carbon dioxide, oxygen and vitamin K hydroquinone (the reduced form of vitamin K) as cofactors. With the incorporation of each carbon dioxide molecule into a glutamic acid side chain, a molecule of vitamin K hydroquinone (VKH_2) is simultaneously oxidized to vitamin K-2,3-epoxide (KO). Since the amount of VKH_2 in the cell is limited, it must be regenerated to maintain a continuous supply of the cofactor by an enzyme called vitamin K epoxide reductase (VKOR), which reduces KO back to VKH_2 for subsequent GGCX reactions. The set of enzyme-catalyzed reactions involved in the inter-conversion of the oxidized and reduced forms of vitamin K is known as the vitamin K cycle [24] (Figure 1.4). Interference of this cycle is the mechanism of action of oral anticoagulant drugs, such as warfarin. Also known as vitamin K antagonists, (VKAs), these compounds specifically inhibit the activity of vitamin K epoxide reductase, thereby preventing the recycling of VKH_2 and the synthesis of functional clotting proteins. Interestingly, the identity of VKOR as the target of vitamin K antagonists was not revealed until some 60 years after warfarin was approved for medical use.

1.2 VKOR , the Pharmacological Target of 4-hydroxycoumarins

Discovery of the Anti-clotting Properties of 4-Hydroxycoumarins

During the 1920s, cattle in Canada and the northern part of the United States were afflicted with an unknown hemorrhagic disease. Frank Schofield, a veterinary pathologist, linked the disease to an anticoagulant compound produced by spoiled sweet clover in cattle feed. This compound was eventually isolated, characterized, and identified as 3-3'-methyl-bis-4-hydroxycoumarin (later named dicoumarol) by Mark Stahmann, a graduate student working in Karl Link's laboratory in Wisconsin [25]. Dicoumarol (Figure 1.5) was patented as a drug in 1941 and quickly became widely used for the prevention of thromboembolic diseases. Warfarin, 3-(α-phenyl-β-acetylethyl)-4-hydroxycoumarin, as it was referred to during Karl Link's investigation of dicoumarol analogs, was compound 42 on a list of 106 substances tested that were tested for improved anti-clotting properties [26]. In comparison to dicoumarol, compound 42 (Figure 1.5), had a longer duration of action and was more toxic to mice and rats than rabbits or dogs [26]. Therefore, after receiving the name Warfarin (WARF + (coum)arin), in honor of the Wisconsin Alumni Research Foundation that funded Link's work, the drug was marketed first as a rodenticide in 1942. Only after it was used to treat President Eisenhower when he suffered a heart attack in 1955 [27], did warfarin become well-accepted as a clinically useful anticoagulant, eventually replacing dicoumarol as the drug of choice [25]. All 4-hydroxycoumarin anticoagulants, e.g. warfarin, acenocoumarol, and phenprocoumon, have VKOR as their pharmacological target.

In 1970, Matschiner observed the accumulation of vitamin K epoxide in warfarin-treated rat liver microsomes [28]. This was the first evidence for VKOR activity. Later that year, Bell and

Matschiner reported an unknown liver enzyme that converted vitamin K epoxide to vitamin K [29]. It was also discovered that the coagulant property of vitamin K epoxide could be blocked by warfarin [28]. These observations led to the hypothesis that warfarin inhibited a cyclic interconversion between vitamin K and vitamin K epoxide [30], which has been the subject of thousands of publications over the intervening decades.

1.3 Biochemical Characterization of VKOR

The redox protein partner of VKOR

The customary in vitro assay used to measure VKOR activity requires an enzyme source (typically liver microsomes), the substrate (vitamin K epoxide), and a source of reducing equivalents. The latter is most commonly satisfied by dithiothreitol (DTT), which is thought to substitute for an endogenous protein that reduces the oxidized form of VKOR enzyme in order to initiate catalysis [31]. The physiological reductant that can be replaced by DTT in vitro has not yet been identified, but several candidates have been investigated: reduced glutathione [32], reduced lipoic acid, reduced lipoamide/microsomal lipoamide reductase [32] [33] and thioredoxin [34-36]. Gardhill and Suttie demonstrated that thioredoxin was capable of reducing VKOR in the reduction pathway of vitamin K epoxide and vitamin K. Preusch, however argued that thioredoxin probably is not the in vivo reductant, because it is predominantly a soluble cytosolic protein that is unlikely to have access to VKOR, which is located on the luminal side of the ER, as suggested by its inability to support VKOR reduction in whole microsomes without additional detergent [37]. Thioredoxin has the capacity to support VKOR activity only in the presence of detergent at concentrations higher than needed to observe DTT-dependent reduction [37]. This result is also consistent with a later report from Wallin et al [38], who demonstrated

that the thiol redox center of VKOR resides in a hydrophobic environment by comparing the ability of hydrophilic and hydrophobic thiol reducing trialkylphosphines to reduce the active site.

More recently, Wallin presented evidence for another member of the thioredoxin family, protein disulfide isomerase (PDI), as a candidate for the endogenous reductant of VKOR [39]. PDI, a thioredoxin-like protein that functions in disulfide-dependent protein folding, was shown to bind tightly with VKOR in liver microsomes by immuno-precipitation and 2D SDS-PAGE methods. Oxidative folding of reduced RNase was shown to be as effective as reduced vitamin K at triggering the reduction of vitamin K epoxide and subsequent γ-carboxylation reactions by GGCX. RNase-triggered VKOR activity was significantly inhibited by bacitracin in rat liver microsomes, and by PDI-silencing RNA in HEK 293 cells. Based on these data, Wajih et al. hypothesized that PDI and VKOR form a complex in the ER membrane through which disulfide-dependent oxidative folding of proteins by PDI provides electrons for the reduction of the VKOR redox center. Still, it is uncertain whether the in vitro behavior of any of the candidate proteins observed experimentally is relevant to the in vivo system, or how these proteins might be physically associated with VKOR in the ER membrane.

Catalytic Activities of VKOR

VKOR was thought to be a multi-enzyme complex in the ER after many failed attempts to purify catalytically active VKOR from rat and bovine hepatic microsomes [40,41]. The conversion of vitamin K epoxide to vitamin K hydroquinone, the form utilized by GGCX, occurs in two 2 electron reduction steps (Figure 1.4): 1) conversion of vitamin K epoxide to vitamin K quinone followed by 2) vitamin K quinone conversion to vitamin K hydroquinone. Until recently, it was

uncertain whether these reductions were performed by a single enzyme or multiple enzymes [42]. Besides VKOR, NAD(P)H-dependent quinone oxidoreductase (NQO1) can accomplish the second reduction step [2,4] (Figure 1.4). Gardill and Suttie observed that the enzyme activity responsible for epoxide reduction and vitamin K quinone reduction shared several characteristics, including sensitivity to a variety of 4-hydroxycoumarin compounds, co-fractionation, protection from N-ethylmaleimide (NEM) inactivation by the presence of either vitamin KO or vitamin K quinone, and the thiol reducing agent-dependent catalytic activity [35]. It was therefore concluded that a single enzyme reduces vitamin K quinone to vitamin K hydroquinone in two sequential reactions. Confirmation of this was obtained once it was found that recombinant VKOR, which could be purified as an active enzyme, possessed both reductase activities [42].

Stereoselectivity of Vitamin K Epoxide Reduction by VKOR

While the formation of KO by GGCX is highly stereospecific [43], VKOR-catalyzed reduction at the 2,3 position of the epoxide ring is not stereoselective (Figure 1.3). In vitro studies have demonstrated that the reductase reduces both enantiomers non-selectively, suggesting the epoxide substrate binds to VKOR in both possible orientations of the methyl and phytyl side chain relative to the epoxide ring [44]. The authors noted that these observations were consistent with the wide variability in substituent size of 4-hydroxycoumarin anticoagulants that are able to inhibit VKOR.

Discovery of the VKOR gene

VKORC1, the gene that encodes VKOR, is comprised of 5,126 base pairs on human chromosome 16, three exon regions encoding a protein of 163 amino acids, and has a calculated relative molecular mass of 18 kDa. In adults, *VKORC1* mRNA is expressed most highly in liver tissue, followed by the kidney, lung, and pancreas [45]. In 2004, *VKORC1,* was identified in two independent studies that were published in *Nature* [45,46].

Because previous reports had mapped two human coagulation disorders: warfarin resistance (WR) and combined deficiency of vitamin-K-dependent clotting factors type 2 (VKCFD2) to the same chromosomal region [47], Li et al. chose to focus on a candidate locus on chromosome 16. First, genes within this locus with known (non-oxidoreductase) function were ruled out. Per the suggestion that VKOR is a trans-membrane protein found in the ER [8,48], only genes encoding proteins predicted to have trans-membrane regions were considered further as candidate genes for VKOR. Finally, using a A549 cell line as a model with sufficiently high levels of VKOR activity, siRNA was used to systematically knock down 13 candidate genes. Knockdown of a single gene, *VKORC1*, led to specific inhibition of VKOR activity. Verification that this was the correct gene was obtained by recombinant expression and biochemical characterization of the over-expressed protein as a warfarin-sensitive VKOR enzyme.

These results were corroborated by the second study, which took a pharmacogenomic approach [45]. Rost et al. used a positional cloning approach to screen for mutations in DNA from two VKCFD2 patients, 4 WR patients, and several rat strains that exhibited warfarin resistance. Since missense mutations present on the same gene were discovered in every individual and resistant

rat strain examined, it was named vitamin K epoxide reductase complex 1 (*VKORC1*), in recognition of the possibility that VKOR and other protein partners, including the putative endogenous thiol reductant make up a larger complex.

1.4 Anticoagulation therapy

Medical Indications

A thrombotic disorder occurs when an unwanted blood clot (or thrombus) forms. These are life-threatening events because they involve the major vasculature of the heart, brain, and lung. Thrombotic conditions that require anticoagulation therapy to prevent new clot formation or break down thrombi include stroke, pulmonary embolism, deep vein thrombosis and a number of cardiac conditions, including myocardial infarction and atrial fibrillation.

Several factors influence the therapeutic agent chosen to treat a thrombotic disorder, one of which is the stage of the coagulation process to be targeted. Oral VKAs, heparin, and antiplatelet drugs prevent thrombus formation at different sites within the coagulation cascade (Figure 1.1), while thrombolytic drugs are used to dissolve existing clots.

Vitamin K Antagonists

Two classes of VKAs that have been approved for use in the United States are 4-hydroxycoumarins and 1,3-indanediones (Figure 1.6). Despite structural differences, they share the same mechanism of action. Years after Karl Link isolated dicoumarol, 1,3-indanedione derivatives were also identified as anticoagulants [49]. Currently, these agents are used as potent rat poisons and as alternative drugs prescribed to patients that are intolerant to 4-hydroxycoumarins.

1.5 Warfarin Therapy

Warfarin has a chiral center at carbon-9, but is administered to patients as the racemic mixture of equal amounts of (R)- and (S)-warfarin [50,51]. In vivo, the S-enantiomer of warfarin is 3-5 times more potent as an anticoagulant than the R-enantiomer [52,53] (Figure 1.5). Similarly, for phenproucomon, the S-enantiomer is 1.5-2.6 times more potent than the (R)-enantiomer [53]. Interestingly, enantiomers of acenocoumarol exhibit the opposite behavior [54], but this is a consequence of the much shorter half-life for S-acenocoumarol (2 hours), such that it does not accumulate significantly in plasma.

Warfarin Pharmacokinetics

Warfarin is completely absorbed and is 100% bioavailable following oral administration. The drug is highly bound to plasma proteins (>99%) and has a long half-life ($t_{1/2}$= 15-70 hrs). Practically none of the parent drug is excreted unchanged in the urine [55], but both warfarin enantiomers are metabolized by hepatic cytochrome P450s (CYPs) (Figure 1.7) that are partially glucuronidated before being excreted in the bile and urine. (S)-warfarin is metabolized to (S)-7-hydroxywarfarin, its major metabolite, as well as (S)-6-hydroxywarfarin by CYP2C9 [56]. (R)-warfarin is metabolized predominantly by CYP2C19 to (R)-8-hydroxywarfrin and CYP3A4 to (R)-10-hydroxywarfarin [57], and by a carbonyl reductase to diastereomeric (R)-warfarin alcohols that are excreted in the urine [58] (Figure 1.7). Specific human UGT isoforms have been identified recently that can glucuronidate many of the phenolic metabolites, but not the parent drug enantiomers [59]. In humans, the half-life of (R)-warfarin is about twice as long as that of (S)-warfarin and so the higher in vivo potency of the latter cannot be explained by preferential metabolic elimination of the former.

Warfarin Dosing

Warfarin is the current drug of choice for the prevention and treatment of thromboembolic disorders. Unfortunately, administration of warfarin and other coumarin analogs used as anticoagulation drugs is complicated. Warfarin has a relatively narrow therapeutic window and a highly variable inter-individual dose response among patients which together results in either over- or under-coagulation when the drug is given, especially at the beginning stage of treatment [60,61]. The 'normal' dosing range for warfrain is about 2-8 mg/day, but a small percentage of the patient population responds well to doses as low as 0.5 mg/day (Higashi et al., 2002). In addition, a severe phenotype is observed rarely wherein some patients lack any response to the drug with doses up to 50 mg/day (Watzka et al., 2010). Warfarin dose requirement is determined by demographic factors such as age, weight, gender, and race as well as environmental factors such as vitamin K intake and co-administration of warfarin-interfering drugs [62,63]. More recently, dosing algorithms have been designed [64,65] combining these factors with pharmacogenetic determinants of warfarin dose.

Warfarin Pharmacogenomics

To date, about 50% of the variance in maintenance dose of warfarin can be accounted for by common polymorphisms in just three genes; *CYP2C9*, *CYP4F2* and *VKORC1* [66]. Each of these genes is intrinsically linked either to warfarin metabolism or vitamin K metabolism [57,67], thereby offering a plausible rationale for their effects in modulating warfarin dose in patients.

Of the three genes identified above, *VKORC1* dominates as the single best genetic indicator of warfarin maintenance dose (Figure 2.1). Common (non-coding) polymorphisms in *VKORC1*

predict ~25% of the variance in maintenance dose of warfarin, whereas approximately 12% and up to 4% of warfarin response is attributable to common (coding) polymorphisms in *CYP2C9* and *CYP4F2,* respectively [68,69].

Influence of VKORC1 Genotype on Warfarin Pharmacodynamics

In a retrospective study of 186 Caucasian warfarin patients, Rieder et al. [70] identified 10 SNPs, from which a high dose-haplotype group (B) and a low dose haplotype group (A) were defined [70]. These researchers found that carriers of group B haplotypes, which are associated with high warfarin dose requirements, expressed elevated levels of *VKORC1* mRNA in human liver, relative to carriers of A group haplotypes which associate with low warfarin dose. According to Rieder et al., warfarin dose response appeared to be determined by *VKORC1* mRNA expression which is regulated by the two major haplotype groups. The association between *VKORC1* genotype and mRNA expression has since been reported by others [71,72].

VKORC1 haplotype prevalence also help to explain inter-ethnic differences in therapeutic response to 4-hydroxycoumarin drugs. The incidence of the low-dose haplotype A is very much higher in the Asian population, and lower in the African population than in Caucasians. These observations are consistent with the stratification of dose requirement among these ethnic groups, wherein the mean maintenance warfarin dose is 3 mg/day (Asians), 5 mg/day (Caucasians) and 6 mg/day (Africans), respectively (Dang et al. 2005).

The discovery of *VKORC1* has also been important for understanding the rare occurrence of warfarin resistance in humans. A number of mutations in the *VKORC1* gene have been identified

in warfarin-resistant patients (e.g. R58, V29L, V45L, V45A, L128R), each of which conferred resistance when recombinantly expressed [45].

Influence of CYP2C9 Genotype on Warfarin Metabolism

CYP2C9, the major P450 isoform responsible for the inactivation of warfarin in humans has two common genetic variants: *CYP2C9*2* (Arg144Cys) and *CYP2C9*3* (Ile359Leu) which possess 50-70% and ~10%, respectively, of the enzymatic activity of the wild-type enzyme towards (S)-warfarin metabolism [73]. Patients carrying either of these variants are predisposed to over-anticoagulation when initiated with the 'standard' 5 mg dose of the drug.

Influence of CYP4F2 Genotype on Vitamin K Metabolism

In a genetic screening of DNA variants of genes that code for drug-metabolizing and drug transport enzymes, Caldwell et al. [74] identified V433M, a variant of *CYP4F2,* as a new determinant of warfarin dose. Two of three separate cohorts of Caucasian warfarin patients possessing this variant allele that were examined provided evidence that carriers of the variant allele required an elevated maintenance dose of the drug. Not knowing the physiological function of CYP4F2 with respect to vitamin K metabolism or warfarin pharmacodynamics, the authors postulated that the enzyme either alters arachidonic acid metabolism or hydroxylates the vitamin K phytyl side chain to affect warfarin dose. CYP4F2 was known to metabolize arachidonic acid (Stec et al., 2007), but metabolism of vitamin K itself had not been demonstrated, although the enzyme was known to hydroxylate the phytyl side chain of vitamin E (Sontag and Parker, 2002). Metabolism of vitamin K by CYP4F2 was an attractive hypothesis in that patients carrying a variant allele would be expected to have a defective enzyme that would not be able to metabolize

vitamin K and would, therefore, need a higher dose of a VKA to achieve the target anticoagulant response. This hypothesis was supported by McDonald et al. [67], who showed in vitro that VK_1 was oxidized only by recombinant Supersomes expressing the CYP4F2 isoform. By steady-state kinetic and immune-quantitation measurements, it was demonstrated further that the V433M variant of CYP4F2 present in genotyped human liver microsomes possessed less enzymatic activity and was expressed in lower concentrations than the wild-type enzyme.

Because of the influence that genetic polymorphisms can have on drug dosing, a method to screen with combinations of risk alleles of *VKORC1*, *CYP2C9* and *CYP4F2*, could be useful to predict warfarin dose requirements and prevent overdosing that may result in hemorrhagic complications.

1.6 Interactions Between VKOR, KO and VKAs

VKOR-catalyzed reduction of KO

While much recent attention has been devoted recently to the clinical consequences of genetic variation in warfarin response genes, mechanistic studies of VKOR action and inhibition of the enzyme by VKAs has progressed little in the past 15 years. In the early 1980s, Silverman proposed a reaction pathway by which VKOR reduces vitamin K epoxide to vitamin K based on a chemical model study in which he observed that the epoxide could be non-enzymatically reduced by thiol compounds [14]. In this pathway (Figure 1.8), Silverman proposed that the VKOR active site disulfide is first reduced by a thiol reductant. The epoxide binds to reduced VKOR, becomes protonated by an acidic residue and then attacked by a sulfhydryl to open up the ring, resulting in a β-hydroxy sulfide adduct. Protonation of the β-hydroxyl group makes it a

good leaving group for reductive elimination by attack of a second sulfhydryl group on the first active site sulfide. At the end of each reaction with the epoxide, vitamin K is generated and the oxidized disulfide in the VKOR active site is restored. (Silverman's mechanism can also be drawn as a base-catalyzed reaction (Figure 4.3) as well for the reduction of vitamin K quinone).

This proposal for the mechanism of vitamin K epoxide reduction is supported by evidence for the postulated enolate intermediate between the thiol adduct and vitamin K in the form of its keto tautomer, since 3-hydroxyvitamin K is observed as a product of DTT-promoted vitamin K epoxide reduction [75] and as an in vitro product formed by vitamin K epoxide reductase in warfarin-resistant rat liver microsomes [76]. (The observation of a new vitamin K metabolite formed only by warfarin-resistant rats suggested that a genetically altered VKOR caused structural changes in the active site).

Evidence of participation in this mechanism by a sulfhydryl group was first obtained from in vitro studies by Lee and Fasco [32], who investigated the effects of thiols and sulfhydryl-modifying reagents on the conversion of vitamin K epoxide to vitamin K and vitamin K to vitamin K hydoquinone of VKOR in rat liver microsomes. From a panel of monothiol and dithiol compounds, they found that the rate of both reduction reactions, (KO to quinone and quinone to hydroquinone) was faster in the presence of a dithiol than a monothiol, suggesting that a pair of thiols is the only structural constituent needed to reduce VKOR. The slower reduction of VKOR in the presence of a monothiol suggested that the single reduction undergoes re-oxidation before a second molecule of monothiol can react. Therefore, for maximal VKOR activity, both sulfhydryl groups need to stay reduced. The addition of NEM, a compound that reacts with

sulfhydryl groups, resulted in VKOR inactivation in rat hepatic microsomes more effectively when the enzyme had been pre-reduced by DTT. Furthermore, vitamin K and vitamin K epoxide were able to prevent inhibition by NEM of their own metabolism in pre-reduced liver microsomes.

All biochemical studies of VKOR had been conducted in microsomal preparations until the discovery of the gene encoding VKOR, allowing for modern methods of experimentation to answer unresolved questions about VKOR catalysis. One of the earliest of such studies was conducted by Goodstadt and Ponting [77], who carried out a sequence alignment of the predicted protein sequences of VKORC1 from several species and discovered that *VKORC1* homologues are present in vertebrates, plants, bacteria, archae, and arthropods. The alignment also revealed 4 absolutely conserved cysteine amino acids (Cys43, Cys51, Cys132, and Cys135, as well as a conserved serine or threonine at position 57. Cys132 and Cys135 were proposed to make up the VKOR active site based on previous data demonstrating that they; 1) are located in a predicted transmembrane region [48], an observation that corroborated prior evidence of VKOR active site residing in a hydrophobic environment [38], 2) constitute a CXXC motif which is known to function as a redox center in other enzymes that belong to the thioredoxin family. Goodstadt and Ponting suggested further that the sulfhydryl groups of Cys132 and Cys135 catalyze a nucleophilic attack on vitamin K epoxide in a mechanism similar to a cysteine thiol-disulfide exchange performed by thioredoxin-like enzymes. The role of all 7 cysteines in the VKOR sequence was further investigated by site-directed mutagenesis and recombinant expression. Mutation of Cys132 and/or Cys135 to serine or alanine rendered the enzyme inactive for the conversion of KO to vitamin K [78,79], thereby supporting the existence of a CXXC redox

center in the active site of VKOR and the earlier suggestions that the presence of a cysteine residue in the active site was a requirement for KO reduction [80].

Chu et al (ref) 2006), also showed that Cys132 and Cys135 were required for the recombinant enzyme to reduce KO to VK_1 and VK_1 to VKH_2. Conversely, mutagenesis of Cys43 and Cys51 did not appear to affect catalytic activity driven by DTT [81], and so it has now become well accepted that Cys132 and Cys135 constitute the active redox center of VKOR.

Chemical Classes of VKAs

There are two major chemical classes of vitamin K antagonists: 4-hydroxycoumarin derivatives and 1,3-indandione derivatives.

4-Hydroxycoumarin derivatives

All of the compounds in this class have a 4-hydroxycoumarin ring with a different subsituent at carbon 3. Link and coworkers showed that, for this class of compounds, the hydroxyl group at the 4-position, the substituent at the 3-position on the coumarin and the benzopyrone backbone are required for anticoagulant activity (7). The most widely used 4-hydroxycoumarin derivative is warfarin, which has been a prototype for the design of more potent analogs. Examples of other VKAs used clinically are acenocoumarol and phenprocoumon (both used outside the US, mainly in Continental Europe). Since the 1950s, these various derivatives of 4-hydroxycoumarin have been used world-wide in both humans and animals [82]. The emergence of genetic resistance in rodents after extensive use of the first generation of anticoagulant agents necessitated the development of a second generation of more potent chemicals. Also known as ‘Superwarfarins,’

these compounds (eg. brodifacoum, difenacoum, and bromadiolone) generally have larger and more lipophilic substituents attached to carbon 3 of the 4-hydroxycoumarin ring. The increased lipophilicity greatly extends their half-lives, an attribute that makes them especially effective as rodenticides.

The 4-hydroxycoumarin derivatives are weakly acidic (pKa of ~5) lactones. NMR studies of warfarin indicate that in solution, the compound exists in at least three conformations, the ring opened form, and two distereomeric cyclic hemiketals (Figure 1.9) that result when the 4-hydroxy oxyanion attacks the carbonyl carbon of the side chain to form a new ring closure [1]. It is presumed that it is the ring opened form of warfarin that inhibits VKOR. Recently, several novel derivatives of warfarin were synthesized by Gebauer [83] and tested for their ability to inhibit rat liver VKOR. These comparisons showed that the potency of warfarin inhibition does indeed depend on the acidity of the 4-hydroxy group and that it is increased by more hydrophobic substituents on carbon-3.

1,3-Indandione derivatives

This class of vitamin K antagonists have an aromatic diketone nucleus and a substituent at the carbon 2-position. The most well-known of these derivatives are anisidione, the only one used clinically in the US, and pindone, chlorophacinone, and diphacinone which are used as rodenticides. Like 4-hydroxycoumarins, 1,3-indanediones are highly lipophilic compounds that inhibit VKOR, but they are faster-acting and have longer half-lives than warfarin [84]. Also like 4-hydroxycoumarins, resistance to inhibition by 1,3-indanediones has been reported [85].

Molecular mechanism of VKOR inhibition by VKAs

Based on his proposed mechanism of reduction of KO, Silverman also suggested that 4-hydroxycoumarins and 1,3-indandiones are mechanism-based inactivators of VKOR [86,87] (Figure 1.10). This view emerged because the VKAs and vitamin K epoxide are structurally similar, and so one might expect them to bind to VKOR in similar manner. Silverman proposed that the enzyme protonates the double bond in warfarin to form a 3-substituted 2,4-chromadione, an unstable tautomer of warfarin that has a lactone carbonyl group that is susceptible to nucleophilic attack by a reactive site nucleophile, such as a thiol, thereby generating a covalent adduct to VKOR. **(**A similar mechanism can be drawn for VKOR inhibition by 1,3-indanediones). The existence of a covalent bond between warfarin and VKOR has not been substantiated, but there is evidence suggesting that there is a tight interaction, in that dilution and repeated washing of rat liver microsomes that had minimal remaining VKOR activity after treatment with warfarin did not fully restore enzyme activity to normal levels [88,89]. It was concluded by these latter workers that warfarin binds to VKOR essentially irreversibly.

In Silverman's proposed mechanism for VKOR inhibition [86], the inhibitor binds to the reduced form of the VKOR active site, however, there is alternative evidence that warfarin may bind, in fact, to the oxidized form of the enzyme. A study of the interactions between KO, warfarin, and DTT revealed that increasing concentrations of DTT lowered warfarin inactivation [90]. Moreover, when the enzyme was incubated with warfarin before exposure to DTT, inhibition was greater than when it was exposed to DTT first. It was shown that maximal rates of inhibition were reached when the reductase was exposed to warfarin before DTT and that the level of inhibition was greater at higher concentrations of substrate. Based on these observations, it was

concluded that warfarin binds to the disulfide (oxidized) form of VKOR active site, whereas the substrate binds to the thiol (reduced) form. These observations, that warfarin and the KO substrate bind to oxidized and reduced forms of the enzyme, respectively, may help explain why warfarin's inhibition of the enzyme appears to be non-competitive [12,90].

Finally, structural details of the interaction between warfarin and its therapeutic target are not yet available, in part because membrane proteins, like VKOR, are extremely difficult to crystallize. 4-Hydroxycoumarin anticoagulants have been crystallized in complex with the cytosolic enzyme, NQO1 [18] with the observation that Tyr128 of that enzyme stabilizes binding of dicoumarol through electrostatic interaction with the coumarin nucleus. The same tri-peptide that harbors Tyr128; Thr-^{128}Tyr-Ala, is found near the active site of VKOR, as in Thr-^{139}Tyr-Ala. This has led to speculation that Tyr139 of VKOR is a critical binding determinant of warfarin [20], but no kinetic studies have yet appeared regarding the contribution of these residues to either VKOR catalysis or inhibition by VKAs.

It is not surprising that the discovery of *VKORC1* has greatly renewed interest in the study of VKOR, as implementation of the current recombinant DNA technology offers the potential to surpass past efforts to understand its interactions with warfarin at a mechanistic level, a goal that has remained clinically relevant for over 60 years. In Chapter 2 of this manuscript, a mechanism by which *VKORC1* genotype regulates the maintenance dose of warfarin is proposed and tested using an in vitro system of genotyped human liver microsomes. Chapter 3 explores the previously proposed mechanisms of VKOR inhibition (reversible and irreversible) with respect to agents in the two major chemical classes of vitamin K antagonists, using bovine liver

microsomes as a high activity enzyme source. In Chapter 4, the role of a single tyrosine residue, (Y139) that is found near the VKOR active site, is evaluated in terms of its contribution to catalysis and inhibition by warfarin. Finally, Chapter 5 summarizes the conclusions deriving from work that that has been accomplished in this project, and discusses future research in this area.

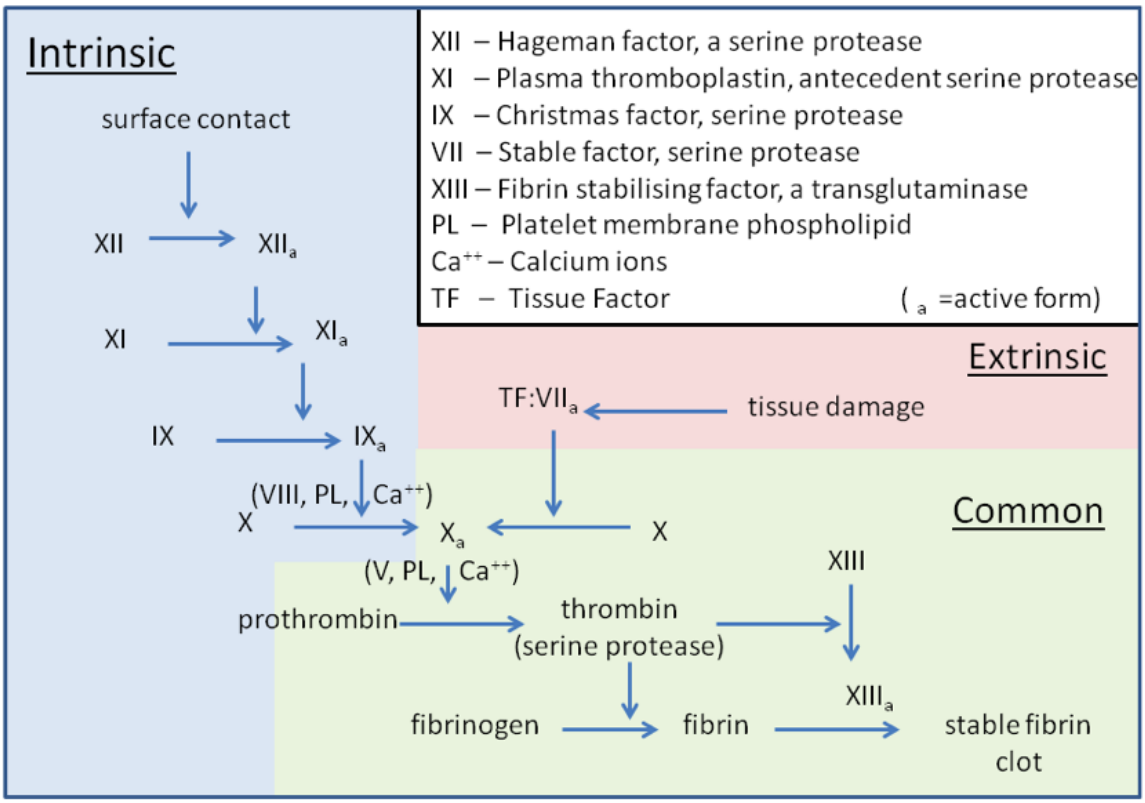

FIGURE 1.1: **The blood coagulation cascade, as taken from**[91]

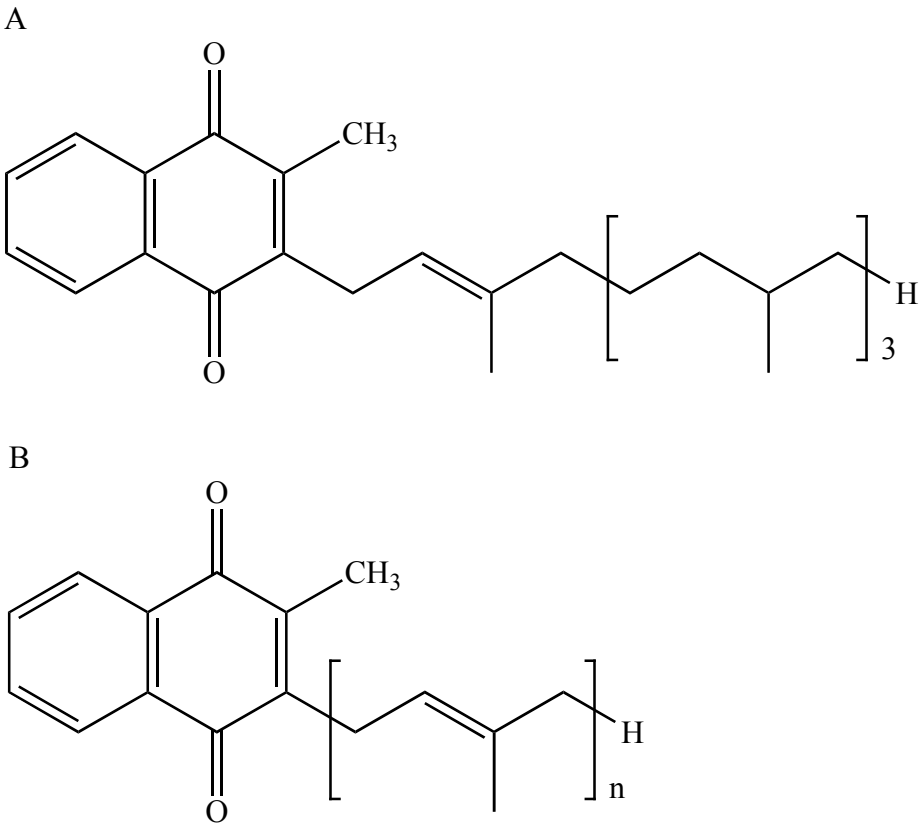

FIGURE 1.2: **Chemical structure of (A) Phylloquinone (VK_1) and (B) Menaquinones (MK-n).**

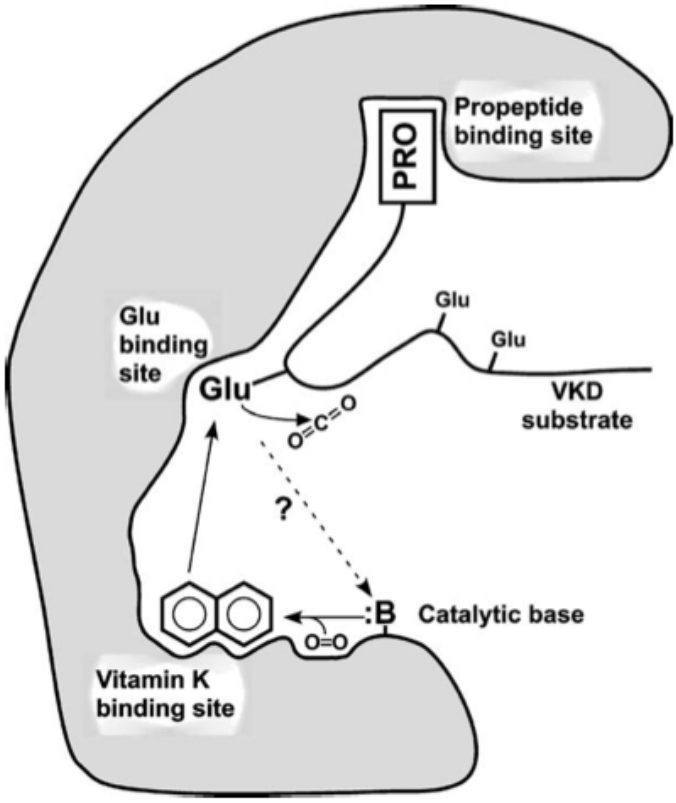

FIGURE 1.3: **Binding of a vitamin K-dependent protein to GGCX and subsequent carboxylation of a glutamic acid as taken from** [21]**.**

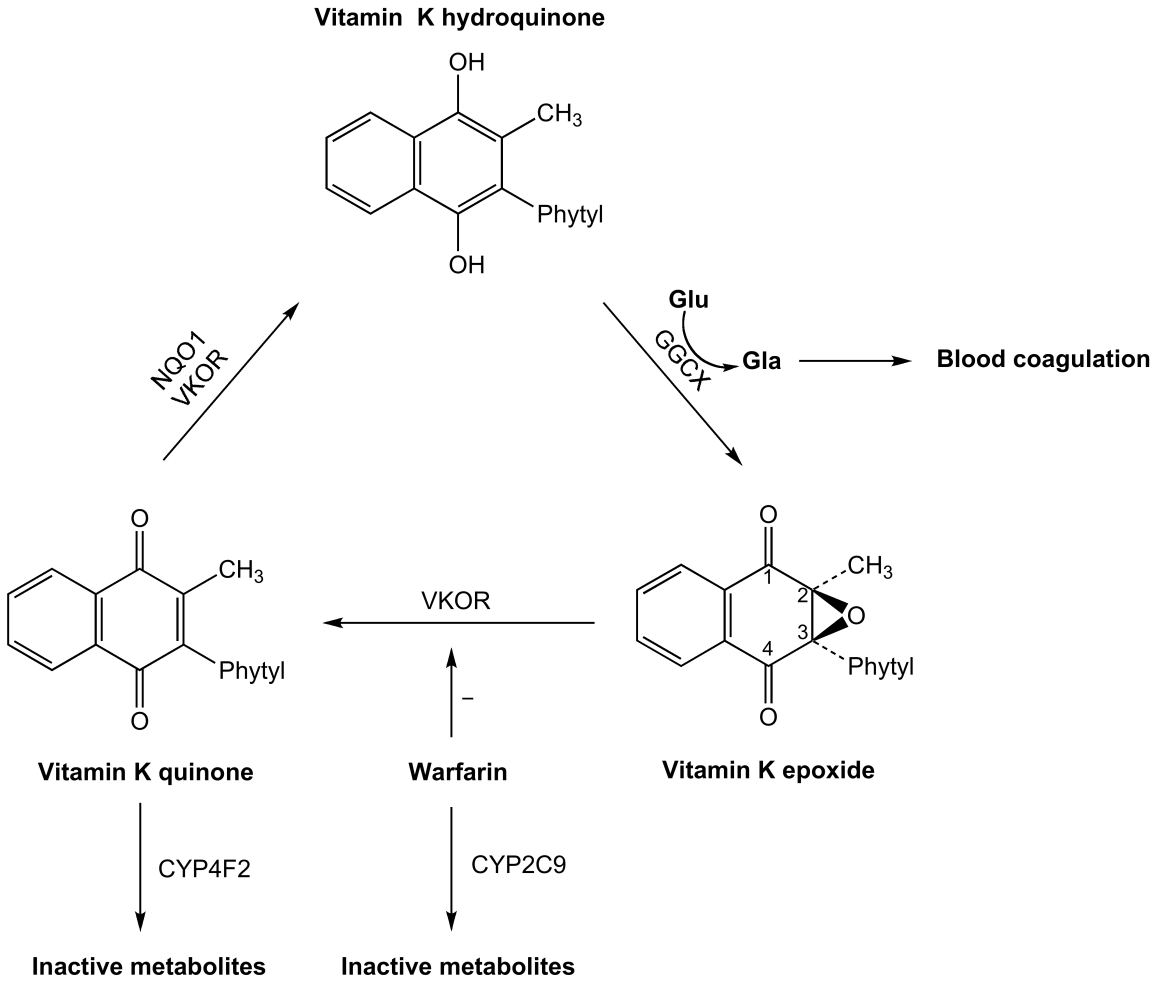

FIGURE 1.4: **The vitamin K cycle.**

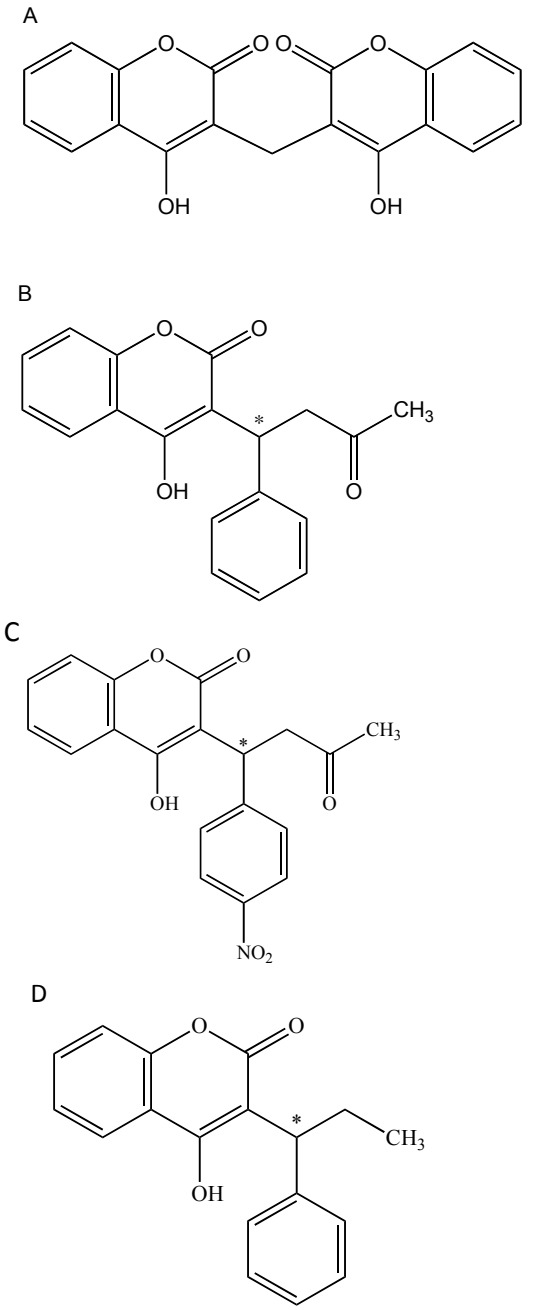

FIGURE 1.5: **4-Hydroxycoumarin anticoagulants:** (A) dicoumarol, (B) warfarin, (C) acenocoumarol, and (D) phenprocoumon. Asymmetric centers are labeled with an '*.'

A

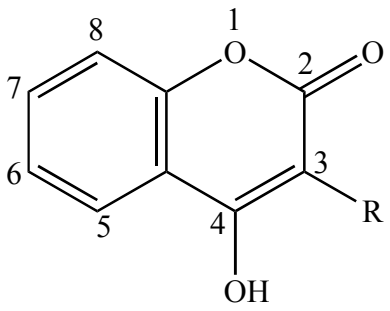

B

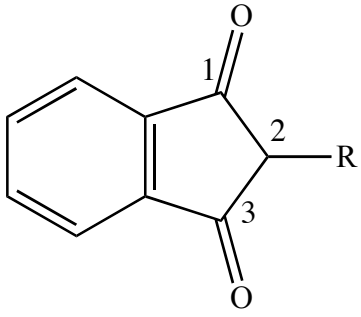

FIGURE 1.6: **Chemical classes of vitamin K antagonists: (A) 4-hydroxycoumarin and (B) 1,3-indanedione nucleus.**

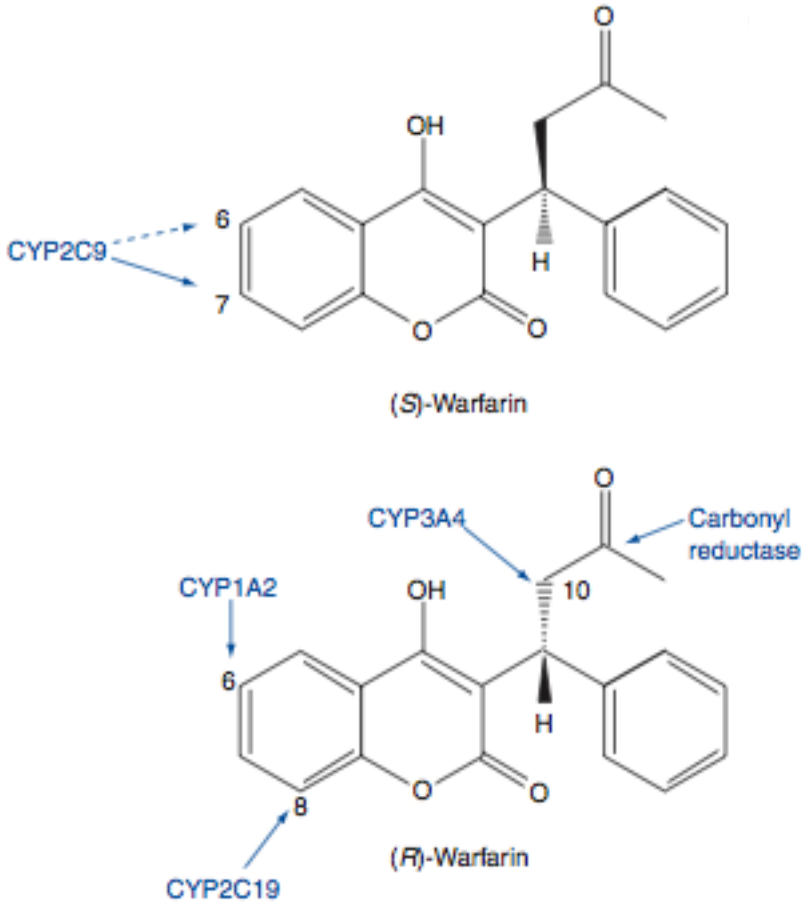

FIGURE 1.7: **Sites of (S)-warfarin and (R)-warfarin metabolism and the enzymes responsible for catalysis as taken from** [57]**.**

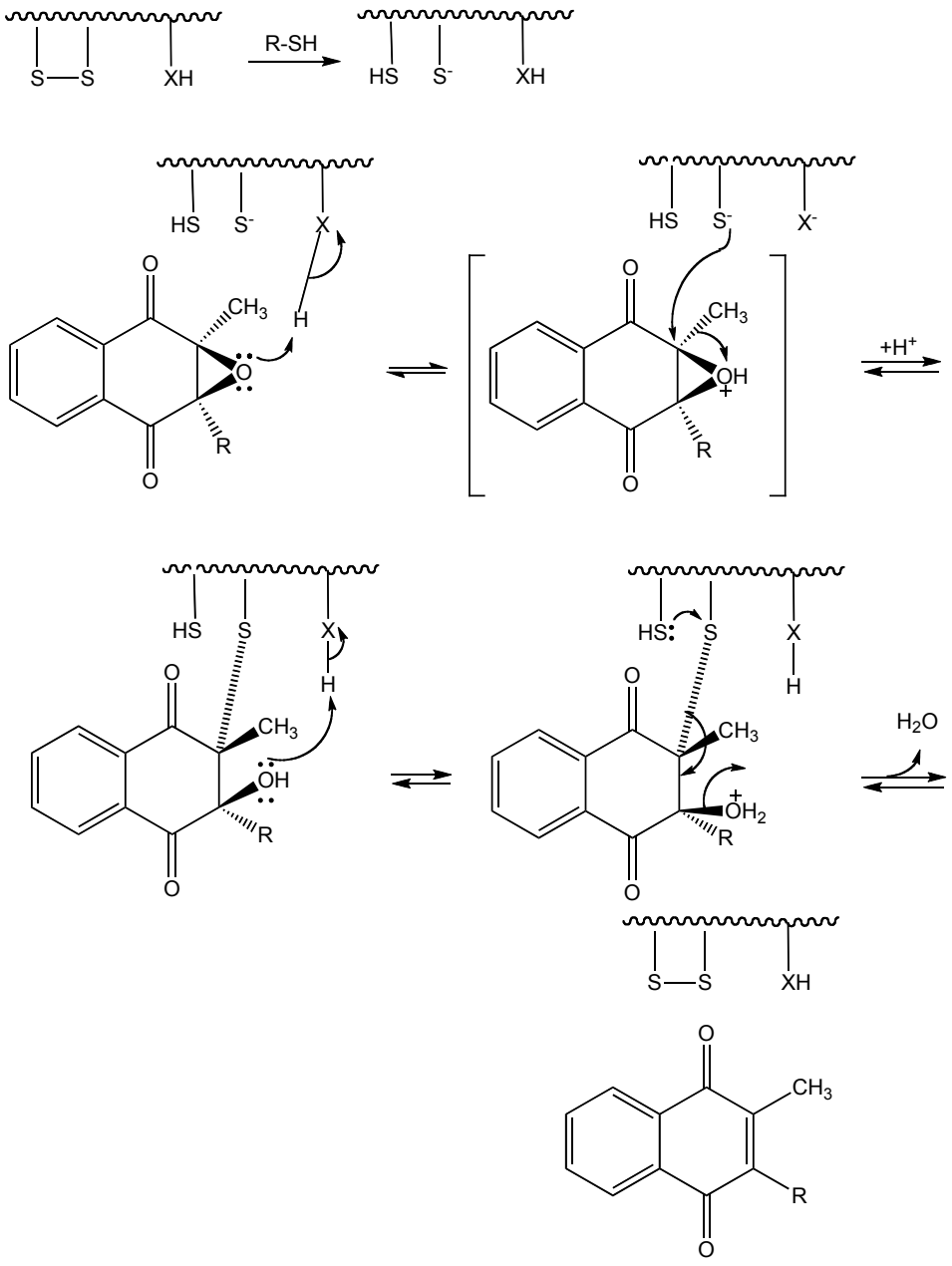

FIGURE 1.8: **Proposed mechanism of VKOR-(acid) catalyzed reduction of vitamin K epoxide as taken from** [14]**.**

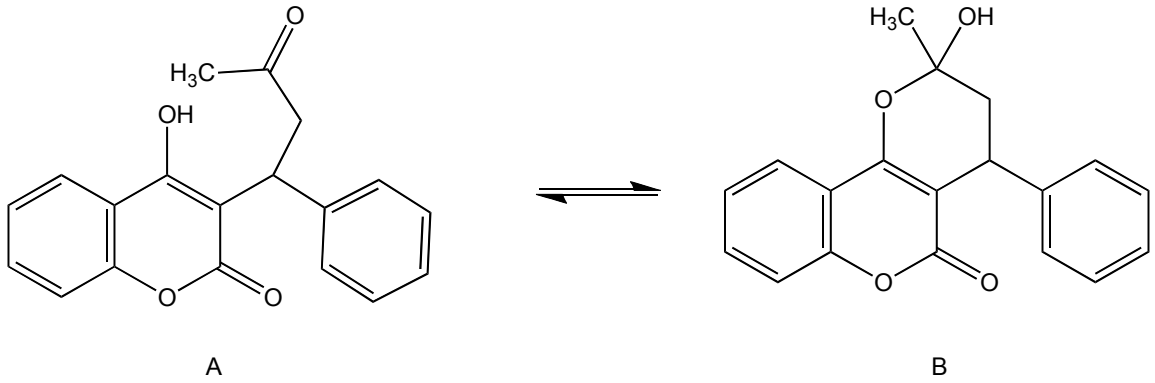

A B

FIGURE 1.9: **Conformations of warfarin in solution (A) ring opened form (B) ring closed hemiketal form.**

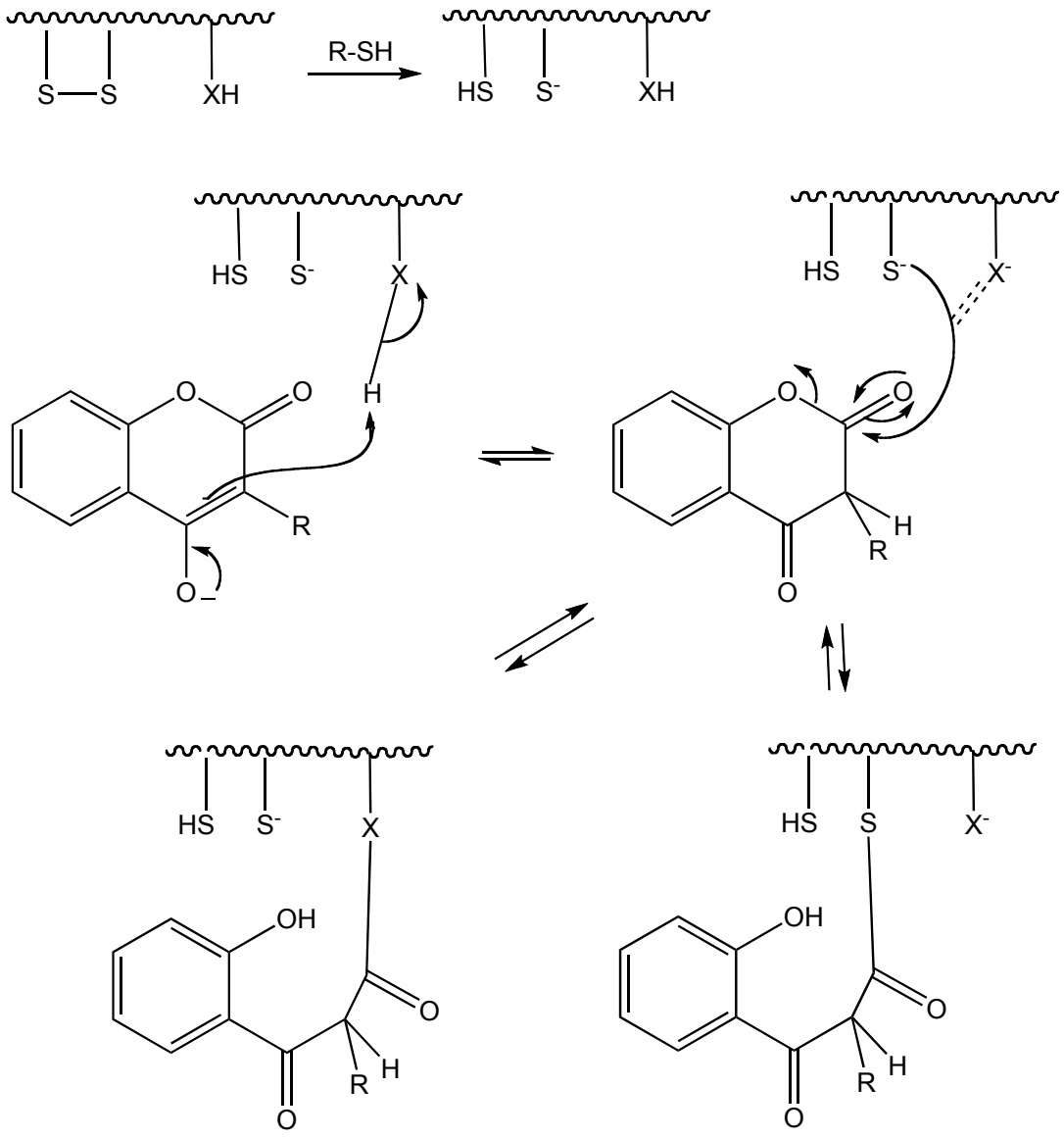

FIGURE 1.10: **Proposed mechanism of VKOR inactivation by 4-hydroxycoumarin anticoagulants as taken from** [86]**.**

Chapter 2

Biochemical and Pharmacogenetic Characterization of Human Liver Vitamin K Epoxide Reductase Activity

2.1 Introduction

In the post-genomic era, data from ever increasing numbers of candidate gene and genome-wide association studies continue to identify sequence variation in genes that can be linked to disease and drug treatment outcomes. From a basic research perspective, it seems intuitive that a full mechanistic understanding of how specific genes influence disease susceptibility/drug response can only positively impact the progress of translational medicine. However, there are often tremendous gaps in our understanding of the biochemical pathways that are modulated by even well established genetic biomarkers. A notable exception is the pharmacogenomics of warfarin, the most frequently administered oral anticoagulant to prevent thromboembolic diseases. Warfarin is a 4-hydroxycoumarin drug that blocks recycling of reduced vitamin K, a cofactor essential to the activation of clotting proteins. About 50% of the variance in the maintenance dose of warfarin can be accounted for by common polymorphisms in just three genes; *CYP2C9*, *CYP4F2* and *VKORC1* [37,66]. Each of these genes is explicitly linked either to warfarin metabolism or vitamin K metabolism [37,67,92] thereby offering a plausible rationale for their effects in modulating warfarin dose in patients.

Of the three genes identified above, *VKORC1* dominates as the single best genetic indicator of warfarin maintenance dose (Figure 2.1). Common (non-coding) polymorphisms in *VKORC1* predict ~25% of the variance in maintenance dose of warfarin [38,70] whereas approximately

12% and as much as 4% of warfarin response is attributable to common (coding) polymorphisms in *CYP2C9* and *CYP4F2,* respectively [39,68,69]. Beyond the impressive quantitative role of *VKORC1* variation in determining warfarin dose response, some information is also available on the mechanism whereby *VKORC1* variants influence warfarin dose. Rieder et al. [40,41,70] have described a transcriptional mechanism, wherein 5-flanking/intron/3'-UTR polymorphisms defining two major haplotype groups regulate *VKORC1* mRNA expression. Specifically, carriers of B haplotypes, which are associated with high warfarin dose requirements, expressed elevated levels of *VKORC1* mRNA in human liver, relative to carriers of group A haplotypes which associate with low warfarin dose. These gentoype-mRNA associations have since been replicated by others [42,71,72]. Presumably, higher levels of *VKORC1* mRNA translate to increased enzymatic activity of the hepatic vitamin K epoxide reductase (VKOR), thus requiring a higher concentration (dose) of warfarin to maintain the same degree of anticoagulation – i.e. an International Normalized Ratio of between 2 and 3 [70]. The primary purpose of the current study was to test this hypothesis by characterizing VKOR expression and activity in genotyped human liver samples.

Prior to the discovery of the gene that encodes vitamin K epoxide reductase, *VKORC1,* the microsomal systems involved in vitamin K metabolism and anticoagulation by coumarins were studied most extensively in the rat [93,94] and bovine liver [95]. Kinetic data for human VKOR has rarely appeared in the literature presumably because of limited availability of suitable tissue for analysis. Access to the Human Liver Bank in the Department of Medicinal Chemistry at the University of Washington was a key component of study feasibility. However, in initial studies using pooled human liver microsomes that had been previously prepared for P450-based

research, we found extremely low, barely detectable, levels of VKOR activity (Figure 2.2, Table 2.1). Therefore, we adapted the established HPLC-based analytical method [35,96] by replacing UV-based detection with a more sensitive (by more than 1000-fold) fluorescence-based detection method following a post-column reduction step [42,97]. This allowed for quantitation of vitamin K at the levels produced by human liver VKOR. We used this assay, firstly to optimize liver microsomal preparation and storage methods to best facilitate kinetic analysis of human VKOR and then secondly, to investigate the effect of *VKORC1* haplotype on the catalytic activity of human liver VKOR.

2.2 Materials and Methods

2.2.1 Synthesis and Purification of KO

Racemic vitamin K_1 epoxide (KO) was synthesized and purified as described in the literature [43,98]. Crude KO, as a yellow oil (50 mg) was dissolved in ethanol (10 mg/mL solution) and purified on a reverse phase-HPLC semi-preparatory column (Ultrasphere ODS; 10 mm x 25 cm, 5 micron particle size; Beckman Coulter, Inc., Brea, CA). KO, detected by UV absorbance at 228 nm and 264 nm (Shimadzu Diode Array Detector SPD-M10AVP, Kyoto, Japan), was eluted isocratically with 100% methanol (HPLC grade) at a flow rate of 4 mL/min (Shimadzu pump LC10ADVP, Kyoto, Japan). KO, which eluted at 16 minutes under these conditions, was collected and solvent-removed mostly by rotary evaporation in a 40^{o}C water bath followed by high vacuum at room temperature over night. Working stock solutions of KO were prepared in ethanol (USP grade) over a range of concentrations (25 μM - 21 mM). The concentration of KO was determined spectrophotometrically using an extinction coefficient of 30,800 $M^{-1}cm^{-1}$ (225 nm) [44,96].

2.2.2 Preparation of Chemical Standards

Standard solutions of vitamin K_1, VK_1, (0.1 μM, 1, μM and 10 μM) and VK_2, (10 μM) in isopropanol (HPLC grade) were stored at -20°C. The concentration of VK_1 and VK_2 stock solutions were determined spectrophotometrically using an extinction coefficient of 18,900 $M^{-1}cm^{-1}$ (248nm), and 11,800 $M^{-1}cm^{-1}$ (248 nm), respectively [45,96].

2.2.3 Preparation of Liver Microsomes

Adult human liver tissues were obtained from the Liver Bank housed within the Medicinal Chemistry Department of the University of Washington (UW) School of Pharmacy. Individually frozen rat and bovine liver samples were purchased from Pel-Freez® Biologicals (Rogers, AR). All tissues were stored at -80°C and all tissue-processing operations were performed at 4°C or on ice. Typically, pieces of liver tissue were thawed on ice in 3 mL homogenization buffer per gram of dry tissue. After the fat and connective tissue were removed, the remaining tissue was cut into fine pieces. Two techniques were applied to homogenize the tissue samples: 1) **grinding** the tissue with a piston-type Teflon®-tipped pestle (Wheaton Industries, Millville, NJ) powered by an electric drill in a borosilicate glass round-bottom tube (6 passes) and 2) **blending** the ground mixture with a blade-type VirTishear homogenizer (VirTis, Gardiner, NY) on ice for 10 seconds at a power setting of 10. The homogenate was fractionated by ultracentrifugation (9000 x g for 20 minutes at 4°C) in a Sorvall® Ultra80 ultracentrifuge (DuPont Instruments, Corp., Miami, FL). The post-mitochondrial supernatant was filtered through a pre-chilled glass funnel covered with a layer of cotton gauze to strain out residual fat and then centrifuged at 110,000 x g for 70 minutes at 4°C. The resultant microsomal pellet was resuspended (by grinding as described in **Section 2.2.3**) in wash buffer and the microsomes were re-sedimented at 110,000 x g for 70 min

at 4°C. The final pellet was resuspended (grinding) in a minimal amount of storage buffer and frozen at -80°C. The total protein content in each microsome sample was quantitated according to instructions in the BCA™ Protein Assay kit (Thermo Scientific, Rockford, IL).

The combination and composition of buffers that were specifically used in the experiments to optimize the detection of human liver microsomal VK_1 production are listed in the legend of Table 2.2. The buffers used to isolate human liver microsomes from genotyped livers are listed in Table 2.2 under the column heading 'Sequence 4.' For the preliminary experiments with bovine liver microsomes, the microsomal pellet was washed with 'B' as described in the legend for Table 2.2, and supplemented with solid NaCl to a final concentration of 1M.

2.2.4 Measurement of VKOR Activity in Liver Microsomes

Each reaction mixture was prepared in a 1.5 mL microcentrifuge tube containing 1 mg/mL microsomal protein, 2 mM DTT (added from a freshly prepared stock in reaction buffer), and reaction buffer (250 mM potassium phosphate, pH 7.86, 500 mM potassium chloride, 20% glycerol, 0.75% CHAPS), in a total volume of 250 or 500 µL (samples maintained a final CHAPS concentration of 0.5-0.7%) unless otherwise stated. Incubation mixtures were pre-incubated in a shaking water bath at 30°C, 70 rpm for 3 minutes prior to initiating the reaction by adding KO (substrate) in a volume that maintains a final organic solvent concentration of 1% v/v. After 20 minutes, the reaction was quenched by adding 50 µL of a 15% w/v solution of aqueous zinc sulfate to precipitate proteins. One hundred pmol of VK_2 was added to each incubation mixture as an internal standard. The reaction products were extracted by adding 700 µL hexanes (ACS grade) and 200 µL isopropanol (ACS grade), vortexing the tube for 1 minute, and centrifugation (12,000 x g) at room temperature for 5 minutes. The hexane layer (upper) was

collected, transferred to a borosilicate glass test tube, and evaporated under a stream of nitrogen gas for 20 minutes at room temperature (Zanntek Analytical Evaporator, Glas-Col®, Terre Haute, IN). The dry residue was dissolved in 100 µL of isopropanol (HPLC grade) and transferred to a vial for reverse phase-HPLC fluorescence analysis as described below.

2.2.5 Reverse Phase-HPLC Fluorescence Analysis

HPLC-mediated separation and quantification of VK_1 (product), KO (substrate), and VK_2 (internal standard) was performed over a 20 minute run time on a reverse phase HPLC analytical column (Nucleosil 100-5 C18; 4.6 x 125 mm, 5 micron particle size; Macherey-Nagel, Duren, Germany) and eluted isocratically with a mobile phase of 95% methanol (HPLC grade) containing 11 mM $ZnCl_2$, 5.5 mM NaOAc and 5.5 mM glacial acetic acid at a flow rate of 1 mL/min (Shimadzu pump LC10ADVP, Kyoto, Japan) [45,46,67]. Retention times for VK_2, KO, and VK_1 were 7, 9, and 15 minutes, respectively (Figure 2.2). In the presence of acid, zinc catalyzes the reduction of VK_1 and VK_2 quinones (which are non-fluorescent) to the corresponding dihydroquinone forms (which are highly fluorescent). Therefore, after elution from the C18 column, analytes were passed directly through a guard column packed with zinc powder (-100 mesh, Aldrich, St. Louis, MO) prior to the fluorescence detector (Shimadzu Fluorescence Detector RF-10AXL, Kyoto, Japan). Wavelength settings on the fluorescence detector optimized for VK_1 were 244 nm (excitation) and 430 nm (emission) [47,99,100].

2.2.6 Selection of Human Liver Tissues Samples by *VKORC1* Genotype

Human Liver Bank samples were genotyped as previously described [45,70]. Microsomes were prepared from five non-ischemic human livers that were selected to represent each *VKORC1*

haplotype group combination (A/A, A/B, B/B). Each microsomal pellet was harvested from approximately 10 grams of human liver tissue, resuspended with storage buffer to a final concentration of 5 mg/mL, and stored at -80^{o}C.

2.2.7 Steady-state Enzyme Kinetics

Experiments performed to measure KO binding affinity (K_m) and maximal VKOR activity (V_{max}) in liver microsomes were performed at the following final substrate concentrations: human pool (0.25, 0.50, 1.5, 3.0, 8.5, 16, 32, 85, and 210 μM), rat (0.25, 0.50, 1.5, 3.0, 5.0, 15, 30, 40, and 90 μM), and bovine (0.25, 0.50, 1.0, 2.0, 6.0, 12, 30, 60, and 100 μM). Microsomes reserved for performing replicate sets of kinetic experiments were stored as single-use aliquots containing enough protein for the number of reactions (plus 2 extra) in a single set. For each experiment conducted, a fresh tube of microsomes was thawed on ice and the appropriate volumes of reaction buffer and DTT needed for the complete set of reactions, were added to create a master mix. The master mix was vortexed briefly and divided equally into 1.5 mL microcentrifuge tubes. At each concentration of substrate, incubations with heat-inactivated (10 minutes at 100^{o}C) microsomes were carried out in parallel with catalytically active microsomes.

2.2.8 VK_1 Quantification and Calculations

For each HPLC chromatogram, Shimadzu EZSTART chromatography software version 7.2.1 SP1 was used to compute the peak areas for VK_1 and VK_2, respectively. VK_1 quantification was achieved by applying the method described previously [49,67]. Briefly, data from mock incubations that were performed with known concentrations of VK_1 in the presence of heat-inactivated microsomes, were used to make a standard curve by plotting fluorescence vs. peak

area ratio (VK_1/VK_2). The equation of the linear regression, which typically had a slope of 1, was used to convert peak area ratio to amount ratio (pmol VK_1/pmol VK_2). The amount of VK_1 formed during an incubation reaction was determined by multiplying the amount ratio by 100 (for the amount of VK_2 (internal standard) that was added). The rate of VK_1 production was calculated as pmol/mg microsomal protein/minute.

2.2.9 Kinetic and Statistical Data Analysis

GraphPad Prism, version 5.00, software for Macintosh (GraphPad Software, San Diego, CA, USA), was used to plot and fit data points (each point representing the mean of triplicate measurements). Kinetic constants, K_m and V_{max}, were calculated by non-linear regression curve fitting of the data plotted as the substrate concentration versus the rate of reaction. Goodness of fit was evaluated by the R^2 value. The one-way ANOVA and Student's t-tests using StatPlus® (AnalystSoft Inc., Alexandria, VA) were performed to determine statistical significance.

2.2.10 Quantitation of VKOR Protein in Human Liver Microsomes

Human liver microsomes were pooled according to *VKORC1* genotype (n = 5 per pool; A/A, A/B and B/B). Microsomal proteins in each pool were concentrated by lipid removal according to the following procedure. A mixture of 10 µL of 0.15% sodium cholate and 100 µL of microsomes was incubated for 5 minutes at room temperature. Ten µL of 72% tricholoroacetic acid was added to precipitate proteins and the mixture was incubated for 5 minutes at room temperature followed by centrifugation at 12,000 x g for 2 minutes. The resulting supernatant was decanted and the pellet was washed twice by vortexing in 1 mL of ice cold ethanol:ether mixture (1:1). After the final spin, the supernatant was removed and the pellet was air-dried

before pipette resuspension with 100 µl of resuspension buffer (0.2 M Tris, pH 7.4, 4% SDS, 0.15 M NaOH). Microsomal protein content was assayed by performing a DC Protein Assay (detergent-compatible) with a kit purchased from Bio-Rad Laboratories **(**Hercules, CA).

Recombinantly expressed VKOR protein (the preparation of which is described in Section 4.2.1-4.2.5), and human liver microsomes were heated for 20 minutes at 37^{o}C in Laemmli Sample buffer (1:2 dilution) (Bio-Rad Laboratories, Hercules, CA) containing β-mercaptoethanol (1:20 dilution). Proteins were separated on a 10-20% Acrylamide Tris-HCl gel (Bio-Rad Laboratories, Hercules, CA) and electrophoretically transferred to a nitrocellulose blotting membrane, which was blocked at 4^{o}C for 4 hours in Odyssey® Blocking buffer (LI-COR Biosciences, Lincoln, Nebraska). Each of the following blot incubations was performed in a 50 mL Falcon tube and mixed on a tube rotator. The membrane was first probed with a 1:5,000 dilution of rat anti-VKOR antibody (a gift from Dr. Kathleen Berkner, Lerner Research Institute, Cleveland, Ohio) for 12 hours at 4^{o}C and then with mouse anti-β-actin antibody (1:5,000 dilution) (Sigma-Aldrich, St. Louis, MO) for 1 hour at room temperature in blocking buffer containing 0.1% Tween20® (Sigma-Aldrich, St. Louis, MO). After the membrane was washed extensively with PBS buffer containing 0.1% Tween-20, it was co-incubated with Donkey anti-rabbit IRDye®680 (1:2,500) (LI-COR Biosciences, Lincoln, Nebraska) and Goat anti-mouse IRDye™800 (1:15,000) (LI-COR Biosciences, Lincoln, Nebraska) in blocking buffer containing 0.1% Tween-20 for 1 hour at room temperature in the dark. The membrane was washed extensively with blocking buffer containing 0.1% Tween-20, followed by rinsing with PBS without detergent. The Odyssey® Infared Imaging system (LI-COR Biosciences, Lincoln, Nebraska) was the corresponding Application Software (version 2.2.12) was used to visualize

fluorescent protein bands and quantitate band densities. For each lane, the density of VKOR was normalized to that of the corresponding β-actin band.

2.2.11 Total RNA Extraction from Liver Tissue

Human liver RNA samples were supplied by Dr. Edward Kelly (University of Washington, Seattle, WA) or extracted from flash-frozen tissue from the Liver Bank. Human (pooled) and bovine RNA were purchased from BioChain® (Hayward, CA). Flash-frozen bovine liver tissues were also purchased from Pel-Freez® Biologicals (Rogers, AR). Fresh bovine tissues were acquired and flash-frozen 1 hour after harvest at Schenk Packing Company (Stanwood, WA). In an RNAse-free lab space, total RNA was isolated from approximately 50 μg of each adult liver tissue according to the protocol described by TRI Reagent® Solution (Ambion,® Austin, TX). Briefly, the tissue was homogenized with a pestle for microtubes in 1 mL of TRI Reagent® solution (Ambion,® Austin, TX), vortexed, and incubated at room temperature for 5 minutes. The homogenate was mixed with 100 μL bromochloropropane, shaken vigorously for 15 seconds and incubated at room temperature for 15 minutes, followed by centrifugation at 12,000 x g for 15 minutes at 4°C. The aqueous supernatant was collected, from which RNA was precipitated with isopropanol (ACS grade), washed with 75% ethanol (nuclease-free water, ACS grade), and dissolved in 100 μL of TE buffer. RNA yield was determined by measuring its absorbance at 260 nm on a SmartSpec™ Plus spectrophotometer (Bio-Rad Laboratories, Hercules, CA) and quality was indicated by the A_{260}/A_{280} ratio (1.8-2.2). Quality of the RNA samples was further assessed by RNA gel electrophoresis. All tissues and RNA samples were stored at -80°C.

2.2.12 cDNA Synthesis and Real-Time PCR

For each reaction, 1 μg of RNA was used as a template for reverse transcriptase from a TaqMan® Reverse Transcription Reagents kit (Roche for Applied Biosciences, Carlsbad, CA). Each 10 μL reaction also contained 1 μL of 10X RT buffer, 2 μL of dNTP mix, random hexamers (2.5 μM), $MgCl_2$ (5.5 mM), RNAse inhibitor (0.4 units), and Multiscribe reverse transcriptase (1.25 units). A master mix containing all components except RNA and water was prepared. The master mix was divided evenly into PCR tubes each containing RNA, which were subsequently placed in a PCR thermocycler (Eppendorf Mastercycler Personal, Westbury, NY), under the following PCR conditions: 45^{o}C for 50 minutes, 85^{o}C for 10 minutes, and hold at 4^{o}C. cDNA samples were stored at -20^{o}C or immediately diluted (1:50) with Tris-EDTA buffer. Reaction mixtures containing 100 ng cDNA, 12.5 μL 2X PCR Master Mix (Applied Biosystems, Foster City, CA), 1.25 μl of each species-specific primer probe reaction mix (Applied Biosystems, Foster City, CA) in a total volume of 25 μL, were prepared in a nuclease-free 96-well plate. Real-time PCR analysis was run under standard conditions on an (ABI Prism 7900HT Sequence Detection System, Appied Biosystems, Foster City, CA): 10 minutes at 95 ^{o}C, followed by 41 cycles of 15 seconds at 95^{o}C and 1 minute at 60^{o}C. The threshold cycle (C_T) was set within the linear of signal vs. cycle number graph. C_T values for the endogenous control gene (18S or GusB) were subtracted from the C_T values of the target gene samples to obtain ΔC_T values. The $\Delta\Delta C_T$ method [50,51,101] was applied to calculate the *VKORC1* transcript level in bovine liver tissues expressed as x-fold relative to that observed in human liver (the highest of the human samples).

2.3 Results

2.3.1 Inter-species Differences in Hepatic VKOR Activity

A key observation from preliminary surveys of VKOR activity in liver microsomes from various species was that enzyme activity in human liver was significantly lower (~30-fold) than either rat or bovine liver (Figure 2.3, Table 2.1). However, this early analysis made use of stored hepatic microsomes that had been prepared by a variety of different techniques.

To evaluate the basis for the very large apparent difference between human and bovine VKOR activity, the methods of preparing bovine and human liver microsomes were examined closely. In the published procedure for the preparation of bovine liver microsomes [52,53,102], buffer containing 1M NaCl was used to wash the microsomes before the final pellet was frozen in storage buffer. Possibly, a high amount of salt might remove endogenous inhibitors of VKOR from the microsomes. To rule out any effect of salt as a contributor to the significant inter-species differences in activity, isolated human liver microsomes were washed in high salt-containing buffer prior to incubation with KO, but this treatment had minimal effects on the amount of VK_1 produced (data not shown). (Comparison of recombinantly expressed enzymes (data not shown) showed that the bovine and human VKOR are intrinsically similar in activity).

Next, we made a side-by-side comparison of buffers from the literature [53,76,103] that have been employed to isolate rat liver and human liver microsomes, to determine which procedure would ensure optimal enzyme activity from human liver. Microsomes were prepared under four sets of buffer conditions that are listed in Table 2.2 and assayed for VKOR activity. Conditions listed under ‘Sequence 4’ resulted in the highest rate of reduction of 20 μM KO (Figure 2.4),

although overall buffer conditions had only a modest effect on enzyme activity. Nevertheless, subsequent human liver microsome isolations were performed under 'Sequence 4' conditions.

Finally, liver cDNA for real-time PCR experiments was acquired from various sources of human and bovine liver RNA. When cDNA that was reverse transcribed from total RNA extracted from flash-frozen human liver pieces obtained from the UW Liver Bank were compared with total RNA from flash-frozen bovine liver purchased from Pel-Freez®, the levels of *VKORC1* mRNA expression were about equal (Table 2.3). To attempt to control for differences in sample handling, the experiment was repeated using cDNA reverse transcribed from commercially acquired bovine and human liver RNA samples. In this case, the expression level in bovine liver was slightly higher than human liver by about 2.2-fold (Table 2.3). Finally, when bovine liver RNA was freshly harvested from flash-frozen bovine livers obtained at a local abattoir, transcript levels were ~5-fold higher on average compared to human liver (Table 2.4). When the same set of human and bovine liver samples (as microsomes) were assayed for VKOR activity at 50 μM KO, the average rate of VK_1 production in bovine liver microsomes was ~9-fold higher (Table 2.4).

2.3.2 Evaluation of Microsomal Storage and Assay Conditions for Human VKOR Activity

To establish optimal procedures for preserving microsomal VKOR activity, the stability of the enzyme in human liver microsomes was investigated, a concern that has previously been addressed for other hepatic microsomal enzymes (cytochrome P450s) [54,104]. Human liver microsomes were subjected to 1, 3, or 6 cycles of freezing at -80^{o}C, followed by thawing at 4^{o}C before being assayed for VKOR activity. As indicated in Figure 2.5, after 3 freeze-thaw cycles,

37% of the activity present after 1 cycle was lost and after 5 cycles, activity was no longer detectable.

The ability of DTT to support microsomal vitamin K epoxide reductase activity was investigated. For in vitro VKOR systems, 2 mM DTT, which is believed to reduce an active site disulfide to thiol groups that react with the epoxide [55,105] [14,56], has routinely utilized as a surrogate for the endogenous reductant. To ensure that the active site cysteines were fully reduced by DTT, the amount of VK_1 produced after pre-incubation with DTT for varying amounts of time was measured. The data shown in Fig. 2.6. indicate that reduction of the active site cysteine was maximal after exposure to DTT for 3 minutes at low and high concentrations of substrate.

The possible effect of the zwitterionic detergent CHAPS and alamethicin, a pore-forming antibiotic, as adjuvants for the delivery of KO to the VKOR enzyme was explored. While adding alamethicin alone to the reaction buffer resulted in higher reductase activity than CHAPS, the difference was minimal (~2-fold) (Figure 2.7). Because CHAPS is far more economical for long-term use, all incubations with KO were performed with this detergent in the reaction mixture.

Finally, with the basic reaction conditions optimized, we turned to evaluation of the linearity of human liver microsomal VKOR activity in preparation for steady-state kinetic studies using the new protocols. As demonstrated in Figure 2.3 and Figure 2.11, the reduction of KO exhibits typical monophasic saturation kinetics that is consistent with one-site binding. Pooled human liver microsomes, (n = 10) were used to repeat some of the in vitro experiments that had been performed by earlier investigators to compare VKOR activity in rat liver with that of human liver

[57,96]. As shown in Figure 2.8, production of VK_1 was linear during the first 20 minutes of incubation. Figure 2.9 shows that the relationship between VK_1 formation and microsomal protein concentration, which is also linear up to 1.5 mg/mL. Reduction of KO was dependent on reaction temperature (Figure 2.10). VKOR activity reached a maximum at 30^{o}C above which enzyme activity dropped.

2.3.3 *VKORC1* Genotype vs. VKOR Activity

To investigate the mechanism by which epoxide reductase activity is regulated by *VKORC1* genotype, VKOR steady-state kinetics were evaluated in human liver microsomes representing each *VKORC1* haplotype group combination. The B/B liver microsomes (from high warfarin dose patients) displayed the highest maximal rate of reduction, the A/A liver microsomes (from low warfarin dose patients) exhibited the lowest rate, and the A/B liver microsomes reduced KO at an intermediate rate. Although *VKORC1* haplotype appears to correlate linearly with V_{max}, statistical analysis indicates that the degree of correlation is significant only between B/B and A/A groups, which differ by ~1.7-fold ($P < 0.5$) (Table 2.5). The kinetic constants characterizing the formation of VK_1 by each haplotype group combination are shown in Table 2.5. Unlike V_{max}, K_m values remain constant, independent of genotype.

2.3.4 *VKORC1* genotype vs. VKOR protein expression

The amount of VKOR protein was quantitated by immunoblot analysis in 3 pools each representing a different *VKORC1* haplotype group combination. The amount of VKOR protein in the B/B pool was approximately 1.5-fold higher than the amount in the A/A pool or A/B pool as

shown in Figure 2.12 and Table 2.6. According to a one-way ANOVA test for overall variance and the unpaired t-test, the difference between groups is statistically significant ($P < 0.05$).

2.4 Discussion

The purpose of these studies was to evaluate the hypothesis that warfarin dose response is dependent on transcript level of *VKORC1,* which in turn is directed by *VKORC1* haplotype [58,70]. Therefore, carriers of the *VKORC1* A haplotype, who exhibit reduced hepatic mRNA expression of *VKORC1,* would be expected to possess lower liver levels of VKOR protein and, therefore, have a diminished enzymatic capacity for KO reduction, the target of warfarin therapy. In the current study, we sought to test this by examining the downstream effect of altered mRNA expression through in vitro evaluation of VKOR activity and quantitation of VKOR protein in genotyped human liver microsomes.

Since the initial discovery of VKOR as the molecular target for warfarin's pharmacological properties [59,106], much effort has been devoted to characterizing this microsomal enzyme and its interaction with oral anticoagulants. Most of these early studies employed rat and bovine liver microsomes [60,61,88,107,108], due to their ready availability and the difficulties encountered in purification of the enzyme [41,62,63]. An initial characterization of human VKOR using liver biopsies from morbidly obese patients concluded that the human and rat enzymes had similar kinetic properties [64,65,96] [66,109]. For the studies described currently, we had access to a well characterized human liver bank containing tissue that had been obtained from otherwise healthy transplant donors [57,67,110] [68,69,111]. Thus initial experiments were directed towards characterization of VKOR activity from high quality human liver specimens.

A survey of the VKOR literature, much of it from the 1980s and 90s, revealed that a wide variety of different buffer systems have been used to prepare microsomal fractions for analysis of enzyme activity. As part of our assay optimization procedure we prepared several batches of microsomes from a single liver using different combinations of commonly used buffers. Only slight differences in enzyme activity were observed across the buffer combinations tested and so it was concluded that this is not a critical variable in the experimental design.

In order to improve the sensitivity and selectivity of VK_1 detection, we used a post-column reduction procedure that permits analyte detection as the highly fluorescent dihydroquinones. In preliminary studies with this assay, under conditions of product formation that were linear with respect to incubation time and protein concentration, K_m determination for human liver microsomal reduction of KO returned a value of 5 μM. These data are consistent with the small amount of pre-existing data for human VKOR in the literature [70,96] [70,103] [71,72,112] that used either biopsy or commercially available human liver microsomes. It should be noted that there are no literature reports of human VKOR in autopsy material, possibly due to the instability of VKOR activity as suggested by our finding that enzyme activity decreased substantially on repeated freezing and thawing of human liver microsomes. Consequently, all of our enzymatic studies were conducted on liver samples that were thawed and re-frozen no more than once.

Other variables in the assay procedure include DTT, the most common reducing agent used to drive this enzymatic reaction in microsomes, and detergent concentration. A DTT concentration of 2 mM was selected because it was the lowest concentration that saturated the enzyme, thereby providing a low background for the non-enzymatic reaction (Figure 2.11). The stimulating

effects of the detergent CHAPS is reminiscent of the 'latency' exhibited by UDPGA-dependent microsomal glucuronyl transferases (UGTs) [113]. The UGT active site is known to face the lumenal space of the endoplasmic reticulum and so treatment with detergents or the pore-former, alamethicin, is required to maximize microsomal activities by overcoming diffusional barriers for substrates and cofactors [45,114]. The membrane topology of VKOR is less well-defined than that of the UGTs [48,73,77], although a recent X-ray structure for a bacterial ortholog of the enzyme suggests that the active site is also lumenal [74,115]. That arrangement is true also for the eukaryotic enzyme is supported by alamethicin effectively being able to replace CHAPS in the in vitro assay.

Having established well-suited conditions for monitoring the reduction of KO in human liver microsomes, these new protocols were applied routinely to measure kinetic parameters of the reaction in a panel of 15 liver microsomes of known *VKORC1* genotype. The overall effect that haplotype had on maximal rates of KO reduction and VKOR protein expression in human liver microsomes emulates the linear relationship between *VKORC1* haplotype-directed mRNA expression and warfarin dose observed by Rieder et al.. [70]. While VKOR activity appears to be directed by haplotype, affinity of VKOR for KO does not, as suggested by K_m measurements of approximately 2 μM for the entire panel of livers. This is expected because the *VKORC1* haplotypes examined here do not change the coding-region of the protein. The trends observed here for V_{max} and K_m are consistent with VKOR protein synthesis and enzymatic activity regulation by *VKORC1* haplotypes occurring at the level of mRNA transcription.

Since the statistical correlation between haplotype and VKOR activity was not significant (P > 0.5) when the data was subjected to tests for global significance, we evaluated a number of scenarios that might have confounded the data analysis. First, human livers that yielded outlier rates of KO reduction (1 in the A/A cohort and 1 in the B/B cohort) (Figure 2.7), were resubmitted for DNA sequence analysis, but no new coding mutations in the exon regions were detected (data not shown) that might explain their anomalous enzyme activities. Secondly, the sample size was increased. The initial size of the genotyped panel had been capped at 15 livers based on the availability of tissues in the Liver Bank carrying the A/A genotype. Evaluating the activity of microsomes from all available livers (n = 48) at 50 μM KO, the substrate concentration at saturation, however, did not improve the P-value for significance (Table 2.8).

A tight correlation between activity and haplotype could be difficult to observe experimentally due to the role of other enzymes involved in the vitamin K system as modulators of VKOR in human liver micosomes. Numerous attempts to purify VKOR from animal liver microsomes with various detergents to achieve solubilization have also [14,42] [75,116] rendered the enzyme inactive leading to the conclusion that reductase activity may depend on lipid content and multiple proteins that are associated as a complex in the microsomes [41,76] 39, [32,117]. Proteins associated with microsomes that have been investigated as potential members of the 'VKOR enzyme complex' include calumenin [77,118] , microsomal epoxide hydrolase, and glutathione-S-transferase [41,48]. Recent work demonstrating that the activity of purified recombinantly expressed human VKOR can be restored in the presence of lipids argues against the requirement of the multi-enzyme complex for KO reduction in vitro [38,42]. (Lipids were

presumed to assemble into liposomes, act as membrane-like scaffolds in which the native structure of the active site is preserved).

The current consensus is that VKOR harbors a thioredoxin-like CXXC active site motif that is involved in reducing KO, an activity that can be stimulated in vitro by reducing the enzyme with DTT and other thiol reductants. These reductants serve the role of an endogenous reducing protein that has yet to be identified definitively. Strong evidence points towards endoplasmic reticular proteins in the thioredoxin family, such as protein disulfide isomerase [39,78,79] and thioredoxin [34,80,119]. If in vivo VKOR activity is associated with another protein (such as the physiological reductant), any variations in the regulation of that protein's gene or protein expression, stability, or interactions with VKOR could potentially mask the changes in the intrinsic activity that occur solely as a result of altered *VKORC1* mRNA expression.

The second measurable down-stream effect of changes in *VKORC1* mRNA transcript levels we detected in genotyped human liver microsomes was VKOR protein quantity. The impact that *VKORC1* haplotype had on protein expression paralleled the association between haplotype and either mRNA expression or activity. Protein levels were significantly correlated with haplotype group ($P < 0.05$) overall. Data from our preliminary kinetic studies in human liver microsomes and past reports of VKOR purification attempts suggest that VKOR activity is relatively labile and requires specific conditions to turn over substrate optimally. Therefore, a differential loss of enzymatic activity between livers could hinder the ability to obtain a strong relationship between the amount of enzyme present and its ability to turn over KO.

Normalization of reaction rates by the exact amount of VKOR present in the microsomes, rather than total microsomal protein, would presumably tease out the specific activity of VKOR and improve correlation with haplotype, but our attempts to quantitate the protein in 48 individual genotyped microsome samples with minimal variability proved to be too difficult by our methods. Therefore, we immunoblotted microsomal pools as the closest and most attainable alternate means of quantitation.

Regulation of VKOR activity by mRNA expression was also demonstrated in this study, by the linear relationship between *VKORC1* transcript levels in the liver and VKOR activity in microsomes that was observed in both human and bovine livers. Under the conditions optimized for microsome isolation and assessment of human liver microsomal VKOR activity, the difference in human and bovine VKOR activity that was observed in preliminary experiments (with aged and multiply thawed human liver microsomes) was reduced from 30-fold to 9-fold. (A 5-fold difference mRNA transcript level is much more consistent with a 9-fold difference in enzymatic activity). Furthermore, it is not surprising that the greatest differences in expression could be detected when experiments were conducted with the freshest bovine tissues available since quantitative real-time PCR experiments can be affected by RNA integrity [81,120].

In summary, these data report the first kinetic study of human VKOR activity by a panel of genotyped human liver microsomes. The influence that potential protein partners of VKOR have on activity is yet to be elucidated, but the results of the current study lend support to the theory that *VKORC1* haplotypes predict warfarin dose requirement by regulating mRNA expression of

VKORC1 and contribute to the mechanistic basis supporting genotyping as a clinical practice in the optimization of warfarin therapy.

TABLE 2.1: **Preliminary kinetic parameters of vitamin K epoxide reduction to vitamin K_1 by VKOR in human, rat, and bovine liver microsomes.** Saturation kinetic curves were best fit using a one-site binding model. Values represent the mean ± SEM for microsomes of each species. The value for each liver was obtained by taking the mean of 2 experiments.

Liver Microsomes	V_{max} (pmol/mg/min)	K_m (μM)	Cl_{int} (V_{max}/K_m)
Human (pooled n = 10)	11.5 ± 0.21	2.6 ± 0.23	4.4 ± 0.46
Rat (n = 1)	142 ± 6.06	1.6 ± 0.37	86.9 ± 23.5
Bovine (n = 1)	345 ± 11.7	3.2 ± 0.49	108 ± 20.4

TABLE 2.2: **Buffers used in human liver microsome isolation**. Each batch of microsomes was isolated from 10 grams of tissue from a single liver with the A/B *VKORC1* genotype. Buffer A: 20 mM Tris-HCl pH 7.4, 250 mM sucrose; B: 100 mM Tris pH 7.4, 150 mM KCl; C: 100 mM HEPES pH 7.4; D: 20% glycerol, 100 mM KPi pH 7.4, 0.1 mM EDTA.

Isolation Stage	Sequence 1	Sequence 2	Sequence 3	Sequence 4
Thaw/Homogenization	A	B	A	B
Wash	A	B	A	B
Storage	C	C	D	D

TABLE 2.3: **Relative quantification of *VKORC1* mRNA in various RNA preparations.** *The ratio of bovine to human levels was calculated using the $2^{-\Delta\Delta Ct}$ method with human liver 1 as a calibrator. The range of the difference derived from the standard deviations of $\Delta\Delta C_t$ is in ().

Source of total RNA	*Fold difference in VKOR mRNA expression relative to human liver	
	Human	Bovine
BioChain®	1.0	1.0 (0.6-1.4)
Flash-frozen liver	1.0	2.2 (1.7-3)

TABLE 2.4: **Relative quantification of *VKORC1* mRNA in flash-frozen human liver (UW) and bovine liver (Schenk) samples and their corresponding microsomal VKOR activities.** *The ratio of bovine to human levels and the ratio of human livers (2-6) to human liver 1 was calculated using the $2^{-\Delta\Delta Ct}$ method with human liver 1 as a calibrator. The range of the difference derived from the standard deviations of $\Delta\Delta C_t$ is in (). The rate of VK_1 production by liver microsomes prepared from flash-frozen tissue samples was measured as described in **Section 2.2.4**.

Total RNA (Flash-frozen)	*Fold difference in VKOR mRNA expression relative to human liver 1	VKOR activity at 50 μM KO (pmol/mg/min)
Human liver 1	1.0	11.3 ± 0.01
Human liver 2	7.5 (5.4-10.4)	27.1 ± 1.8
Human liver 3	2.1 (1.1-4.3)	4.5 ± 0.3
Human liver 4	1.5 (0.9-2.3)	15.1± 1.0
Human liver 5	2.2 (1.3-3.8)	18.2 ± 0.3
Human liver 6	4.4 (2.3-8.3)	29.6 ± 4.3
	3.54 (mean)	17.6 (mean)
Bovine liver 1	14.2 (10.6-19.1)	221.5 ± 6.7
Bovine liver 2	35.3 (19.7-63.1)	151.8 ± 15.5
Bovine liver 3	10.0 (7.4-13.6)	134.5 ± 16.2
Bovine liver 4	13.3 (9.8-18.0)	152.7 ± 17.2
	18.2 (mean)	165.1 (mean)

TABLE 2.5: **Kinetic parameters of KO reduction to VK_1 by VKOR in genotyped human liver microsomes.** Saturation kinetic curves were best fit using a one-site binding model. Values represent the mean ± SD for each *VKORC1* haplotype group combination (n = 5). The value for each liver was obtained by taking the mean of 2 experiments. Overall group differences in V_{max} were not significant according to one-way ANOVA where the statistical significance was taken as $P < 0.5$. According to the Student's t-test performed between A/A and B/B values, $*P < 0.5$.

VKORC1 Haplotype Group Combination	V_{max} (pmol/mg/min)	K_m (μM)	Cl_{int} (V_{max}/K_m)
A/A	25 ± 14	2.3 ± 0.36	11 ± 6.3
A/B	27 ± 9.2	2.2 ± 0.19	17 ± 5.1
B/B	42 ± 25	2.1 ± 0.43	*22 ± 16

TABLE 2.6: **Quantity of VKOR protein was significantly correlated with haplotype group combination according to a one-way ANOVA test with statistical significance set at P < 0.05.** According to the Student's t-test performed on A/A and B/B values, *P <0.01. The density of each VKOR band was normalized to that of the corresponding b-actin band. The data is presented as mean ± SD for each *VKORC1* haplotype group combination.

VKORC1 Haplotype Group Combination	Mean Band Density Ratio
A/A	1.4 ± 0.34
A/B	1.4 ± 0.20
B/B	2.0 ± 0.22*

TABLE 2.7: **Range of maximal rates of KO reduction to VK_1 by VKOR in genotyped human liver microsomes.** Saturation kinetic curves were best fit using a one-site binding model. For each liver, the reported value of V_{max} was obtained by taking the mean of rates from 2 experiments (each rate was within 25% of the mean). Outliers are in bold.

VKORC1 Haplotype Group Combination	HLM Sample ID	V_{max} (pmol/mg/min)
A/A	HLM-L102	25.9
	HLM-L114	13.6
	HLM-L128	**47.8**
	HLM-L132	17.9
	HLM-L158	18.1
A/B	HLM-L120	41.1
	HLM-L146	21.0
	HLM-L149	36.4
	HLM-L154	43.5
	HLM-L167	41.7
B/B	HLM-L118	38.7
	HLM-L133	79.2
	HLM-L140	39.7
	HLM-L144	**7.8**
	HLM-L156	44.0

TABLE 2.8: **Rate of KO reduction to VK_1 by VKOR in genotyped human liver microsomes (n = 48) at 50 µM KO.** Values represent the mean ± SD for each *VKORC1* haplotype group combination. The value for each liver was obtained by taking the mean of 2 experiments (each rate was within 25% of the mean). Overall group differences in V_{max} were not significant according to one-way ANOVA where the statistical significance was taken as $P < 0.5$. According to the Student's t-test performed between A/A and B/B values, *$P < 0.1$.

VKORC1 Haplotype Group Combination	Rate at 50 µM KO (pmol/mg/min)
A/A (n = 6)	11 ± 14.3
A/B (n = 17)	16 ± 7.8
B/B (n = 25)	17 ± 7.9*

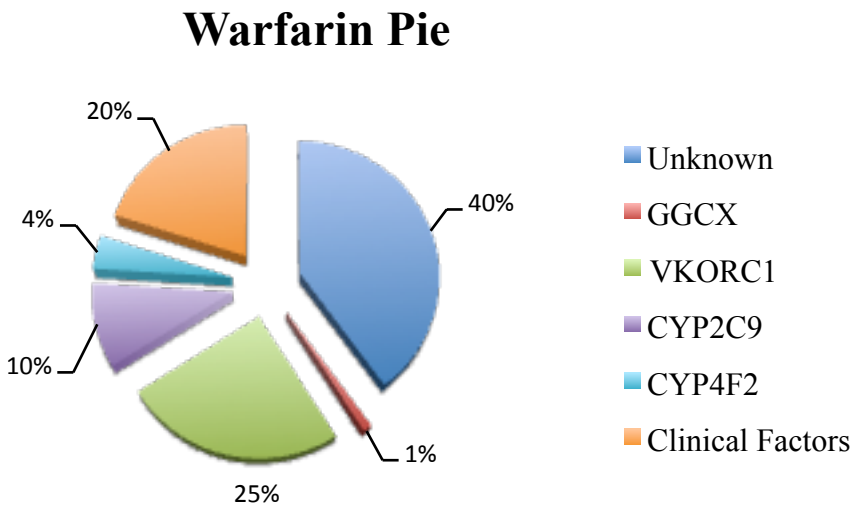

FIGURE 2.1: **The 'Warfarin Pie' showing the genetic and non-genetic factors that have been identified as determinants of warfarin maintenance dose.**

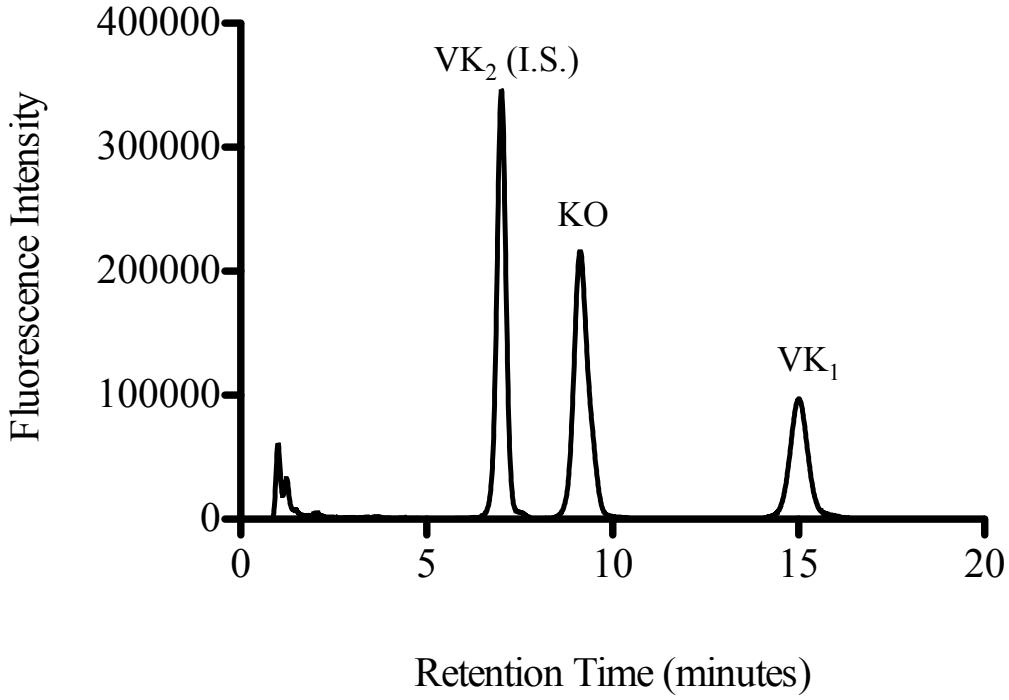

FIGURE 2.2: **Chromatographic separation of vitamin K analytes by HPLC with fluorescence detection**. VK_2, KO, and VK_1 peaks were resolved under the conditions described in **Section 2.2.5**.

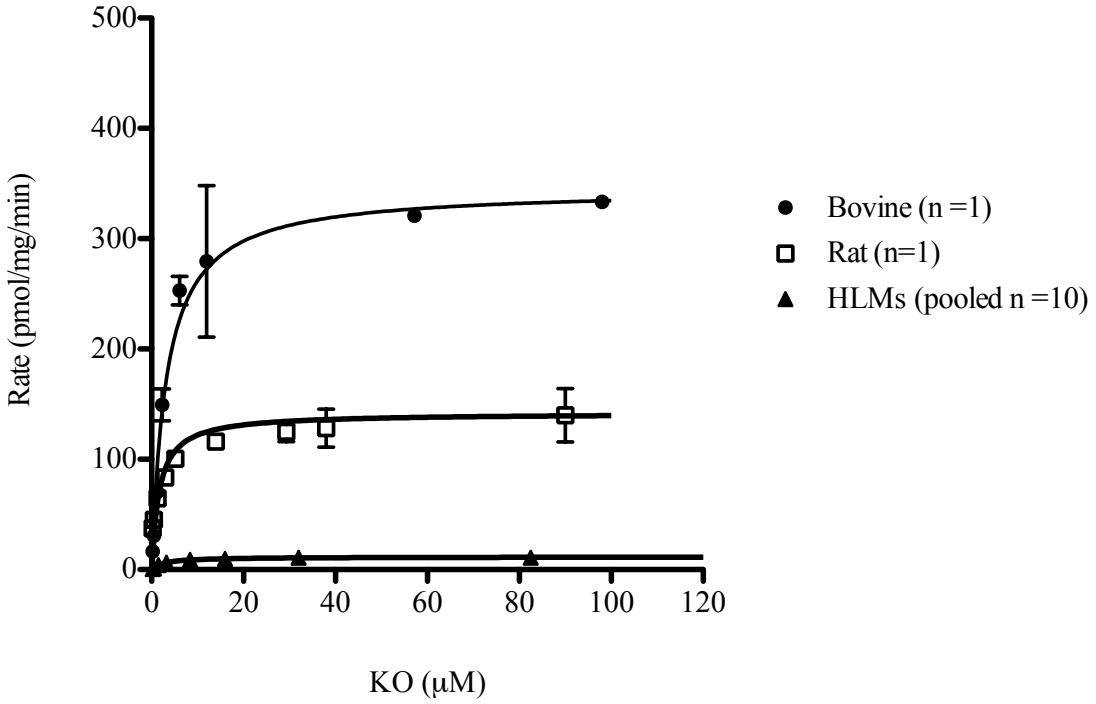

FIGURE 2.3: **Preliminary interspecies comparison of saturation kinetics of VK_1 formation from KO in liver microsomes.** Each data point represents the mean of duplicate measurements in a representative experiment (n = 2) and each error bar represents the standard error of the mean. Data presented on a substrate vs. rate plot was fit with the one-site binding model. Values for kinetic parameters were derived from the curve-fittings for each experiment are reported in Table 2.1 as the mean ± standard error of the mean.

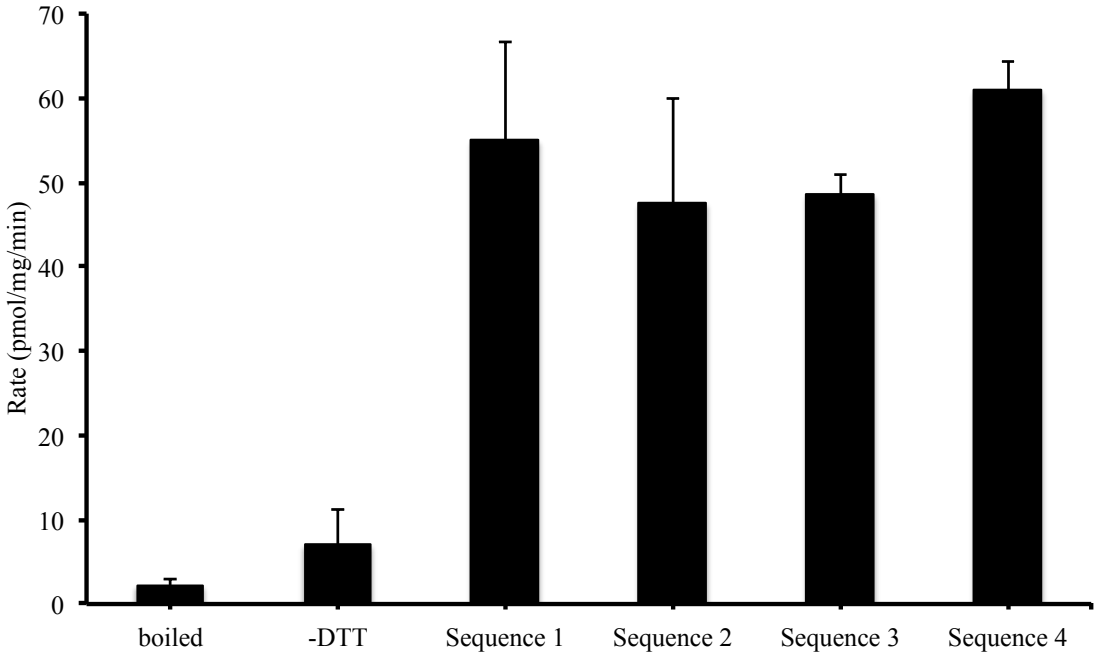

FIGURE 2.4: **Rates of VK_1 formation in human liver microsomes (Batch 1-4).** Human liver microsomes were incubated with 20 μM KO at 25°C in the presence of 2 mM DTT. The amount of VK_1 produced after 20 minutes was measured as described in **Section 2.2.4**. Each bar represents the mean of triplicate measurements and each error bar represents the standard deviation.

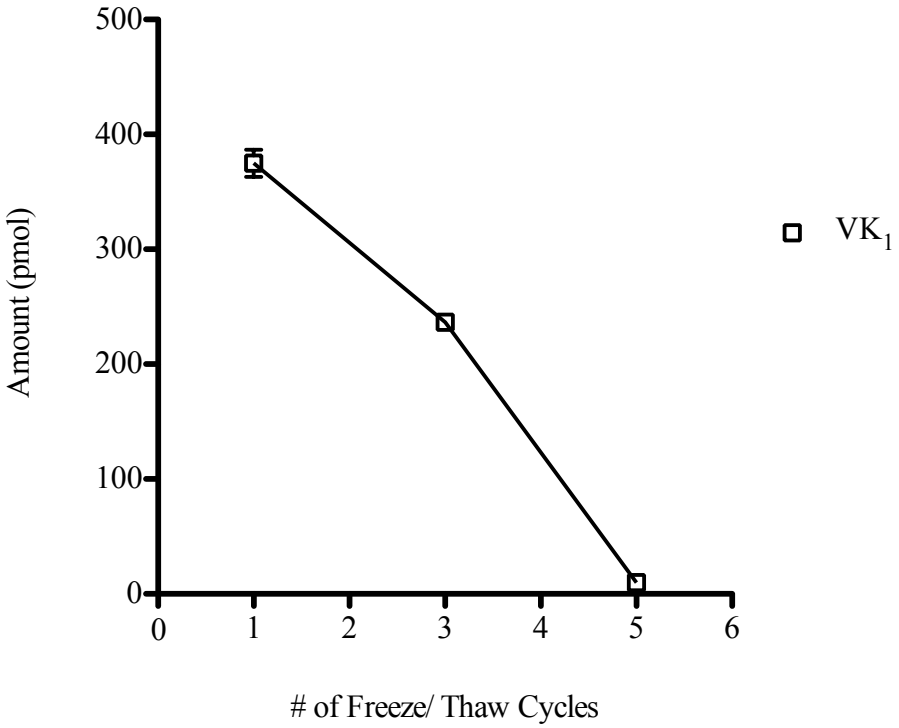

FIGURE 2.5: **Effect of freeze/thaw cycle number on the stability of VKOR activity in human liver microsomes.** Pooled human liver microsomes were incubated with 30 μM KO at 30°C after undergoing to 1, 3, or 5 freeze/thaw cycles. The amount of VK_1 produced after 20 minutes was measured as described in **Section 2.2.4**. Each data point represents the mean of duplicate measurements from a representative experiment (n =2) and each error bar represents standard error of the mean.

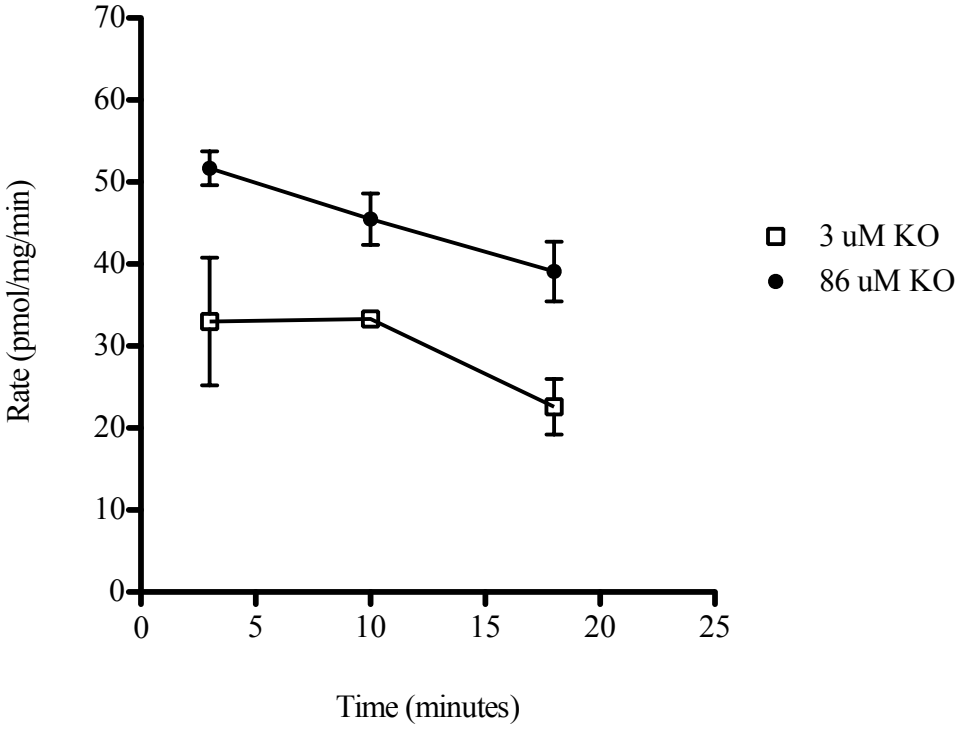

FIGURE 2.6: **Dependence of VKOR activity on pre-incubation time with 2 mM DTT.** Pooled human liver microsomes were incubated at 30°C for 3, 10, and 18 minutes prior to addition of 3.0 μM or 86 μM. The amount of VK_1 produced after 20 minutes was measured as described in **Section 2.2.4**. Each data point represents the mean of duplicate measurements from a representative experiment (n = 2) and each error bar represents standard error of the mean.

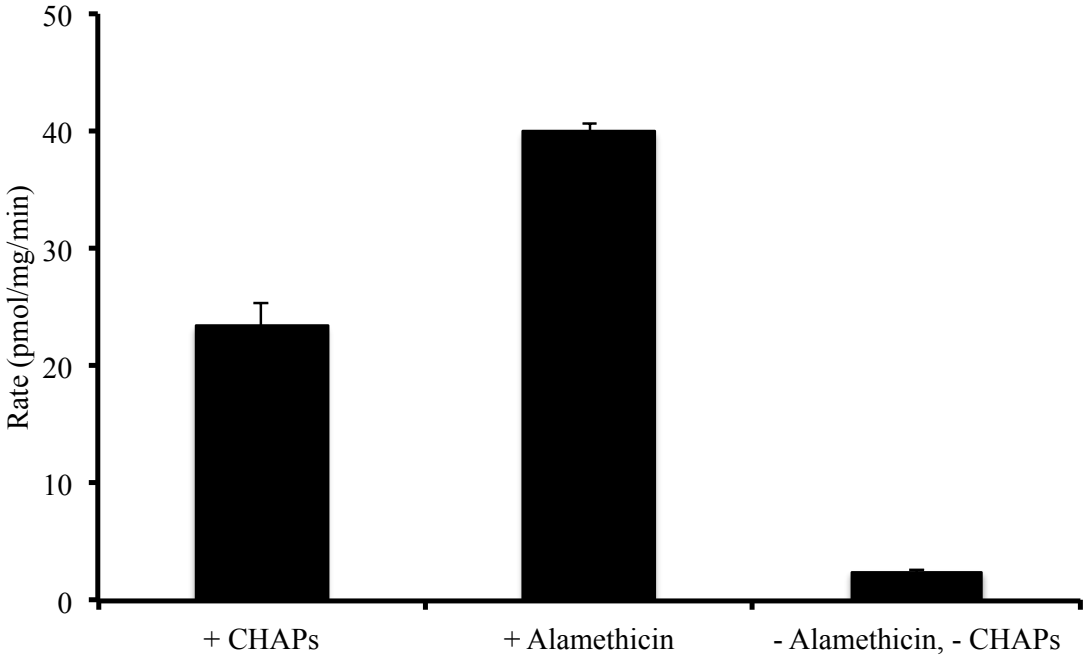

FIGURE 2.7: **Effects of CHAPS detergent and alamethicin on VKOR activity**. Pooled human liver microsomes diluted in reaction buffer containing CHAPS detergent (0.75% w/v), Alamethicin (0.05 mg/mL), or neither were incubated at 30°C with 50 μM KO. The amount of VK_1 produced after 20 minutes was measured as described in **Section 2.2.4**. Each bar represents the mean of triplicate measurements from a representative experiment (n=2) and the error bars represent standard deviations.

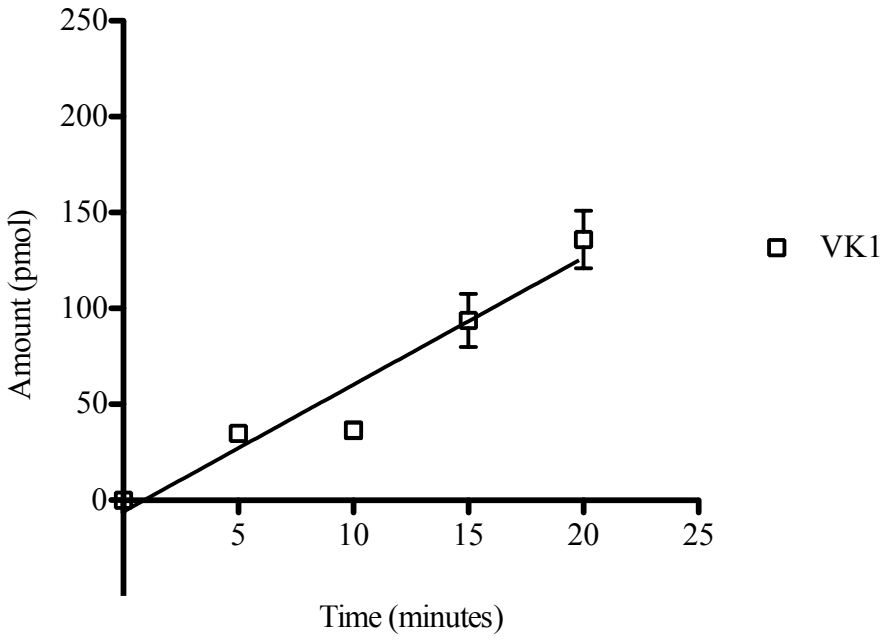

FIGURE 2.8: **Time-dependence of VK_1 production by VKOR in human liver microsomes.** Pooled human liver microsomes were incubated with 20 μM KO at 25°C for various incubation times at a fixed protein concentration of 1 mg/mL The amount of VK_1 produced after 0, 5, 10, 15, 20, and 25 minutes, was measured as described in **Section 2.2.4**. Each data point represents the mean of triplicate measurements in a representative experiment (n = 2) and each error bar represents the standard deviation. The data was fit with a linear regression model.

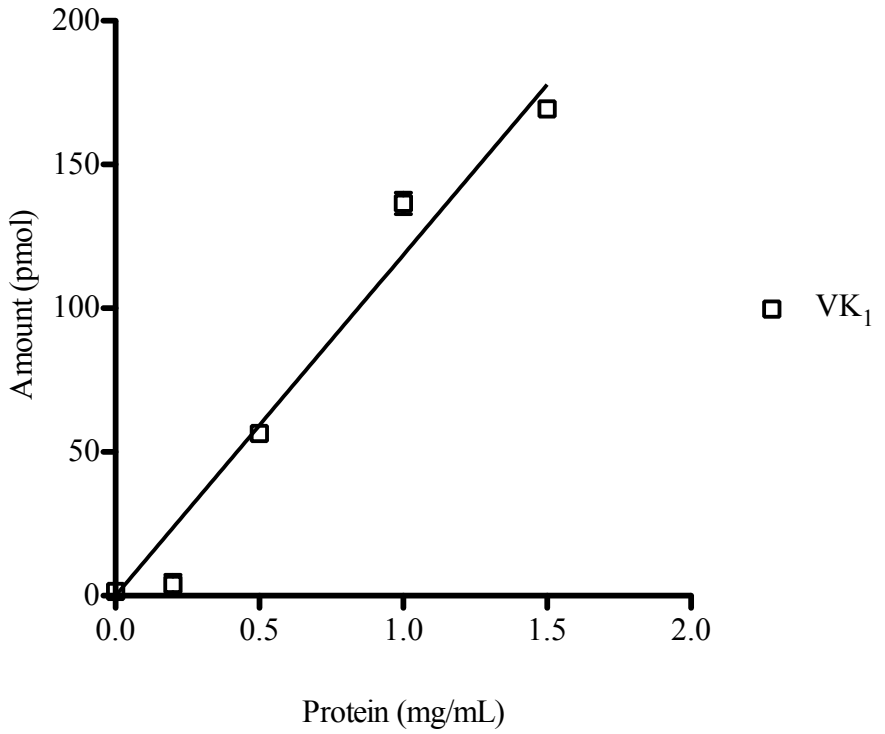

FIGURE 2.9: **Protein concentration-dependence of VK_1 production by VKOR in human liver microsomes.** Various amounts of microsomal protein were incubated with 20 μM KO at 25°C in a fixed volume. The amount of VK_1 produced after 20 minutes was measured as described in **Section 2.2.4**. Each data point represents the mean of triplicate measurements in a representative experiment (n = 2) and each error bar represents the standard deviation. The data was fit with a linear regression model.

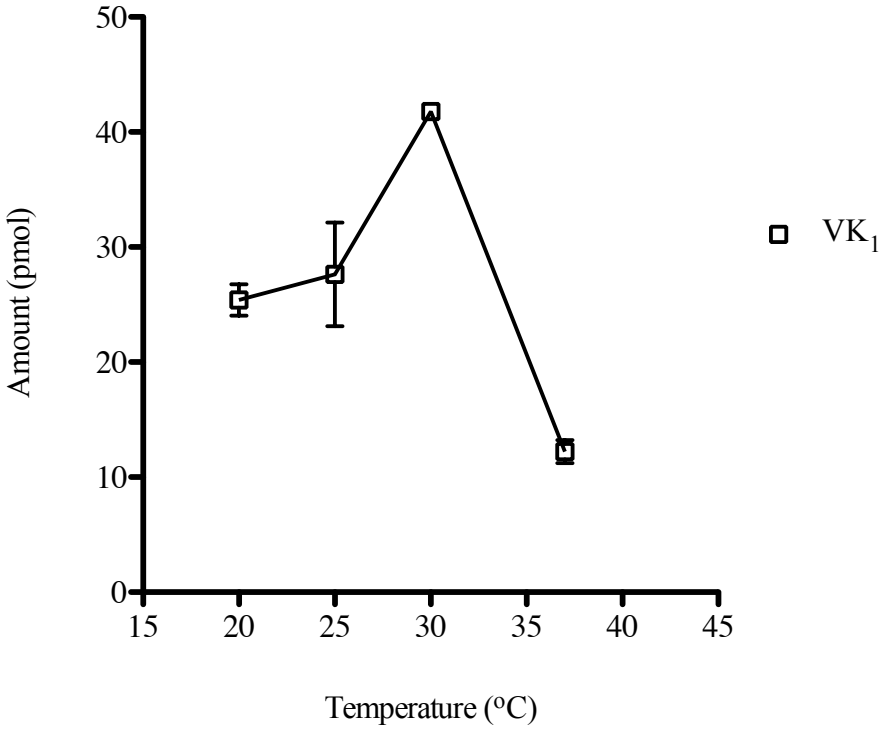

FIGURE 2.10: **Temperature-dependent formation of VK_1 by VKOR in human liver microsomes.** Pooled human liver microsomes containing 1 mg/mL protein and 30 μM KO were incubated at various temperatures. The amount of VK_1 produced after 20 minutes was measured as described in **Section 2.2.4**. Each data point represents the mean of triplicate measurements from a representative experiment (n =2) and the error bars represent standard deviations.

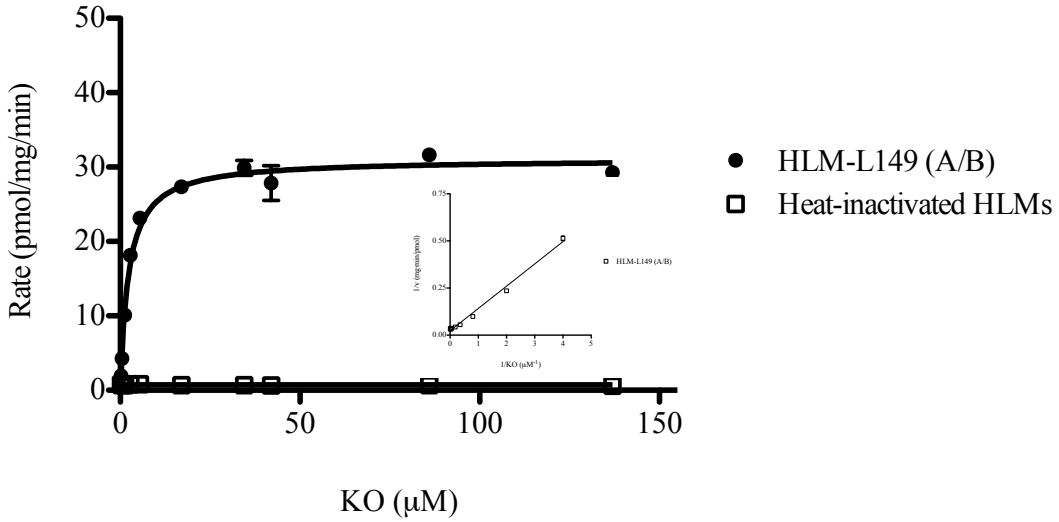

FIGURE 2.11: **Representative curve-fittings of VKOR kinetics exhibited by human liver microsomes with the A/B *VKORC1* genotype and human liver microsomes that were heat-inactivated.** The amount of VK_1 produced after 20 minutes was measured as described in **Section 2.2.4**. Each data point represents the mean of duplicate measurements in a representative experiment (n = 2) and each error bar represents the standard error of the mean. Data presented on a substrate vs. rate plot was fit with the one-site binding model. Data on a Lineweaver-Burk plot (inset) was fit with a linear regression model. Values for kinetic parameters were derived from the curve-fittings for each experiment and reported as the mean ± standard error of the mean.

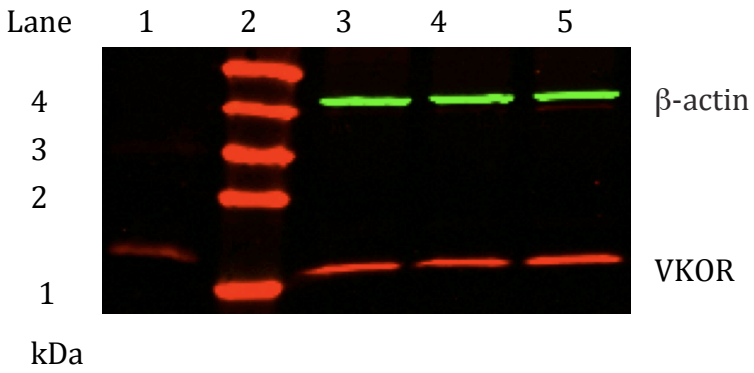

FIGURE 2.12**: Relative quantitation of VKOR protein in HLMs pooled according to *VKORC1* genotype.** Microsomes were immunoblotted with a VKORC1-specific antibody as described in **Section 2.2.10**. Each pool contains equal amounts of microsomal protein from livers representing each *VKORC1* haplotype group combination (A/A, n = 6; A/B, n = 17; B/B, n = 25). Lane 1 contains recombinantly expressed standard for VKOR (19 kDa). Lane 2 contains a molecular weight marker. Lanes 3, 4, and 5 contain 20 ug of protein from pools of A/A, A/B, and B/B microsomes respectively. In human liver microsomes, b-actin appears as a green band (42 kDa) while VKOR appears as a red band (18 kDa).

Chapter 3

An In Vitro Investigation of VKOR Inhibitory Mechanisms by Vitamin K Antagonists in Bovine Liver Microsomes

3.1 Introduction

The first series of vitamin K antagonists (VKAs) consisted of molecules derived from 4-hydroxycoumarin and were introduced as oral anticoagulant drugs and rodenticides during the 1940s [82]. Today, 4-hydroxycoumarins are the mainstay of oral anticoagulation therapy for the treatment and prevention of thromboembolic disorders [121]. In the US, there are two classes of vitamin K antagonists that have been approved by the Food and Drug Administration (FDA): 4-hydroxycoumarins (Figures 3.1-3.2) and 1,3-indanediones (Figure 3.3). For each class, a single drug can be prescribed in the US: warfarin (Figure 3.1D) the current drug of choice, and anisindione (Figure 3.3B), an alternative drug for patients that are intolerant to 4-hydroxycoumarins. The 1,3-indanedione anticoagulants are comprised of molecules with an aromatic diketone nucleus. Like 4-hydroxycoumarins, they possess variable side groups on the eastern half of the molecule. Both chemical classes are effective vitamin K antagonists due to their capacity for inhibiting VKOR [49]. However, the interaction between VKOR and warfarin has been the most extensively studied and appears to be multi-faceted. Conclusions regarding potential molecular mechanism(s) of VKOR inhibition have been drawn on the basis of a few key experimental observations about the interaction between warfarin and the rat form of the enzyme.

First, Fasco and coworkers discovered that rat liver microsomes that had been pre-treated with DTT exhibited VKOR activity that was insensitive to inhibition by warfarin (and other 4-hydroxycoumarins), and concluded that warfarin binds solely to the oxidized (disulfide) form of the enzyme [90].

Second, after observing that the inhibition of VKOR (both epoxide and quinone reductase activities) in warfarin-treated rat liver microsomes was not mitigated by dilution and repeated washing, Fasco and Principe concluded that warfarin binds to its target tightly and inhibits VKOR irreversibly [2]. A similar view was advanced by Silverman who postulated that 4-hydroxycoumarins and 1,3-indanediones were mechanism-based inactivators of VKOR on the basis of chemical studies that supported the idea that VKOR active site thiols might react with substrate ketones [86,87]. However, no evidence of covalent adduct formation between VKOR and VKAs was reported.

Lastly, Thijssen et al. observed that administration of unlabeled warfarin to rats that had been pre-treated with [^{14}C]-warfarin, led to an increase in the plasma radioactivity level. Moreover, liver microsomes prepared from rats pretreated with R- or S-[14C]-warfarin, released these compounds upon treatment with 10 mM DTT [122]. These authors concluded that warfarin binds tightly, not irreversibly, to VKOR, but could not rule out the possibility of a cytseinyl adduct formed between the enzyme active center and the inhibitor.

Historically, studies of VKAs have focused on 4-hydroxycoumarin derivatives, especially warfarin, probably because it is the mostly widely used oral anticoagulant worldwide. In fact,

there is only a single, recent report that compares the efficacy and kinetics of 1,3-indanedione and 4-hydroxycoumarin inhibition of rat liver VKOR [123]. Also, sporadic reports have appeared that various quinone structures perturb the vitamin K cycle [124-126] but no systematic analysis of the various chemical classes of VKA has been performed.

The purpose of the current study was to investigate the structure-activity relationships between the two major classes of VKAs and their anticoagulant activity, taking into account both reversible and irreversible mechanisms of VKOR inhibition as determinants of inhibitor potency. Therefore, the most commonly available agents from each chemical class were selected for our experiments, which were performed in bovine liver microsomes. Bovine liver microsomes were chosen as the enzyme source for these inhibition experiments because they had the highest basal activity among the various species investigated in Chapter 2.

3.2 Materials and Methods

3.2.1 Preparation of Chemical Solutions

KO and VK_2 stock solutions were prepared and stored as described in **Section 2.2.1-2.2.2.** Stock solutions of the following compounds were prepared in DMSO or methanol solvent and stored at -20^{o}C: racemic warfarin (Sigma, St. Louis, MO), R- and S-warfarin, acenocoumarol (American Custom Chemicals Corporation, San Diego, CA), diphacinone (Sigma, St. Louis, MO), chlorophacinone (ChemService, West Chester, PA), pindone (ChemService, West Chester, PA), valone (ChemService, West Chester, PA), brodifacoum (ChemService, West Chester, PA), racemic 4'-azido-warfarin (a gift from the Trager Lab at the University of Washington, Seattle, WA), R- and S-4'-azidowarfarin, and racemic 4'-azido-warfarin alcohol (prepared by reducing

racemic 4'-azido-warfarin with sodium borohydride), 2-hydroxy-1,4-napthoquinone (ChemService, West Chester, PA), lapachol (Sigma, St. Louis, MO), and vitamin E quinone (Tokyo Chemical Industry CO, LTD., Tokyo, Japan).

3.2.2 Chiral Separation of Warfarin (and 4'-Azidowarfarin) Enantiomers

To separate chiral enantiomers of warfarin (and 4'-azidowarfarin), a 10 mg/mL solution in DMSO was on loaded onto a chiral HPLC column (Pirkle (R,R) Whelk®-O1; 10 mm x 25 cm, 5 micron particle size; Regis, Morton Grove, IL). R- and S- warfarin, which were detected by UV absorbance at 257 nm and 308 nm (Shimadzu Diode Array Detector SPD-M10AVP, Kyoto, Japan), were eluted with an isocratic mobile phase of hexane and 60% acetic acid in ethanol at a flow rate of 2.5 mL/min (Shimadzu pump LC10ADVP, Kyoto, Japan). The R-enantiomer, which eluted at 10 minutes, and the S-enantiomer, which eluted at 20.5 minutes, were collected and dried mostly by rotary evaporation in a 40^{o}C water bath and subsequently under high vacuum at room temperature over night.

3.2.3 Preparation of Bovine Liver Microsomes

Bovine liver microsomes were isolated as described in **Section 2.2.3**, from frozen liver tissue purchased from Pel-Freez Biologicals® (Rogers, AR).

Preliminary IC_{50} Experiments

Microsomes reserved for performing replicate sets of kinetic experiments were stored as single-use aliquots containing enough protein for the number of reactions (plus 2 extra) in a single set. A fresh tube of microsomes was thawed on ice and the appropriate volumes of reaction buffer,

KO (to a final concentration of 5.2 μM) needed for a complete set of reactions, were added to create a master mix. The master mix was vortexed briefly and divided equally into 1.5 mL microcentrifuge tubes containing inhibitor over a range of concentrations (listed below). The samples were pre-incubated at 30^{o}C for 3 minutes before the reaction was initiated by adding DTT (2 mM final concentration unless otherwise indicated) and thereafter carried out according to the procedure described in **Section 2.2.4**. The rate of reaction exhibited by negative control reactions, which contained DMSO or methanol solvent, was defined as the rate in the absence of inhibitor. Final inhibitory concentrations tested for racemic warfarin and brodifacoum were 0 μM (negative control), 0.01 μM, 0.1 μM, 1.0 μM, 10 μM, and 100 μM. Final inhibitory concentrations tested for R-warfarin, S-warfarin, and acenocoumarol, were 0 μM (negative control), 0.01 μM, 0.02 μM, 0.05 μM, 0.1 μM, 0.2 μM, 0.5 μM, 1.0 μM, 2.0 μM, 5.0 μM, 10 μM, and 100 μM. Final inhibitory concentrations tested for valone were 0 nM (negative control), 0.2 nM, 2.0 nM, 10 nM, 20 nM, 50 nM, 100 nM, 200 nM, 500 nM, 1.0 μM, 5.0 μM, and 20 μM. Final inhibitory concentrations tested for diphacinone were 0 nM (negative control), 0.2 nM, 2.0 nM, 10 nM, 20 nM, 50 nM, 100 nM, 200 nM, 500 nM, 2.0 μM, and 5.0 μM. Final inhibitory concentrations tested for pindone and chlorophacinone were 0 nM (negative control), 0.2 nM, 2.0 nM, 10 nM, 20 nM, 50 nM, 100 nM, 200 nM, 500 nM, 1.0 μM, 2.0 μM, and 5.0 μM. Final inhibitory concentrations tested for 2-hydroxy-1,4-napthoquinone and lapachol were 0 nM, 2 nM, 10 nM, 20 nM, 50 nM, 100 nM, 200 nM, 500 nM, 1.0 μM, 2.0 μM, 5.0 μM, 10 μM, and 14 μM. Final inhibitory concentrations tested for vitamin E quinone were 0 μM (negative control), 10 nM, 100 nM, 1.0 μM, 10 μM, and 100 μM. The preliminary IC_{50} measurements were used to determine the inhibitor concentration range in subsequent K_i studies.

3.2.4 Determination of Reversible K_i

The initial-velocity steady-state kinetics of VKOR inhibition in bovine liver microsomes was evaluated by reacting the enzyme with a range of substrate (KO) concentrations (0.5 μM, 1.7 μM, 5 μM, and 15 μM) at different concentrations of inhibitor. Reaction mixtures were prepared as described in **Section 3.2.4**. K_i constants were determined for the following inhibitors: 1) racemic, R, and S-warfarin, 2) acenocoumarol 3) diphacinone, and 4) chlorophacinone. Final inhibitory concentrations tested for warfarin (racemic, R-, and S-) were 0 μM (negative control), 0.33 μM, 1.0 μM, and 3.0 μM. Final inhibitory concentrations tested for acenocoumarol were 0 μM (negative control), 0.33 μM, and 1.0 μM. Final inhibitory concentrations tested for diphacinone were 0 nM (negative control), 70 nM, 220 nM, and 650 nM. Final inhibitory concentrations tested for chlorophacinone were 0 nM (positive control), 15 nM, 45 nM, and 135 nM.

3.2.5 'Irreversible' Inhibition Experiments

Experiments that were performed to assess the degree of 'irreversible' inhibition of VKOR by 1) DMSO (negative control), 2) racemic warfarin, 3) acenocoumarol, 4) diphacinone, or 5) chlorophacinone in bovine liver microsomes were modeled after those previously described for warfarin and rat liver microsomal VKOR [2]. All of the following operations were performed on ice or at 4^{o}C. Two ultracentrifuge tubes, each containing 98 mg of bovine liver microsomal protein, were diluted with buffer A (200 mM Tris-HCl, 0.15 M KCl, pH 7.4) to 14 mL (a final protein concentration of 7 mg/mL). To the first tube, inhibitor was added to reach a final concentration of 10 μM and to the second tube, an equal volume of DMSO was added. The tubes were vortexed and incubated on ice for 1 hour. Two 2-mL aliquots were removed from each tube

and stored at -80^{o}C (reserved to be assayed for VKOR activity). After the remaining portions were diluted with: 1) buffer B (20 mM Tris-HCl, 0.15 M KCl, pH 7.4), 2) buffer B containing 20 mM DTT, 3) buffer B containing 4% BSA, or 4) buffer containing 4% BSA + 20 mM DTT, to fill the tubes, the microsomes were sedimented by centrifugation at 105,000 x g for 75 minutes in a Sorvall® Ultra80 ultracentrifuge (DuPont Instruments, Corp., Miami, FL). The supernatants were decanted, and the pellets were resuspended in buffer B by grinding as was described in **Section 2.2.3**. The microsomal protein pellet was re-sedimented. The previous pellet wash step was repeated twice with Buffer B (unless otherwise indicated). The final pellet was resuspended in 10 mL of buffer A. Total protein content of each sample was quantitated according to the BCA™ Protein Assay kit (Thermo Scientific, Rockford, IL) prior to assessment of VKOR activity. The rate of VK_1 production by each microsomal sample was assayed at a saturating substrate of concentration 80 μM KO according to the method previously described in **Section 2.2.4**.

3.2.6 Reverse Phase-HPLC Fluorescence Analysis

HPLC separation and quantification of VK_1 (product), KO (substrate), and VK_2 (internal standard) was performed as described in **Section 2.2.5**.

3.2.7 VK_1 Quantification and Calculations

Quantitation of VK_1 was conducted as described in **Section 2.2.8**. The rate of VK_1 production in bovine liver microsomes at each inhibitor concentration was calculated as pmol/min/mg microsomal protein. For the IC_{50} experiments, the reaction rate for each sample containing inhibitor was normalized to the mean rate of the negative control reaction (organic solvent

control) and converted to % activity. For the 'irreversible' inhibition experiments, each rate was normalized to the mean rate of the appropriate negative control (DMSO-treated microsomes, pre- or post- dilution and washing) and converted to % activity..

3.2.8 Analysis of Kinetic Data

GraphPad Prism, version 4.00, software for Windows (GraphPad Software, San Diego, CA), was used to plot and fit data points (each representing the mean of triplicate measurements). IC_{50} constants were calculated by non-linear regression curve-fitting of the data plotted as log (inhibitor concentration) vs. percentage of negative control reaction rate. The same software was used to generate Lineweaver-Burke plots (1/substrate concentration vs. 1/rate) and Dixon plots (1/inhibitor concentration vs. 1/rate), both of which were best fit by a linear regression equation. K_i values were derived from Dixon plots by calculating the mean x-intercept of the lines. Goodness of fit was evaluated by the R^2 value. Microsoft® Excel® for Mac (2011) was used to generate bar graphs.

3.3 Results

3.3.1 Preliminary IC_{50} experiments

A panel of available compounds that were known or potential VKAs (because of their structural resemblance to vitamin K) was screened for inhibitory activity against bovine liver VKOR. The compounds in this screen included derivatives of 4-hydroxycoumarin (warfarin, 4'-azidowarfarin, 4'-azidowarfarin alcohol, acenocoumarol, brodifacoum), 1,3-indanediones (valone, pindone, diphacinone, chlorophacinone), naphthoquinones (2-hydroxy-1,4-napthoquinone, lapachol), and Vitamin E quinone. Chemical structures of these compounds are

shown in Figures 3.1-3.5. All of the IC_{50} experiments were carried out in bovine liver microsomes at the approximate K_m of bovine VKOR (5.2 μM KO, which was reported in **Chapter 2**). All of the IC_{50} measurements are listed in Table 3.1.

Warfarin

The IC_{50} of racemic warfarin (Figure 3.1D) against bovine liver VKOR was 1.42 ± 0.1 μM (Figure 3.6). Under typical in vitro experimental conditions (2 mM DTT as the VKOR reductant), the individual enantiomers of warfarin were similarly potent (Figure 3.7). However, in the presence of very high DTT concentrations (42 mM), the potency of the S-isomer was 6-fold higher than that of the R-isomer (Figure 3.8).

Acenocoumarol

Acenocoumarol, which differs from warfarin by a nitro substituent at the para position of the phenyl ring (Figure 3.1E), is slightly more potent than warfarin as an inhibitor of bovine VKOR (Figure 3.6). The IC_{50} of acenocoumarol (racemic) was 0.84 ± 0.1 μM.

4'-Azidowarfarin and 4'-Azidowarfarin alcohol

The chemical structure of 4'-azidowarfarin and its alcohol derivative are shown in Figure 3.4. Addition of an azido group to the para position of the phenyl ring of warfarin produced a better VKOR inhibitor than warfarin itself (and acenocoumarol), in bovine liver microsomes. The IC_{50} of racemic 4'-azidowarfarin was 0.78 ± 0.01 μM (Figure 3.9). Furthermore, the mixture of diastereomeric 4'-azidowarfarin alcohols was about 2-fold less potent than 4'-azidowarfarin (Figure 3.9). Similar trends were observed in human liver microsomes (data not shown), in

which the IC_{50} of 4'-azidowarfarin alcohols and 4'-azidowarfarin was 0.85 ± 0.21 μM and 0.25 ± 0.02 μM respectively.

Brodifacoum

With an IC_{50} of 0.26 μM, the 'superwarfarin', brodifacoum (Figure 3.2B) is the strongest inhibitor of the 4-hydroxycoumarin derivatives examined in this study (Figure 3.6).

Valone and Pindone

Valone, a derivative of 1,3-indanedione with an isobutyl acetyl R-group on the 2-carbon (between the ketones) (Figure 3.3C), had an IC_{50} of 0.33 ± 0.02 μM (Figure 3.10). Structurally similar to valone, pindone, which possesses a tert-butyl group on the acetyl moiety (Figure 3.3D), had an IC_{50} of 37 ± 7 nM, and was approximately 8-fold more potent than valone (Figure 3.10).

Diphacinone and Chlorophacinone

Diphacinone (Figure 3.3E) was about 5 times less potent than its chlorinated analog, chlorophacinone (Figure 3.3F). The IC_{50} of chlorophacinone and diphacinone was 44 ± 3 nM and 0.21 ± 0.01 μM respectively (Figure 3.10).

2-Hydroxy-1,4-Naphthoquinone, Lapachol, and Vitamin E Quinone

Despite their structural resemblance to VK_1 (or KO) (Figure 3.5B), 2-hydroxy-1,4-naphthoquinone (Figure 3.5A) and lapachol (Figure 3.5C) were not nearly as effective as the 4-hydroxycoumarins or 1,3-indanediones as inhibitors of bovine liver VKOR activity. The IC_{50}

values for 2-hydroxy-1,4-naphthoquinone and lapachol were greater than 15 μM and 7 μM, respectively (data not shown). We also observed that vitamin E quinone (Figure 3.5D), was not an inhibitor of bovine VKOR at concentrations up to 50-100 uM (data not shown).

3.3.2 Reversible component of VKOR inhibition by vitamin K antagonists

Reversible inhibition of two compounds from each class of VKAs (marked with an '*' in Table 3.1) was characterized quantitatively by observing their effects on the kinetic parameters of VKOR. These changes were visualized graphically on Lineweaver-Burk plot (1/rate vs. 1/substrate concentration). Panel A of Figures 3.11-3.16 shows that the y-intercept of the regression line increased with increasing inhibitor concentration, indicating that the apparent V_{max}, or maximal reaction rate of the enzyme was reduced by the inhibitor and that the lines converged to the left of the y-axis at the same x-intercept, indicating that the K_m, or affinity of the enzyme for KO was unaffected by inhibitor binding. On the basis of these observations, warfarin, acenocoumarol, diphacinone, and chlorophacinone were classified as non-competitive, reversible inhibitors of VKOR with respect to KO.

To determine the dissociation constant, K_i for each inhibitor-enzyme pair, the experimental data was also represented on a Dixon plot (1/V vs. [I]) as shown in panel B of Figures 3.11-3.16. The K_i values, which were derived from the x-intercept of the lines, for the 4-hydroxycoumarins investigated were 1.05 ± 0.07 μM for racemic warfarin, 1.04 ± 0.44 μM for R-warfarin, 1.04 ± 0.49 μM for S-warfarin, and 0.35 ± 0.02 μM for acenocoumarol, with respect to KO. The K_i values for the 1,3-indanediones were 0.10 ± 0.03 μM for chlorophacinone, and 0.17 ± 0.06 μM for diphacinone, again with respect to KO.

3.3.3 'Irreversible' component of VKOR inhibition by vitamin K antagonists

Fasco and Principe first reported that the inhibition of rat liver VKOR by warfarin was irreversible [2]. Their protocol consisted of incubating rat liver microsomes with inhibitor, subsequently diluting several times with buffer to remove inhibitor from the microsomes, and finally assessing the level of remaining VKOR activity relative to the activity of unwashed microsomes. By this method, we demonstrated, in bovine liver microsomes, that Fasco's findings are reproducible for warfarin, and can be extended to the indanedione, chlorophacinone. Figure 3.17A shows that the extent of recovery of VKOR activity from warfarin or chlorophacinone inhibition by mere dilution with buffer B is minimal. However, application of Fasco's inhibitor removal method with a few modifications, produced different results. The effect that various buffer conditions had on VKOR activity after racemic warfarin or chlorophacinone inhibition is illustrated in Figure 3.17B-E and Figure 3.18. Figure 3.17B shows that adding 20 mM DTT (enzymatic activity was measurable up to 42 mM - data not shown), in the first dilution step restored most of the activity in the warfarin-treated microsomes, but left most of the VKOR activity in chlorophacinone-treated microsomes suppressed. As illustrated in Figure 3.17C, the effect of 4% BSA was roughly the same as DTT with respect to warfarin, but more pronounced with respect to chlorophacinone. Figure 3.18 shows that the combination of DTT and BSA in the first dilution step produced approximately the same results for warfarin as DTT or BSA individually. For chlorophacinone, however, the recovery of activity measured was intermediate between that obtained from DTT alone or BSA alone. Adding DTT and BSA to the first dilution step, and increasing the total number of wash steps, reduced the recovery of VKOR activity from either inhibitor (Figure 3.17D). Combining DTT and BSA in all wash steps did not significantly improve recovery of enzyme activity further, as illustrated in Figure 3.18. Table 3.1 reports the

difference between the percentage (of control VKOR activity) post-washing ($\%_{Post}$) and the percentage pre-washing ($\%_{Pre}$) (from the data illustrated in Figure 3.18). Contrary to the work of Fasco et al., we observed that VKOR activity of warfarin-, acenocoumarol-, diphacinone-, or chlorophacinone-inhibited microsomes was highly recoverable, but required 20 mM DTT or 4% BSA in the wash buffers. That said, complete recovery of enzyme activity was not obtained under any conditions, for any inhibitor. For each compound, the value of $\%_{Post}$ -$\%_{Pre}$ trended with the value of IC_{50}.

3.4 Discussion

Most of what is known about the molecular mechanism whereby vitamin K antagonists inhibit VKOR has emerged from the numerous studies that were centered around the interaction between VKOR and warfarin (the most clinically relevant of this drug class). During the 1980s, seemingly conflicting models were proposed based on separate accounts of reversible (in vivo) [127] and irreversible (chemical models (Silverman 1980) as well as in vitro and in vivo) inhibition of VKOR by warfarin [2,128]. In 1987, Thijssen proposed a model to account for the discrepancy between the reported in vitro and in vivo observations of warfarin inhibition [127], but its generality for the various classes of VKAs ,including the FDA-approved 1,3-indanediones, has not been investigated. A single mechanism whereby both 4-hydroxycoumarins and 1,3-indanediones can inactivate VKOR, was advanced by Silverman [87]. He proposed that, in the presence of a reduced active site, an active site nucleophile undergoes acylation by the inhibitor. Although Silverman was able to support this hypothesis using chemical models, no supporting enzymatic evidence (e.g. covalent adducts) was obtained.

Therefore, the primary purpose of these studies was to thoroughly characterize in vitro irreversible inhibition of VKOR by studying the behavior of multiple chemical classes of vitamin K antagonists. To ensure the highest control enzyme activities from which to assess chemical inhibition easily by the analytical method described in Chapter 2, these studies were conducted in bovine liver microsomes. First, a preliminary inhibitor screen was conducted in order to select the most potent compounds from each class for detailed study. Second, the in vitro kinetics of VKOR inhibition by the selected compounds was assessed to confirm that in vitro, reversible inhibitor binding is similar to what was previously observed for warfarin using rat liver microsomes. Finally, we compared the activity level of inhibitor-treated bovine liver microsomes before and after various treatments intended to remove inhibitor from the microsomes in an effort to understand how the extent of 'irreversible' VKOR inhibition changes under different in vitro conditions.

The results of our preliminary screen of known and potential inhibitors of bovine VKOR indicated that certain structural attributes significantly affect the inhibitory kinetic parameters (IC_{50}) determined in vitro. First of all, the lack of potency exhibited by vitamin E quinone, despite its resemblance to VK_1 (quinone moiety with a phytyl side chain), suggests that chemical inhibition of VKOR requires a bicyclic nucleus. This conclusion is supported by the observation that the extremely potent plant toxin, ferulenol, which possesses the same isoprenyl side chain as VK_1 and vitamin E quinone, on carbon-3 of its 4-hydroxycoumarin ring is a much stronger inhibitor than warfarin by ~22-fold [83].

Second, having a substituent on the eastern half of the bicyclic nucleus also appears to be an essential structural attribute for efficacy as demonstrated by the difference between the IC_{50} of 2-hydroxy-1,4-naphthoquinone and the IC_{50} of lapachol. Link's group also came to this conclusion after the discovery that neither unsubstituted 4-hydroxycoumarin nor 1,3-indanedione have the anticoagulant properties possessed by its substituted derivatives [129]. The fact that lapachol, a naphthoquinone that has a carbon-3 side chain comprised of a single isoprenyl unit, has a low potency relative to warfarin agrees with recent reported by Gebauer et al. concerning the effect of isoprenyl side chain length on the IC_{50} of ferulenol derivatives [83].

A third conclusion made from our preliminary experiments is that the 1,3 indanedione nucleus binds to the VKOR binding site more effectively than does the 4-hydroxycoumarin nucleus. The 1,3-indanediones, as a group, were considerably more potent reversible inhibitors than the 4-hydroxycoumarin derivatives examined. These results, obtained, using bovine liver microsomes as the enzyme source are, similar to previous vitro work conducted in rat liver microsomes [123].

It has been shown that inhibitor structural variation on the eastern half of 4-hydroxycoumarins is better tolerated than the western half [83,118] and that VKOR is not stereospecific for KO binding [44]. This suggested that the portion of the VKOR active site that accommodates the eastern side of the 4-hydroxycoumarin ring (or substrate) is the more capacious part of the binding site. However, this trend did not extend to the indanediones, where increasing size of the carbon-3 substituent of 4-hydroxycoumarin did not lead to led to a lower IC_{50} and K_i, and so VKA inhibitor potency must be driven by more than just the lipophilicity of the side-chains. Log P was poorly correlated with IC_{50} ($R^2 = 0.09$) for the compounds in this study.

The afore-mentioned structural requirements fit the model previously proposed to explain the substrate/inhibitor selectivity of VKOR binding [124,130], in which VKOR in the oxidized form binds to compounds that are structural analogs of the transition state of VKOR that exists for the reductive elimination step that occurs during the latter stages of the catalytic cycle [94,124].

Next, we focused on the strongest inhibitors of bovine liver VKOR (two 4-hydroxycoumarins and two 1,3-indanediones) in subsequent experiments, in order to explore reversible and irreversible mechanisms of inhibition. Non-competitive type inhibition kinetics (with respect to KO) were demonstrated by warfarin, acenocoumarol, diphacinone, and chlorophacinone in the current study. These results are consistent with what others have reported for warfarin-susceptible and resistant rats [123]. Non-competitive type inhibition supports Fasco's hypothesis that the substrate and inhibitor bind different oxidation states of the same VKOR active site.

At first glance, irreversible inhibition also appeared to be a general phenomenon that occurs for all of inhibitors studied based on results obtained by replicating Fasco and Principe's reversal methodology in bovine liver microsomes (shown in Figure 3.17A). Taking into consideration the work of Thijssen et al. [122], and the affinity for VKOR that 4-hydroxycoumarin and 1,3-indanediones have exhibited [131,132], we modified the wash conditions previously employed by Fasco and Principe and made the following observations regarding the VKOR activity of warfarin- and/or chlorophacinone-inhibited bovine liver microsomes: 1) 4% BSA and 20 mM DTT individually and equally effectively partially reverse warfarin inhibition, 2) 1,3-indanedione inhibition is reversed in the presence of 4% BSA, but is resistant to the effect of 20 mM DTT, 3) the response to 4% BSA and 20 mM DTT is not synergistic, 4) recovery of VKOR activity

cannot be improved by subjecting the microsomes to additional numbers of wash steps, and 5) maximal inhibitor removal occurs during the first dilution. Based on our observations of the selected 4-hydroxycoumarins and 1,3-indanediones, we present a model (as a modified version of Thijssen's [127] in Figure 3.19, which illustrates the chemical equilibrium that exists between the bound and unbound states of an inhibitor/VKOR in the presence or absence of 4% BSA and/or 20 mM DTT during the first wash step.

In the absence of DTT or BSA, the association of **B,** the oxidized form of the VKOR and free inhibitor is favored to form **A**, as demonstrated by the reversible K_i (Table 3.1) as well as the minimal recovery of microsomal reductase activity from inhibition by mere dilution. Catalytically active VKOR, however requires that the enzyme be in the reduced state, **C**, to which KO binds with a higher affinity than the oxidized state [90]. This model illustrates the possible pathways by which **A,** the inactive and inhibitor-bound state of VKOR is converted to **C**, the active and unbound state under the experimental conditions.

We propose that at a high concentration, DTT, which is a competitive inhibitor of VKOR with respect to warfarin (data not shown), reduces the VKOR active site and releases the inhibitor (which has a much lower affinity for the reduced than oxidized state) almost simultaneously. The dramatic increase in activity exhibited after warfarin-treated microsomes were washed with 20 mM DTT (in the first dilution step) suggests that this is the pathway by which VKOR reactivation occurs. The difference between the results for warfarin shown in Figures 3.17A and 3.17B are consistent with the increased amount of radioactivity that was released by diluting [^{14}C]-warfarin-bound rat liver microsomes with buffer containing high amounts of DTT ([127].

The reduction of **B,** the unbound oxidized form of VKOR to **C,** is a less favored pathway because it depends on the dissociation of **A**. In the presence of BSA, the equilibrium between **A** and **B** is driven towards **B**, the unbound oxidized state of VKOR, because of the high affinity of free inhibitor (4-hydroxycoumarins and 1,3-indanediones) to BSA. Under in vitro KO turnover conditions (2 mM DTT), **B** is reduced to **C.** The ability of BSA was to effectively remove inhibitor from the active site was demonstrated by the greater extent of VKOR activity recovered from warfarin- and chlorophacinone-treated microsomes by washing with BSA (Figure 3.17C) than with buffer alone.

The findings presented here do not support Fasco and Principe's general conclusion that warfarin inhibits VKOR irreversibly. They also do not support the mechanism of covalent modification to VKOR by vitamin K antagonists that was proposed by Silverman (on account of the fact that even if chlorophacinone inhibition is irreversible, it occurs under oxidized active site conditions). Our results do agree, however, with the work of Thijssen and Baars, who demonstrated that a much higher concentration of DTT than 2 mM (the standard used for in vitro experiments) was required to more accurately simulate the efficiency of the endogenous reductant in vivo [127]. They proposed that in vivo, the 4-hydroxycoumarin-enzyme complex dissociates upon reactivation of the active site by an endogenous reductant and re-associates when the enzyme becomes re-oxidized during substrate reduction. Therefore, when the active site is complexed with 4-hydroxycoumarin, the rate of active site reduction (and KO turnover) is greatly retarded, but not blocked irreversibly. This model can also be used to explain the basis for the in vivo stereoselectivity of warfarin inhibition. Our comparison of the stereoselectivity of warfarin inhibition in bovine liver microsomes at 2 mM and 42 mM DTT indicated that S-warfarin was a

better VKOR inhibitor only at high DTT concentrations that likely better simulate the efficiency of the in vivo reductant. This parallels the faster release of R-warfarin, compared to S-warfarin, from the binding site of rat VKOR [122]. Our inability to recover 100% VKOR activity under any of the wash conditions also may stem from the difference between the efficiency of VKOR reduction by low concentrations of DTT (2 mM) that was routinely used to analyze baseline activity and by the in vivo reductant. (All in vitro assays for VKOR activity were performed at 2 mM DTT, at which saturating kinetics was observed by our lab and others [38]).

Based on our study of available 4-hydroxycoumarins and 1,3-indanedione compounds, we conclude that VKAs are not irreversible VKOR inhibitors in the strict sense, but are primarily tight-binding, reversible inhibitors of VKOR, at least in bovine liver microsomes. A direct relationship between the extent of 'irreversibility' and potency was evident for potent inhibitors selected from each chemical class of vitamin K antagonist. Expanding the variety and size of our panel of inhibitors as well as the methods of inhibitor removal in future studies will help us to identify structural features that distinguish or are shared by the two classes are determinants of inhibitor potency.

Table 3.1: **Calculated parameters describing the inhibition of VKOR in bovine liver microsomes by various compounds.**

Compound	IC_{50} (μM)	SEM	K_i (μM)	SD	** $\%_{Post}$ -$\%_{Pre}$
4-hydroxycoumarins					
***Warfarin**					
2 mM DTT					
R,S	1.42	0.10	1.05	0.07	58
R	0.95	0.04	1.04	0.44	
S	1.16	0.05	1.04	0.49	
42 mM DTT					
R	33.88	3.77	-	-	
S	5.50	1.33	-	-	
4'-Azidowarfarin					
R,S	0.78	0.01	-	-	
R	-	-	-	-	
S	-	-	-	-	
R,S-OH	1.68	0.15	-	-	
***Acenocoumarol**	0.84	0.10	0.35	0.02	16
Brodifacoum	0.26	0.00	-	-	
1,3-Indanediones					
Pindone	0.037	0.007	-	-	
Valone	0.33	0.02	-	-	
***Chlorophacinone**	0.044	0.003	0.10	0.03	21
***Diphacinone**	0.21	0.01	0.17	0.06	44
Naphthoquinones					
2-hydroxy-1,4-napthoquinone	>15				
Lapachol	7.00				
Vitamine E quinone	~100				

** Difference between inhibitor post-wash and 10 μM inhibitor bar graph values on Figure 3.18.

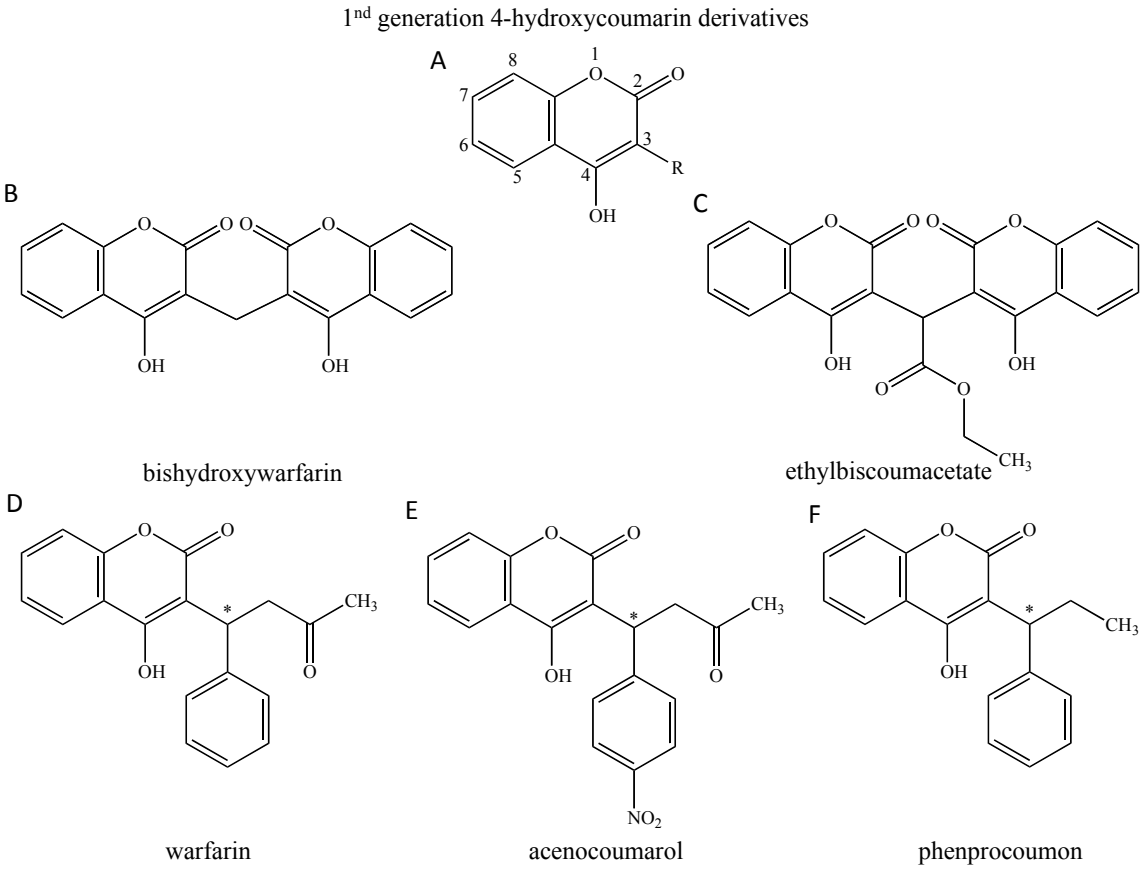

FIGURE 3.1: **Chemical structures and common names of first generation derivatives of (A) 4-hydroxycoumarin that are used as oral anticoagulants pharmaceutically worldwide.** Asymmetric carbons are marked with an '*.' Trade names are (B) Dicumarol,® (C) Tromexan,® (D) Coumadin,® (E) Sintrom,® and (F) Marcoumar.®

2nd generation 4-hydroxycoumarin derivatives

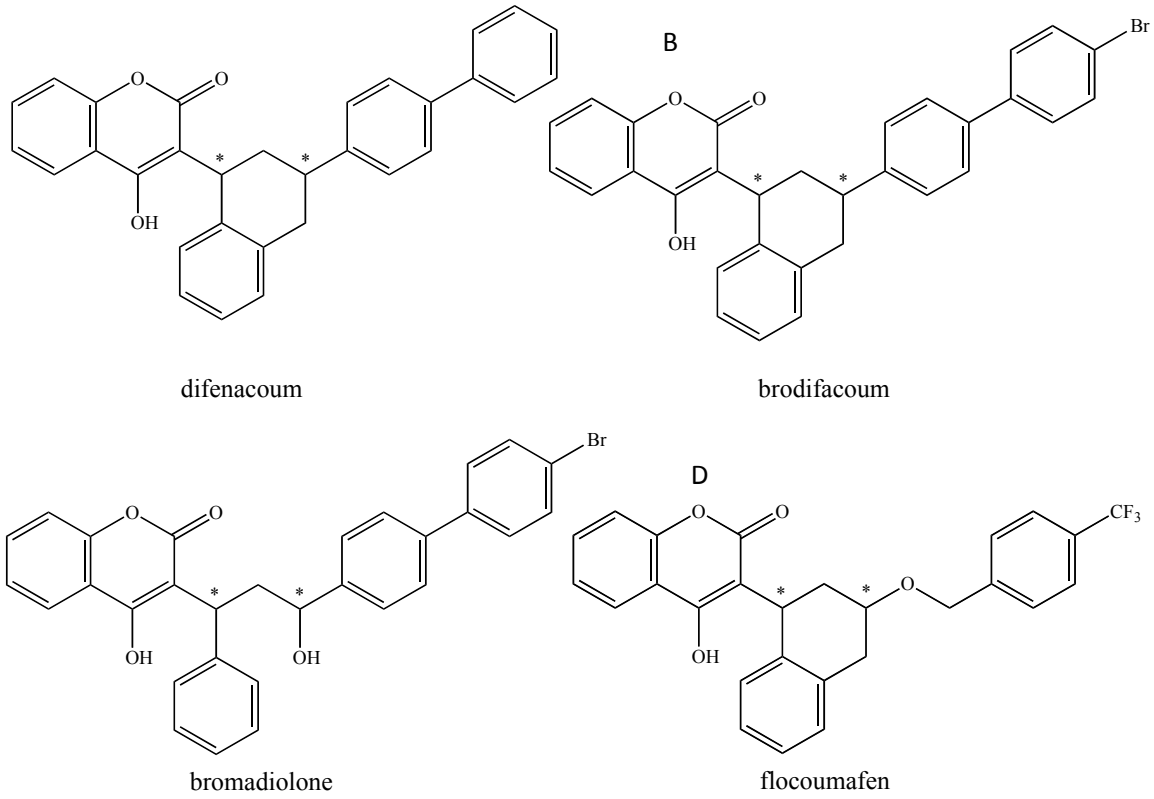

FIGURE 3.2: **Chemical structures and common names of second generation derivatives of 4-hydroxycoumarin that are used as rodenticides.** Asymmetric carbons are marked with an '*.' Trade names are (A) Compo,® (B) Finale,® (C) Apobas,® and (D) Stratagem.®

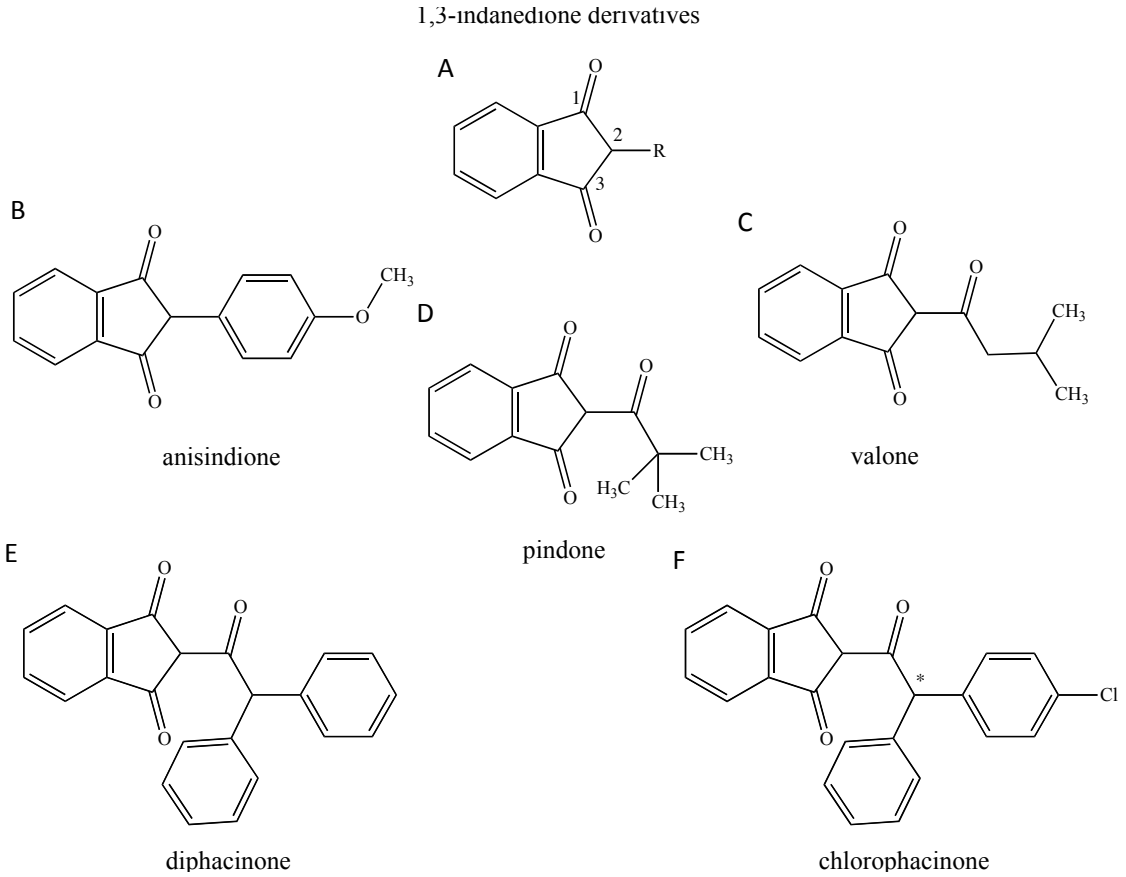

FIGURE 3.3: **Chemical structures and common names of derivatives of (A) 1,3-indanedione that are used as anticoagulants in humans and rats.** Asymmetric carbons are marked with an '*'. Trade names are (B) Miradon,® (C) Motomco trading powder,® (D) Pival,® (E) Diphacine,® and (F) Caid.®

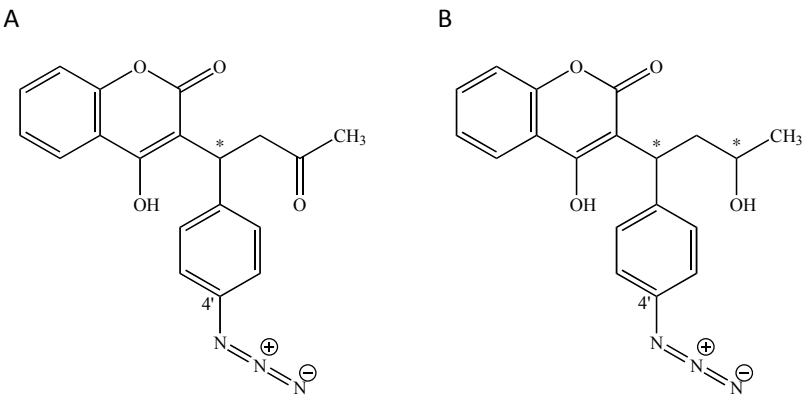

FIGURE 3.4: **Chemical structures of 4'-Azidowarfarin and 4'-Azidowarfarin alcohol.** Asymmetric carbons are marked with an '*.'

A

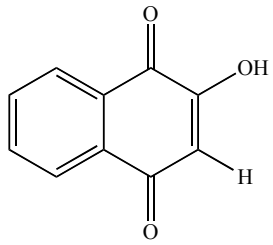

2-hydroxy-1,4-napthoquinone

B

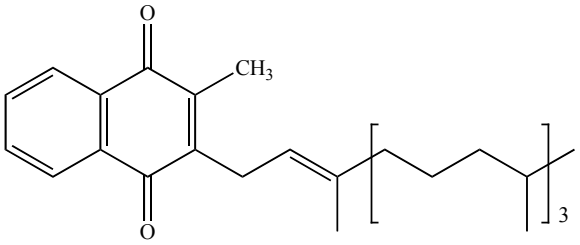

vitamin K_1

C

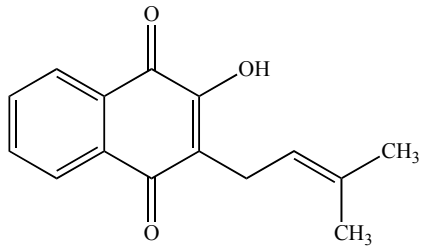

lapachol

D

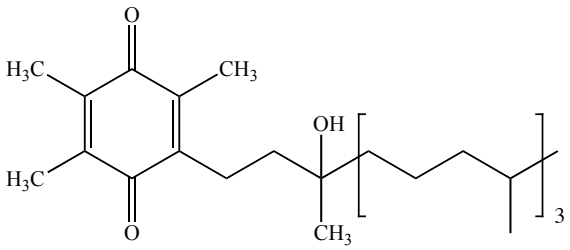

vitamin E quinone

FIGURE 3.5: **Chemical structures of naphthoquinones (A-C) and vitamin E quinone. (D).**

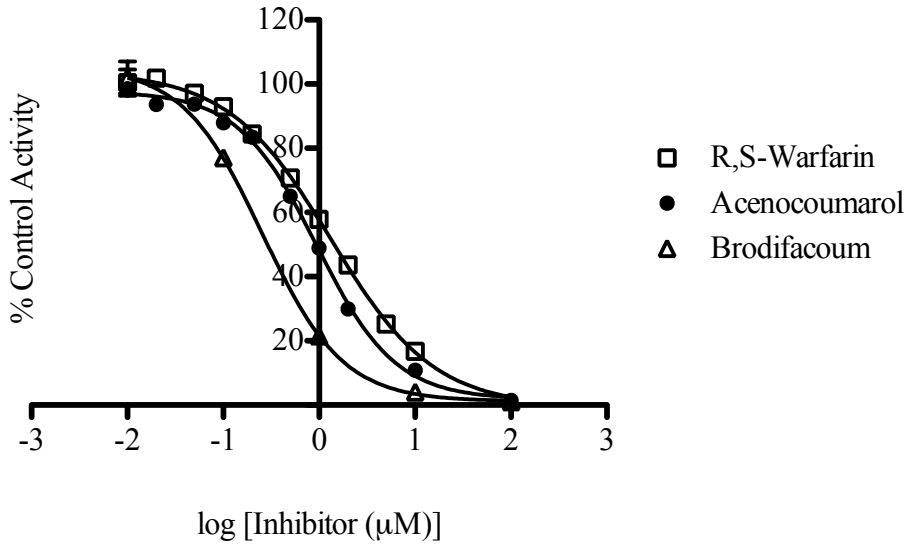

FIGURE 3.6: **Inhibition of VKOR in bovine liver microsomes by 4-hydroxycoumarins.** Data points represent the mean of triplicate measurements from a representative experiment and error bars represent standard deviations. IC_{50} values were calculated by fitting the data with a sigmoidal dose-response (variable slope) equation. The mean IC_{50} and the standard error of the mean of two experiments performed with each inhibitor are listed in Table 3.1.

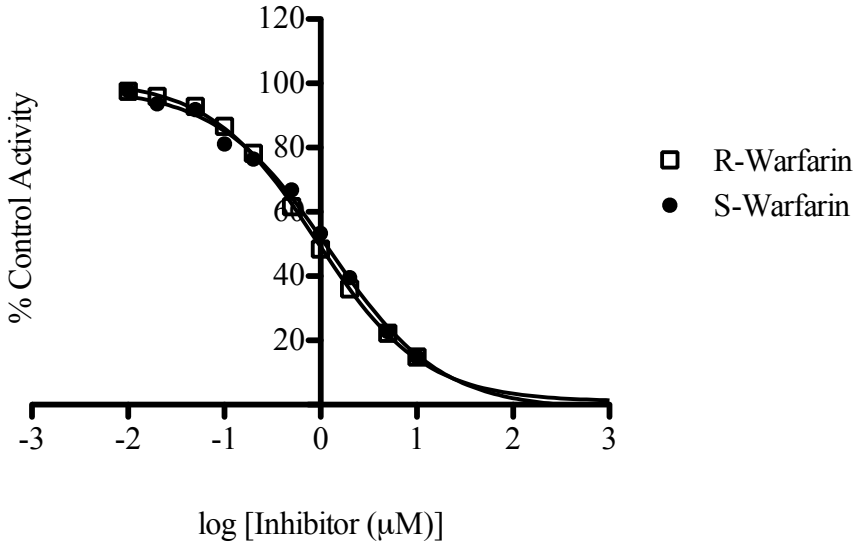

FIGURE 3.7: **Inhibition of VKOR in bovine liver microsomes by individual enantiomers of warfarin in the presence of 2 mM DTT.** Data points represent the mean of triplicate measurements from a representative experiment and error bars represent standard deviations. IC_{50} values were calculated by fitting the data with a sigmoidal dose-response (variable slope) equation. The mean IC_{50} and the standard error of the mean of two experiments performed with each inhibitor are listed in Table 3.1.

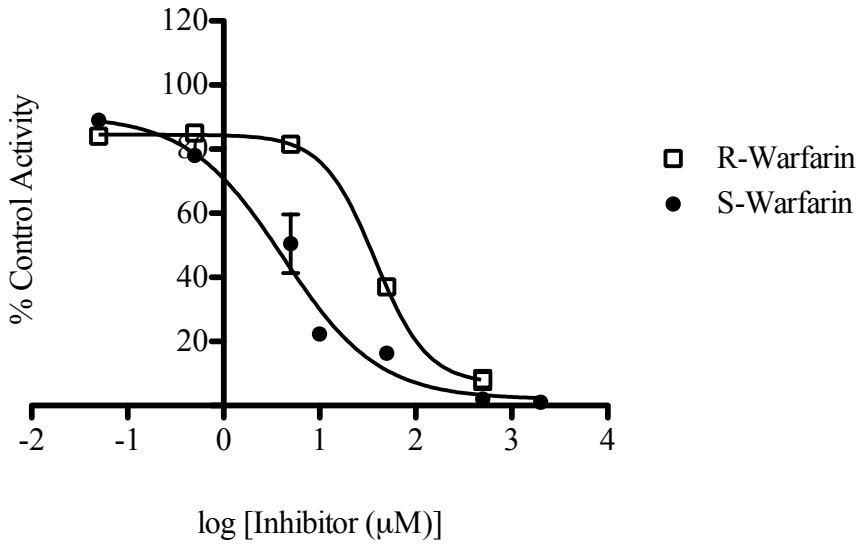

FIGURE 3.8: **Stereoselective Inhibition of VKOR in bovine liver microsomes by warfarin enantiomers in the presence of 42 mM DTT.** Data points represent the mean of triplicate measurements from a representative experiment and error bars represent standard deviations. IC_{50} values were calculated by fitting the data with a sigmoidal dose-response (variable slope) equation. The mean IC_{50} and the standard error of the mean of two experiments performed with each inhibitor are listed in Table 3.1.

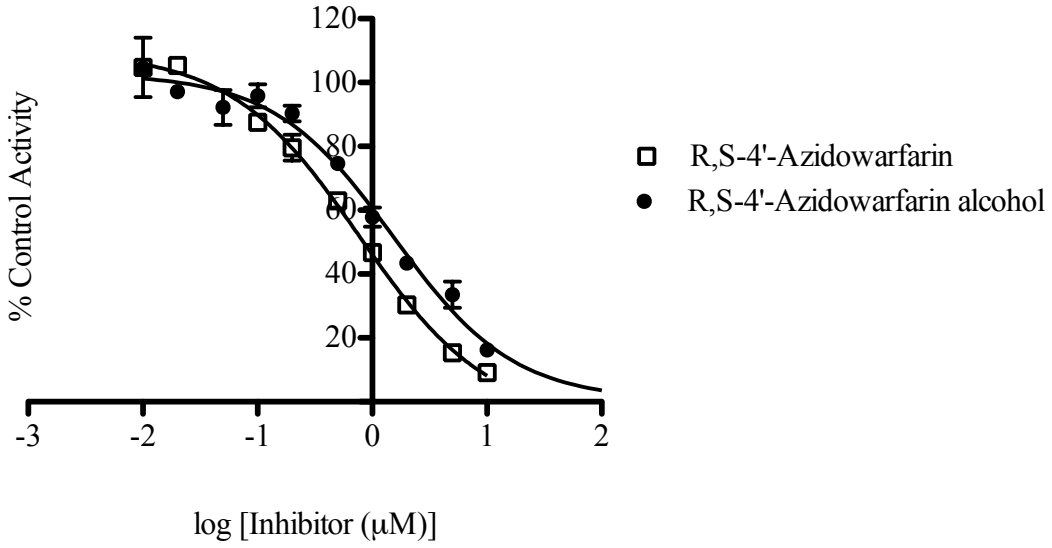

FIGURE 3.9: **Inhibition of VKOR in bovine liver microsomes by racemic 4'-azidowarfarin and racemic 4'-azidowarfarin alcohols.** Data points represent the mean of triplicate measurements from a representative experiment and error bars represent standard deviations. IC_{50} values were calculated by fitting the data with a sigmoidal dose-response (variable slope) equation. The mean IC_{50} and the standard error of the mean of two experiments performed with each inhibitor are listed in Table 3.1.

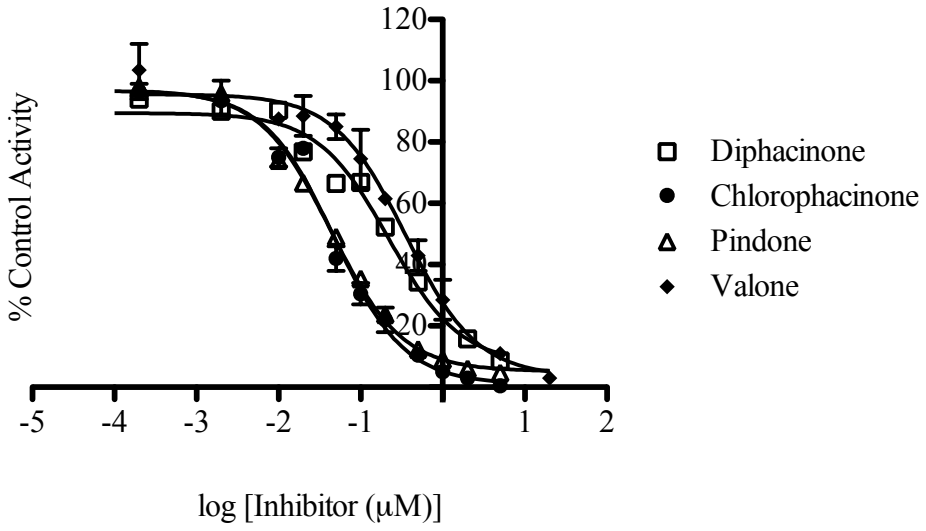

FIGURE 3.10: **Inhibition of VKOR in bovine liver microsomes by 1,3-indanedione derivatives.** Data points represent the mean of triplicate measurements from a representative experiment and error bars represent standard deviations. IC_{50} values were calculated by fitting the data with a sigmoidal dose-response (variable slope) equation. The mean IC_{50} and the standard error of the mean of two experiments performed with each inhibitor are listed in Table 3.1.

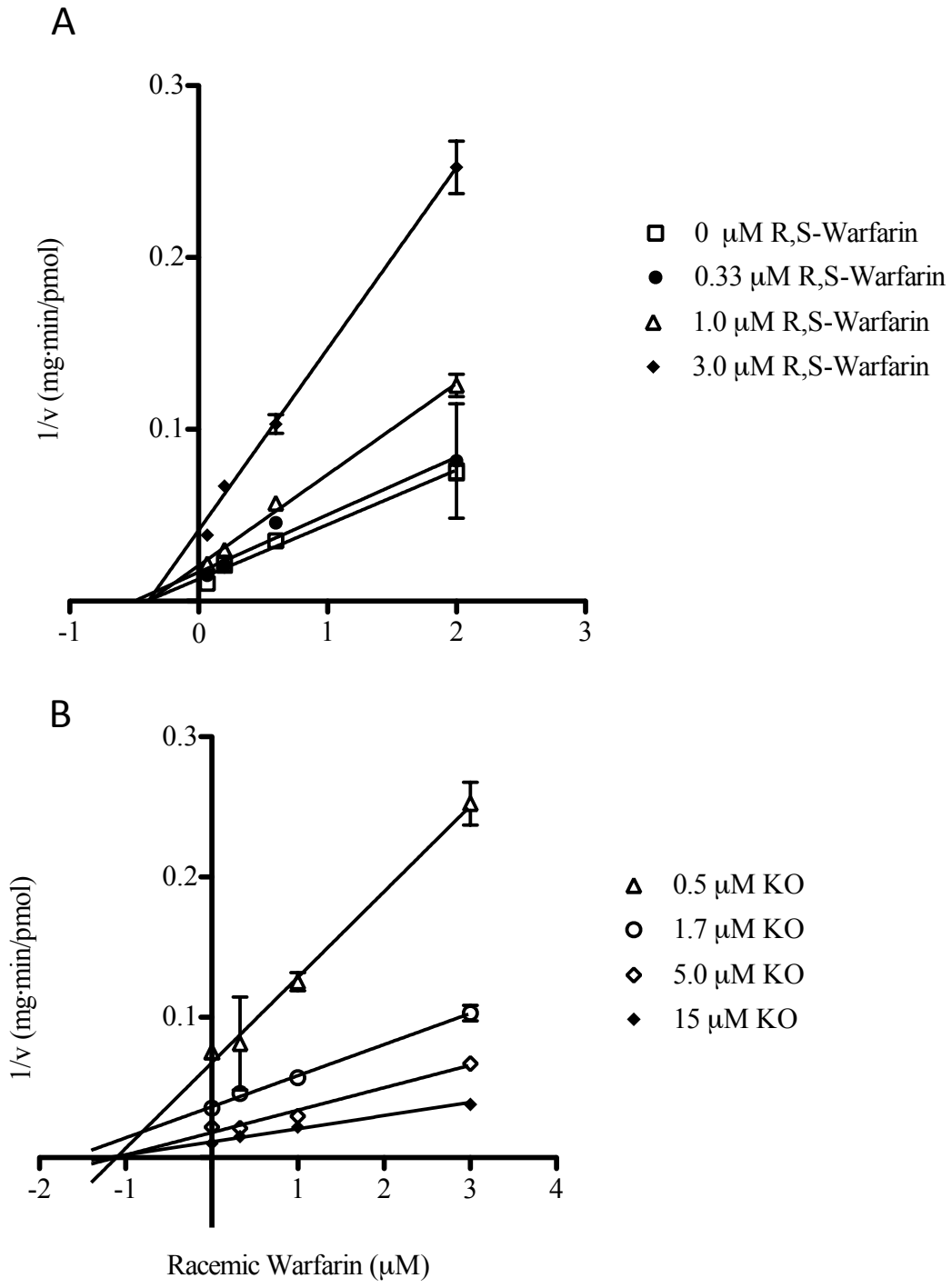

FIGURE 3.11: **(A)** Lineweaver-Burk plot describing VKOR activity at various concentrations of KO (0.5, 1.7, 5.0, and 15 μM) in the presence of 0, 0.33, 1.0, and 3.0 μM racemic warfarin incubated with bovine liver microsomes (0.5 mg/mL). Data points represent the mean of triplicate measurements and error bars represent standard deviations. The data is also presented on a **(B)** Dixon plot, from which the value of K_i was deduced. The K_i for racemic warfarin is listed in the Table 3.1.

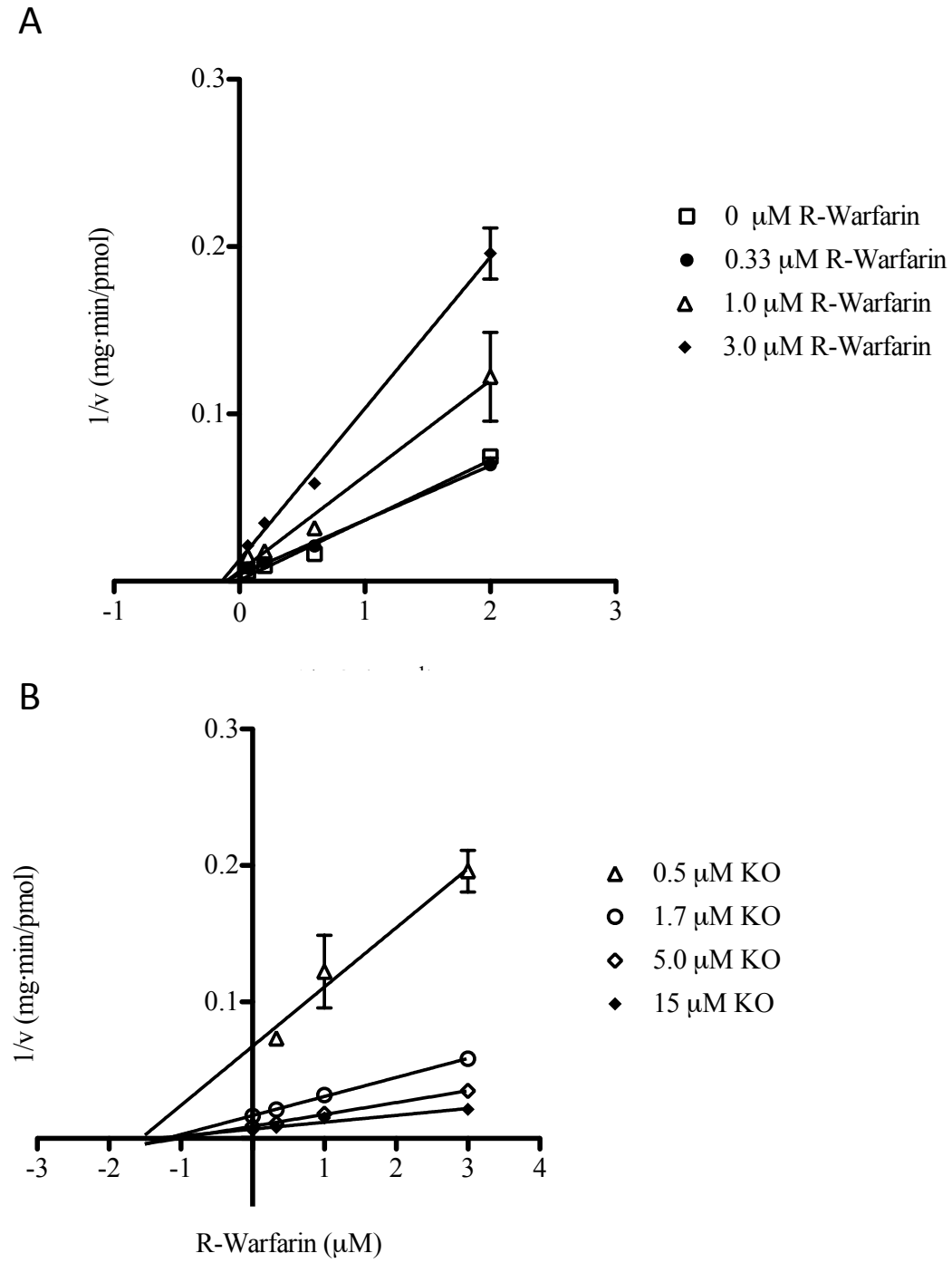

FIGURE 3.12: **(A)** Lineweaver-Burk plot describing VKOR activity at various concentrations of KO (0.5, 1.7, 5.0, and 15 μM) in the presence of 0, 0.33, 1.0, and 3.0 μM R-warfarin incubated with bovine liver microsomes (0.5 mg/mL). Data points represent the mean of triplicate measurements and error bars represent standard deviations. The data is also presented on a **(B)** Dixon plot, from which the value of K_i was deduced. The K_i for R-warfarin is listed in the Table 3.1.

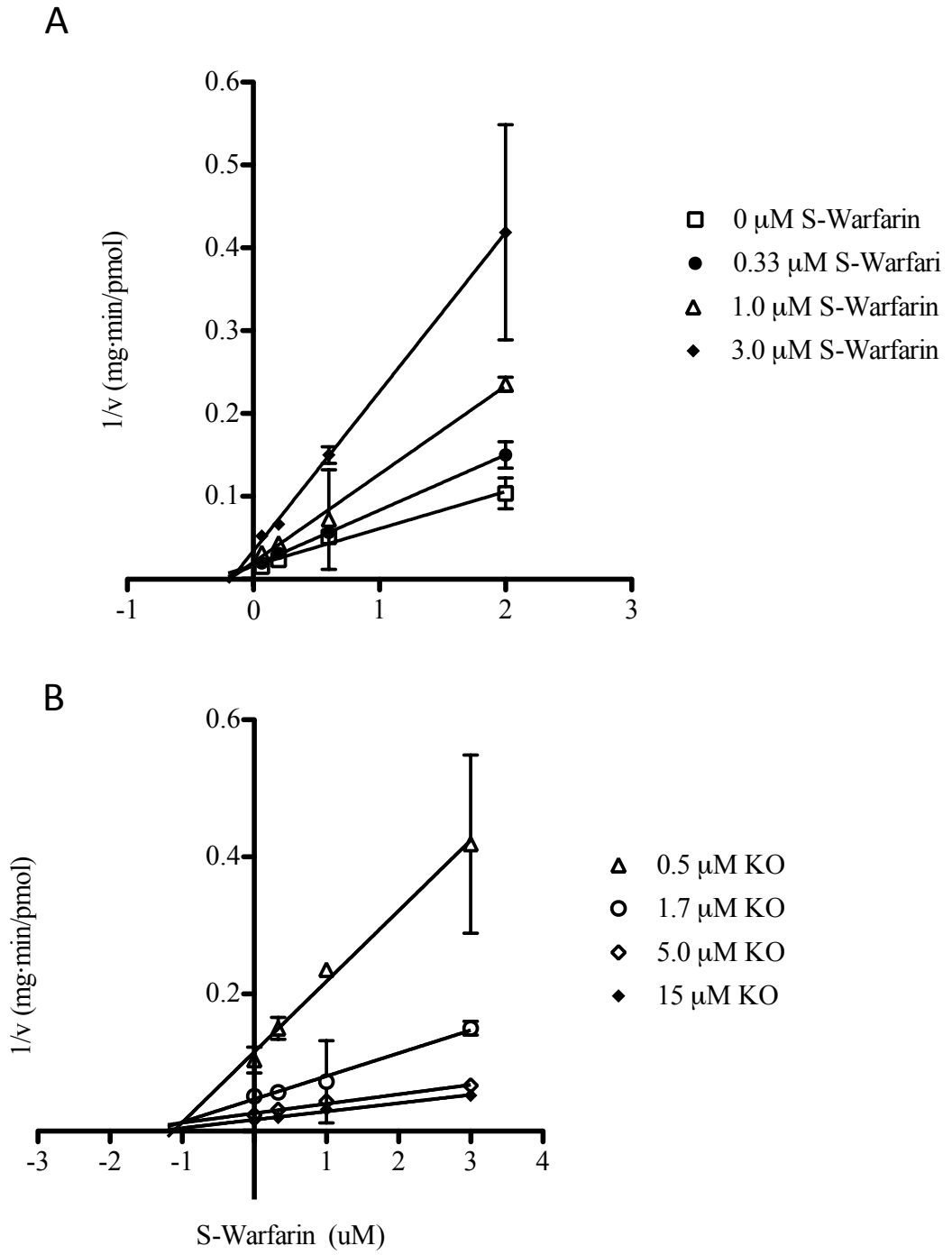

FIGURE 3.13: **(A)** Lineweaver-Burk plot describing VKOR activity at various concentrations of KO (0.5, 1.7, 5.0, and 15 μM) in the presence of 0, 0.33, 1.0, and 3.0 μM S-warfarin incubated with bovine liver microsomes (0.5 mg/mL). Data points represent the mean of triplicate measurements and error bars represent standard deviations. The data is also presented on a **(B)** Dixon plot, from which the value of K_i was deduced. The K_i for S-warfarin is listed in the Table 3.1.

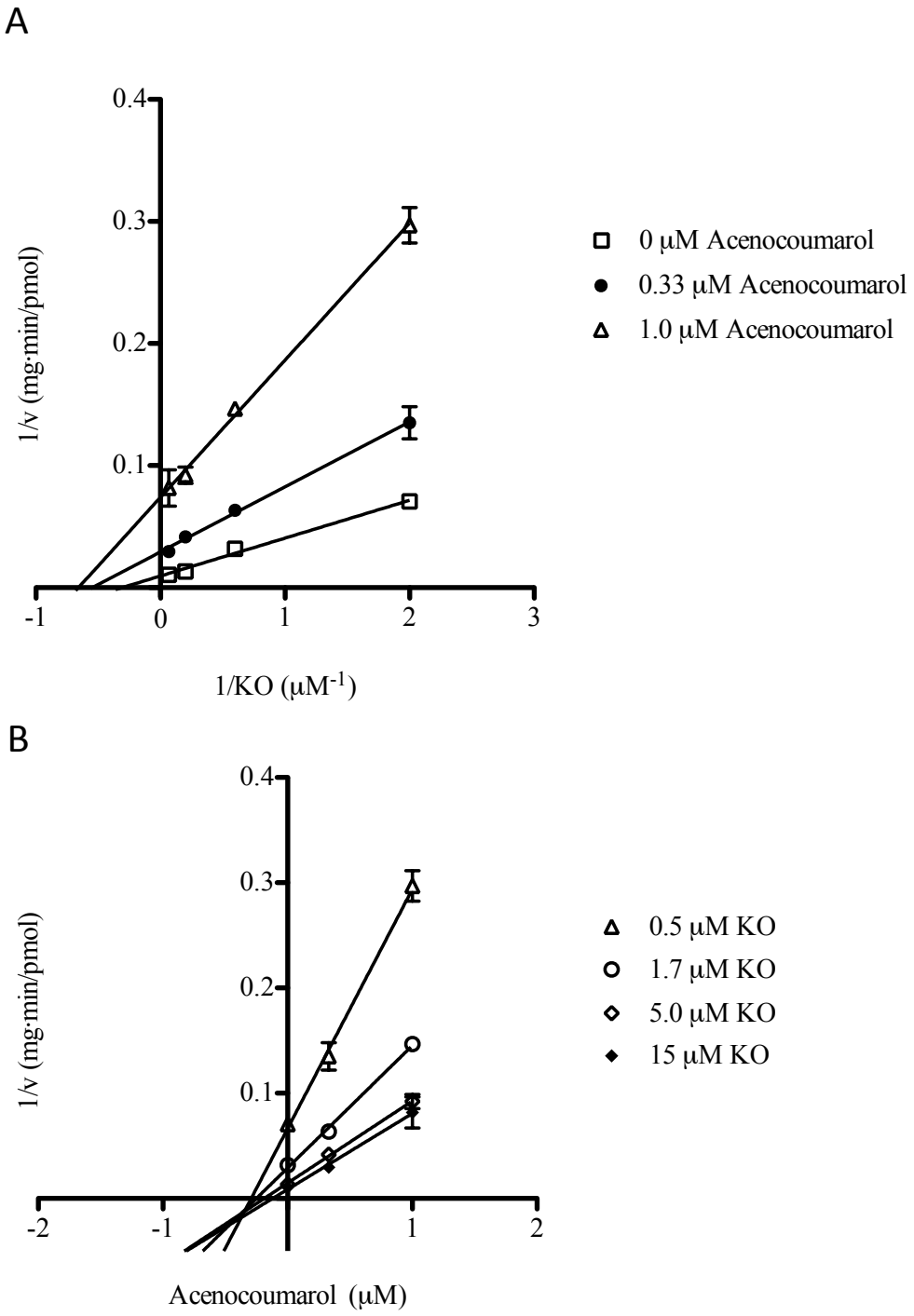

FIGURE 3.14: (**A)** Lineweaver-Burk plot describing VKOR activity at various concentrations of KO (0.5, 1.7, 5.0, and 15 μM) in the presence of 0, 0.33, and 1.0 μM acenocoumarol incubated with bovine liver microsomes (1 mg/mL). Data points represent the mean of triplicate measurements and error bars represent standard deviations. The data is also presented graphically on a **(B)** Dixon plot, from which the value of K_i was deduced. The K_i for acenocoumarol is listed in the Table 3.1

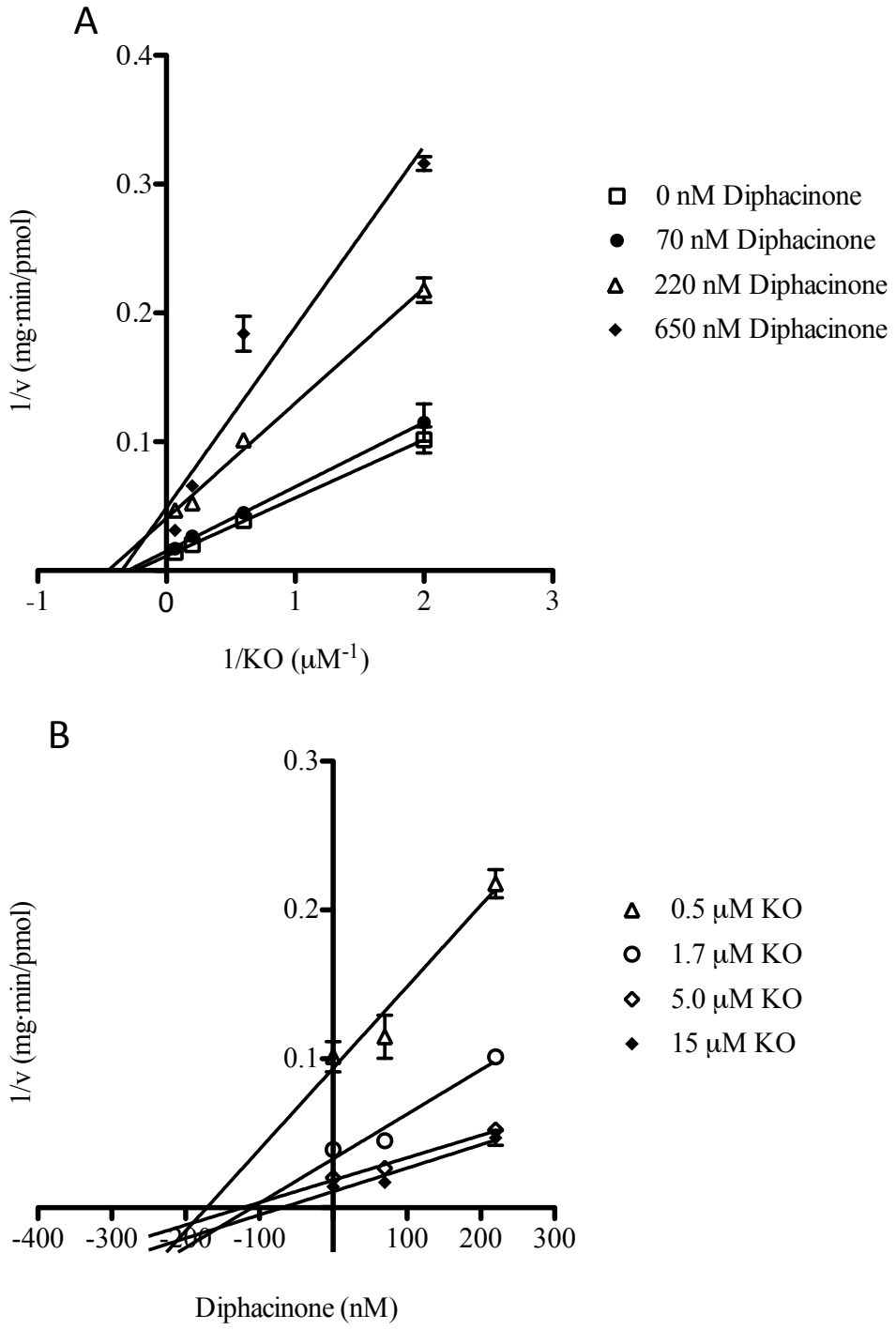

FIGURE 3.15: (**A)** Lineweaver-Burk plot describing VKOR activity at various concentrations of KO (0.5, 1.7, 5.0, and 15 uM) in the presence of 0, 70 nM, and 220 nM, and 650 nM diphacinone incubated with bovine liver microsomes (1 mg/mL). Data points represent the mean of triplicate measurements and error bars represent standard deviations. The data is also presented on a **(B)** Dixon plot, from which the value of K_i was deduced. The K_i for diphacinone is listed in the Table 3.1.

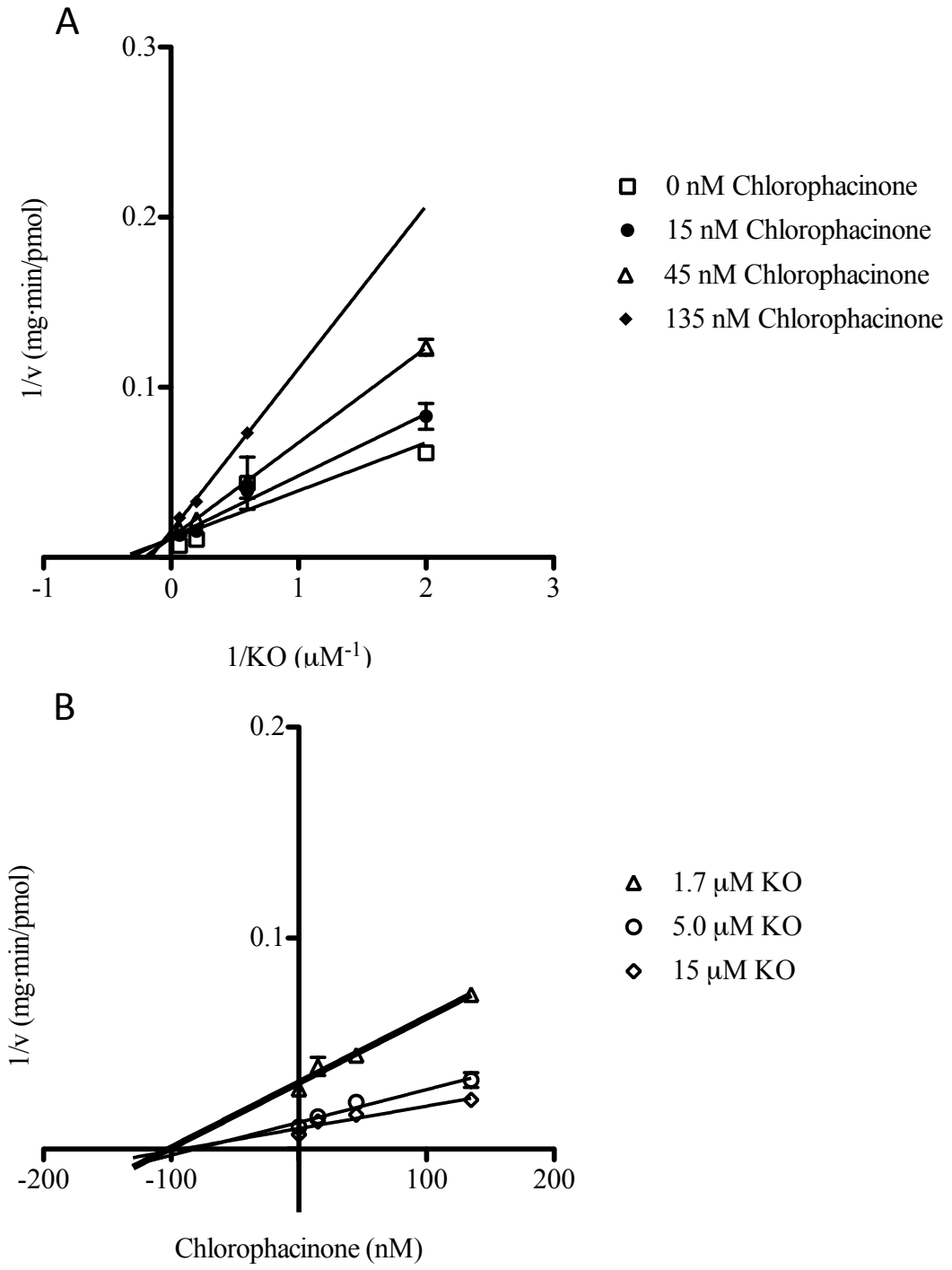

FIGURE 3.16: (**A**) Lineweaver-Burk plot describing VKOR activity at various concentrations of KO (0.5, 1.7, 5.0, and 15 uM) in the presence of 0, 15 nM, and 45 nM, and 135 nM chlorophacinone incubated with bovine liver microsomes (1 mg/mL). Data points represent the mean of triplicate measurements and error bars represent standard deviations. The data is also presented on a **(B)** Dixon plot, from which the value of K_i was deduced. The K_i for chlorophacinone is listed in Table 3.1

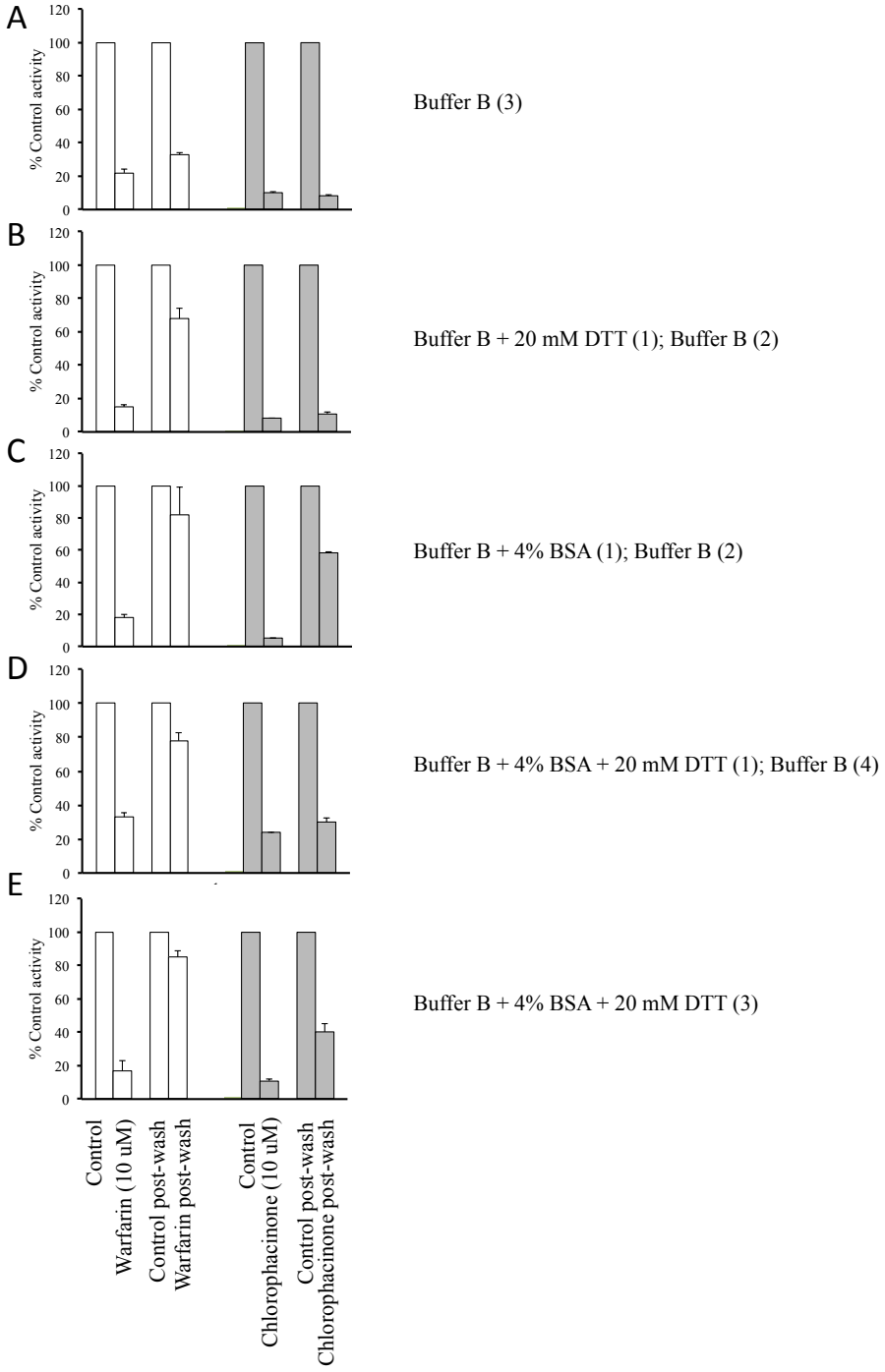

FIGURE 3.17: **VKOR activity of warfarin-treated and chlorophacinone-treated bovine liver microsomes after dilution and wash with various buffers.** Each panel represents data from the experiment performed according to the wash protocol described in the right-hand column. The number of washes applied with each buffer is in (). Inhibition data is reported as the % of activity observed in the corresponding negative control microsomes (solvent control). Bar graphs represent the mean of triplicate measurements and error bars represent standard deviations.

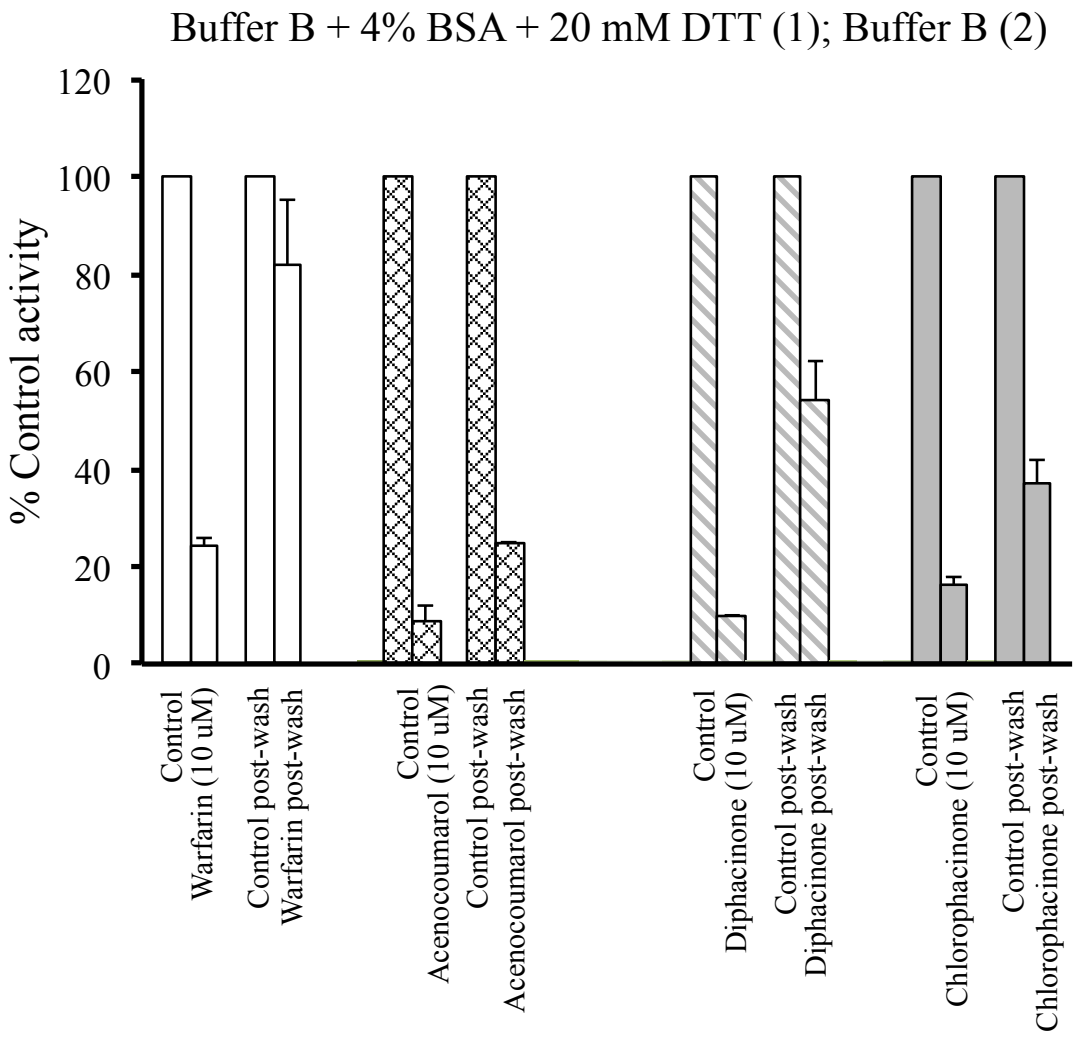

FIGURE 3.18: **VKOR activity of 4-hydroxycoumarin-treated and 1,3-indanedione-treated bovine liver microsomes after dilution and wash with buffer containing BSA and DTT.** Inhibition data is reported as the % of activity observed in the corresponding negative control microsomes (solvent control). Bar graphs represent the mean of triplicate measurements and error bars represent standard deviations.

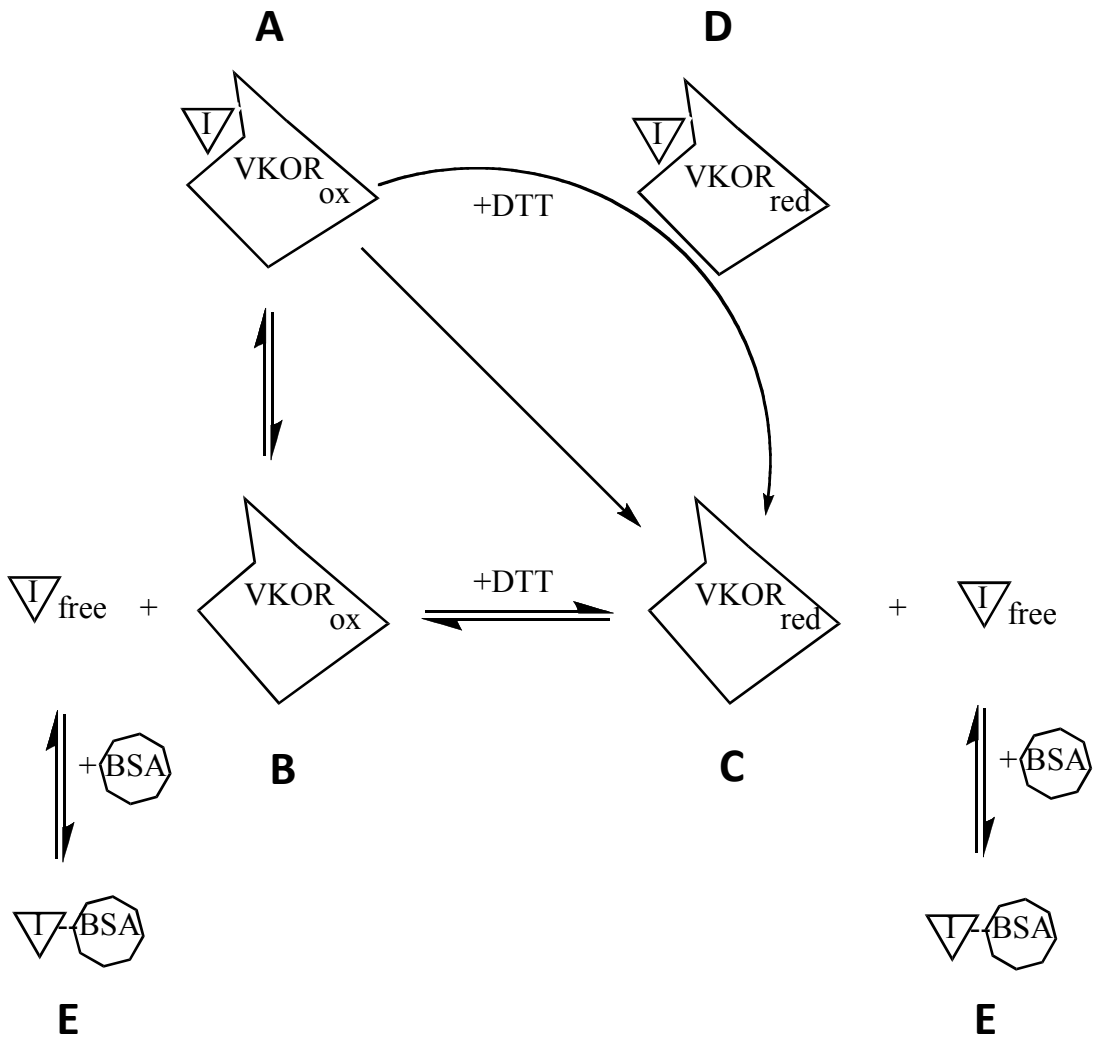

FIGURE 3.19 **Scheme showing the equilibrium between oxidized and reduced forms of VKOR that exist during inhibition by 4-hydroxycoumarin or 1,3-indanediones anticoagulants and the effects that BSA or DTT have on each.** (A) Inhibitor, complexed with the oxidized form of VKOR (B) the unbound oxidized form of VKOR (C) the unbound reduced form of VKOR (D) the hypothetical bound reduced form of VKOR (E) the formation of a BSA-inhibitor complex.

Chapter 4

Role of Tyrosine 139 in the Catalytic Center and Inhibitor Binding Site of VKOR

4.1 Introduction

Identification of the *VKORC1* gene [45,46] has led to numerous publications reporting the discovery of missense mutations that are associated with the warfarin resistance phenotype in both rodents and humans. Warfarin resistance in rats is defined by the World Health Organization as survival following feeding of the rodenticide at a level of 50 ppm in their diet for 6 days [133]. Although some resistant patients exhibit no therapeutic response with doses up to 250 mg/week, warfarin resistance in humans, secondary to the presence of coding-region variants of VKOR, can occur with as little as 80 mg/week of the drug compared to the mean therapeutic dose of 25-35 mg/week [134].

While multiple mechanisms of warfarin resistance may exist, e.g. accelerated warfarin metabolism [135,136] and altered expression of other components of the VKOR complex, like calumenin [137], coding region mutations in VKOR have been found in warfarin resistant rodents at 26 different positions located throughout the primary sequence of mouse and rat VKOR [20]. In addition, in humans, analysis of 134 cases of VKA resistance showed that these patients carry one of 11 missense mutations, also located throughout the primary sequence [134]. Clearly, VKOR mutations are the major cause of warfarin resistance in mammals. It seems likely that these amino acid changes alter the structure of the enzyme so as to adversely affect

warfarin binding. However, no atomic resolution structural data yet exists for this trans-membrane protein that identifies the warfarin-binding site within the enzyme.

Tyrosine 139 (Y139), has been identified as a site of mutation in a single warfarin-resistant human (Y139H) and several populations of warfarin-resistant rodents (Y139F, Y139C, and Y139S) [20]. In the studies reported here, we have focused on this single amino acid because, even in the absence of detailed structural information for the enzyme, it is clear that Y139 is located adjacent to the catalytic cysteines (C132 and C135) on the fourth membrane-spanning alpha helix as illustrated in Figures 4.1 and 4.2 [13]. The proximity of Y139 to the active site cysteines makes it a prime candidate for a role during catalysis in several ways (Figure 4.3). First, Y139 could act as a base to activate the catalytic cysteine that attacks the epoxide ring. Second, Y139 could donate a proton to the hydroxyl group of the putative enolate intermediate in order to eliminate water and generate vitamin K quinone. Third, Y139 might stabilize epoxide binding as appears to be the case for microsomal epoxide hydrolase [138].

In the human VKOR sequence, Y139 occurs within the tripeptide, TYA, a sequence motif that houses Y128 in NQO1, which makes up part of the dicoumarol binding site in this cytosolic quinone reductase (Figure 4.4). In NQO1, Tyr128 stabilizes ligand binding by hydrogen bonding to the lactone oxygen (at position 1) of dicoumarol [18]. Therefore, it is also possible that in addition to a role in substrate turnover, Y139 makes up part the warfarin-binding site of VKOR and interacts similarly with an oxygen atom of the 4-hydroxycoumarin nucleus.

In the current study, we hypothesized that Y139 plays a role in the mechanism of KO turnover as well as binding of the inhibitor to VKOR. We therefore constructed a series of Y139 mutants; Y139F, Y139S, Y139C, Y139V and sought to determine their effects on the kinetics of human VKOR activity and response to warfarin inhibition. For comparative purposes, we also constructed an L128Q mutant. L128 is a second mutational 'hot-spot' in warfarin-resistant rodents (L128Q, L128S) [20] and has been identified as a site of mutation in humans (L128R) [134]. To assess changes in response to warfarin we measured IC_{50}s. To assess changes in catalytic activity, we measured the kinetics for the generation of two products, VK_1 and 3-hydroxyvitamin K (3-OH VK_1). 3-OH VK_1, is reported to be an in vitro product of KO metabolism that has been observed in microsomes from warfarin-resistant rats.

4.2 Materials and Methods

4.2.1 Synthesis of 3-Hydroxyvitamin K Chemical Standard

3-Hydroxyvitamin K (3-$OHVK_1$) was synthesized from racemic vitamin 2,3 epoxide and purified by HPLC according to 'Method A' that was published previously [76]. The 3-hydroxy isomer (Figure 4.5) was identified (versus the 2-hydroxy isomer) by spectrophotometric, ^{1}H-NMR, and mass spectral analysis. The UV absorbance spectrum of the synthetic product had a maximal absorbance at 249 nm and 302 nm as was previously reported. ^{1}H-NMR resonances (in ^{2}H-chloroform solvent) of the product are listed in Table 4.1. Peak splitting at 1.45 ppm (2-methyl), 3.10 ppm (2-hydrogen), and 2.00 and 2.50 ppm (1- methylene) uniquely distinguished the 3-hydroxy product as the only isomer present. Mass spectra were obtained by direction injection-ESI tandem mass spectrometrometry on a Micromass Quattro II Tandem Quadrupole Mass Spectrometer (Micromass, Ltd., Manchester, UK). The major fragments observed in

positive ion mode were daughter ion 1 with m/z = 451 from the loss of water from parent ion (m/z = 469), and daughter ion 2 with m/z = 187 from the loss of the phytyl chain from the parent ion (m/z = 469).

4.2.2 Preparation of Chemical Standards

Standard solutions of VK_1 and VK_2, were prepared and stored as described in **Section 2.2.2**. Stocks of 3-OH VK_1 in isopropanol (HPLC grade) were stored at -80°C. Warfarin solutions were made in DMSO or DMF and stored at -20°C.

4.2.3 Site-Directed Mutagenesis of *VKORC1*

To construct single site mutants of human VKOR, the QuikChange®XL Site-Directed Mutagenesis kit (Stratagene, La Jolla, CA) was used perform mutagenic PCR in a Mastercycler Personal (Eppendorf, Westbury, NY) using a pFastBa**c** expression construct containing full length and C-terminal FLAG-tagged human *VKORC1* (pFBhVF) as a template. Mutagenic primers with the following sequences were used to mutate either Leu128 or Tyr139: L128Q forward, 5'- C CTG TTC TTC GTG C***AA*** TAT GAT TTC TGC ATT G-3', L128Q reverse, 5'-C AAT GCA GAA ATC ATA ***TT***G CAC GAA GAA CAG G-3'; Y139C forward, 5'-GTT TGT ATC ACC ACC T***G***T GCT ATC AAC GTG AGC-3', Y139C reverse, 5'-GCT CAC GTT GAT AGC A***C***A GGT GGT GAT ACA AAC-3'; Y139F, forward, 5'-GTT TGT ATC ACC ACC T***T***T GCT ATC AAC GTG AGC-3', Y139F reverse 5'-GCT CAC GTT GAT AGC A***A***A GGT GGT GAT ACA AAC-3'; Y139S forward, 5'-GTT TGT ATC ACC ACC T***C***T GCT ATC AAC GTG AGC-3', Y139S reverse, 5'-GCT CAC GTT GAT AGC A***G*****A** GGT GGT GAT ACA AAC-3'; Y139V, forward, 5'-GTT TGT ATC ACC ACC ***GT***T GCT ATC AAC GTG AGC-3', Y139V

reverse, 5'-GCT CAC GTT GAT AGC A***AC*** GGT GGT GAT ACA AAC-3'. (Boldface italics indicate the altered nucleotide). All pFastbac plasmids containing wild-type or mutant VKORC1 cDNA were examined for errors by DNA sequencing with *VKORC1*-specific primers: forward, 5'-TCTTCTCCTCCAGGTGGGGCA, and reverse, 5'-AGACACCAGGGAGCTCAG-3.'

4.2.4 Generation of Recombinant Baculoviruses

The Bac-to-Bac® Baculovirus Expression System (Invitrogen, Carlsbad, CA) method of recombinant baculovirus generation was implemented with few modifications. Wild-type or mutant pFBhVF was transformed into MAX Efficiency® DH10Bac™ chemically competent *Escherichia coli* cells. Antibiotic LB agar plates (50 µg/mL kanamycin, 7 µg/mL gentamicin, 10 µg/mL tetracycline, 100 µg/mL Bluo-gal, and 40 IPTG µg/mL), were streaked with a 10-, 100-, or 1000-fold dilution (with room temperature S.O.C. medium) of the transformation mixture and incubated at 37^{o}C for 48 hours. Isolated, white-colored colonies were picked from the plate with a sterilized pipette tip, and used to innoculate 3 mL LB containing antibiotics (50 µg/mL kanamycin, 7 µg/mL gentamicin, and 10 µg/mL tetracycline). Using a Qiagen® Plasmid Miniprep Kit (Qiagen, Valencia, CA), recombinant bacmid DNA was isolated from the cell culture and analyzed by PCR and DNA sequencing using M13 primers: forward, 5'-CCC AGT CAC GAC GTT GTA AAA CG-3,' reverse, 5'- CAG GAA ACA GCT ATG AC- 3'. Once verified to contain the correct *VKORC1* gene sequence, bacmid DNA was stored at 4^{o}C or transfected into the Sf9 (*Spodoptera frugiperda)* cell line to generate recombinant baculovirus. Viral DNA was extracted from each baculovirus stock and re-sequenced, to further ensure that the mutation would be present in infected Sf9 cells.

4.2.5 Recombinant VKOR Expression

To express FLAG-tagged VKOR proteins, Sf9 cells were infected with recombinant baculoviruses. As a negative control, cells were also infected with a baculovirus containing bacmid without a gene inserted. Sf9 cells were grown as a suspension culture in SF200^{TM} II SFM Serum-Free Medium (Invitrogen, Carlsbad, CA) containing 2.5% Heat-Inactivated Fetal Bovine Serum (Invitrogen, Carlsbad, CA), and 1% antibiotics-antimycotics (Invitrogen, Carlsbad, CA). For a typical large-scale expression culture, 700 mL of Sf9 cells (1x10^6 million cells/mL) was infected with 7.5-12.5 mL of the P2 (amplified) baculovirus stock in a sterile 2.8 L Fernbach culture flask and shaken at 126 rpm at 25^{o}C. Cells were harvested approximately 60 hours post-infection by centrifugation at 3,050 x g for 10 minutes at 4^{o}C in a Sorvall RC3C Plus Centrifuge (Dupont, Miami, FL). The cells were resuspended by vortexing in 30 mL of Sf9 cell homogenization buffer (10 mM KPi, 10 mM EDTA, 150 mM KCl) containing 1 tablet of Complete, EDTA-free Protease Inhibitor Cocktail (Roche Diagnostics, Mannheim, Germany) per 50 mL of resuspension volume. The cells were sedimented at 3,050 x g for 10 minutes at 4^{o}C in a Sorvall RT1 Centrifuge (Thermo Scientific, Rockford, IL) and frozen at -80^{o}C.

4.2.6 Isolation of Recombinant Sf9 Microsomes

All of the following operations were performed on ice or at 4^{o}C. Each cell pellet was thawed and resuspended in 15 mL of Sf9 cell homogenization buffer according to the tissue grinding procedure described in **Section 2.2.3**. The cells were lysed in an ice water bath by sonication for 7 cycles (10 second bursts and 1 minute rest per cycle) with a 4710 Series Ultrasonic Homogenizer (Cole-Palmer Instrument Co., Chicago, IL). The cell lysate was fractionated by ultracentrifugation at 8,000 x g for 20 minutes at 4^{o}C and the resultant supernatant was spun at

100,000 x g for 60 minutes at 4^{o}C in a Sorvall ® Ultra80 ultracentrifuge (DuPont Instruments, Corp., Miami, FL). The resulting microsomal pellet was resuspended as above with storage buffer and stored at -80^{o}C. The total protein content of the Sf9 microsomes was determined by performing a kit-based BCA^{TM} protein assay (Thermo Scientific, Rockford, IL).

4.2.7 Relative Quantitation of Recombinant VKOR protein in Sf9 Microsomes

Recombinant VKOR proteins were resolved by gradient gel electrophoresis and visualized by immunoblot analysis according to the protocol used previously for quantitating VKOR protein in human liver microsomes (**Section 2.2.10**). To detect GAPDH (as a loading control) in Sf9 microsomes, the membrane was incubated with the anti-GAPDH antibody (1:2,500 dilution) (Sigma-Aldrich, St. Louis, MO).

4.2.8 Measurement of Recombinant VKOR Activity in Sf9 Microsomes

The catalytic activity of recombinant VKOR enzymes was characterized by monitoring the formation of VK_1 and 3-OH VK_1. Activity assays were conducted as described previously in **Section 2.2.4** with the following modifications: 1) reactions were stopped (and extracted) by adding ice-cold hexanes (700 µL) and IPA (200 µL) and 2) operations after quenching were performed at 4^{o}C or on ice. For sensitive detection of 3-OH VK_1, samples were analyzed by Liquid Chromatography Atmospheric Chemical Ionization Tandem Mass Spectrometry (LC-APCI-MS/MS)**,** immediately after preparation.

4.2.9 LC-APCI-MS/MS Analysis

The current method of LC-APCI-MS/MS analysis was adapted from one that has been reported in the literature for similar compounds [139]. HPLC-mediated separation and quantification of 3-OH VK_1 (product), VK_1 (product), KO (substrate), and VK_2 (internal standard) over a 18 min run time on a reverse phase HPLC analytical column (Nucleosil 100-5 C18; 4.6 x 125 mm, 5 m particle size; Macherey-Nagel, Duren, Germany) and eluted with a mobile phase of A) water and B) methanol at a flow rate of 1 mL/min (Shimadzu pump LC10AD VP) over a gradient: 0-11 min, 95%-97% B; 11-15 min, 97-100% B; 15-17 minutes, 100% B; 17-18 minutes, 100%-95% B. Approximate retention times for 3-OH VK1, VK_2, KO, and VK_1 were 6.4, 9.2, 11, and 15 minutes, respectively (Figure 4.6). Eluents from the column entered an API 4000 mass spectrophotometer (MDS Sciex, Ontario, Canada) and were detected by MRM in APCI negative mode. Settings for the mass spectrometer were as follows: capillary voltage, 3.5 kV; cone voltage, 30 kV; source temperature, 450°C, collision gas, nitrogen. The following parent to daughter ion mass transitions were monitored: m/z 467.3 → 187.8 (3-OH VK_1); m/z 444.2 → 184.8 (VK_2 (internal standard); m/z 466.3 → 186.8 (KO); m/z 450.3 m/z → 185 (VK_1). The collision energy for each transition was -32 eV (3-OH VK_1), -40 eV (VK_2 (internal standard) -32 eV(KO), and -40 eV (VK_1).

4.2.10 Steady-State Enzyme Kinetics

Experiments performed to measure KO binding affinity (K_m) and maximal VKOR activity (V_{max}) in Sf9 microsomes containing recombinant VKOR enzymes (wild-type, VKORC1, L128Q, Y139F, or Y139V) or negative control microsomes were performed at the following substrate concentrations: 0.25 μM, 0.5 μM, 1.0 μM, 3.3 μM, 5.0 μM, 20, μM 50 μM, 80 μM, and 160 μM.

The activity of the Y139C and Y139S mutants was measured at 50 μM and 100 μM KO only, due to insufficient enzyme sample for complete kinetic characterization. Replicate sets of kinetic experiments were prepared and performed as described in **Section 2.2.7**.

4.2.11 VK_1 and 3-OH VK_1 Quantification and Calculations

For each chromatogram, Analyst® Software version 5.1 for Window 7 OS was used to compute the peak area for 3-OH VK_1, VK_1 and VK_2, individually. Data from mock incubations that were performed with known concentrations of 3-OH VK_1 or VK_1 in the presence of negative control microsomes, were used to make a standard curve by plotting the peak area ratio vs amount of chemical standard. Under standard assay and analysis conditions, 3-OH VK_1 was stable against conversion to VK_1 by water elimination, which was minimal relative to the total hydroxyvitamin K amount. The linear regression equation was used to convert peak area ratio to the amount of product. The rate of production was calculated as pmol/mg microsomal protein/minute and normalized to the expression level of VKOR protein per mg of microsomal protein, relative to wild-type expression, as determined from western blotting.

4.2.12 Determination of IC_{50} and K_i of Racemic Warfarin

Briefly, all IC_{50} experimental reactions conducted in recombinant Sf9 microsomes were prepared as described in **Section 3.2.4** with the following modifications: a) microsomes were co-incubated at 30^{o}C with KO (30 μM) and racemic warfarin for 3 minutes before b) the reaction was initiated by adding DTT to the incubation mixture. The rate of reaction exhibited by negative control reactions containing organic solvent was defined as the rate in the absence of inhibitor. Final warfarin inhibitory concentrations tested against wild-type VKOR-containing microsomes

activity were 0 μM (negative control), 0.01 μM, 0.05 μM, 0.25 μM, 1.0 μM, 2.0 μM, 10 μM, 50 μM, and 100 μM. Final inhibitory concentrations tested against L128Q-containing microsomes were 0 μM (negative control), 0.01 μM, 1.0 μM, 2.0 μM, 5 μM, 10 μM, 50 μM, 75 μM, 100 μM, 200 μM, 500 μM, and 1000 μM. Final inhibitory concentrations tested against Y139F-containing microsomes were 0 μM (negative control), 0.05 μM, 0.25 μM, 1.0 μM, 10 μM, 100 μM, 300 μM, 500 μM, 1.0 mM, 3.0 mM, 5.0 mM, and 10 mM. respectively. In some experiments, K_i was determined for wild-type VKOR-containing microsomes with a single concentration of the inhibitor and measuring activity at various KO concentrations (0.5 μM, 1.7 μM, 5 μM, and 15 μM). Reaction mixtures were prepared as illustrated in **Section 3.2.4**. Final inhibitory concentrations tested for racemic warfarin and were 0 μM (negative control), 0.33 μM, 1.0 μM, and 3.0 μM. For IC_{50} or K_i determination, VK_1 detection, VK_1 quantification, and calculations were carried out as described in **Section 2.2.5, Section 2.28**, and **Section 3.2.8**.

4.2.13 Analysis of Kinetic Data

Kinetic constants, K_m and V_{max}, were calculated as described in **Section 2.2.9**. K_i and IC_{50} s were calculated as described **Section 3.2.9.**

4.3 Results

4.3.1 Relative Quantitation of Recombinant hVKOR Enzymes Expressed in Sf9 Microsomes

Wild-type human VKOR and mutants (Y139C, Y139F, Y139S, Y139V, and L128Q) were over-expressed in Sf9 insect cells, which was confirmed by western blot detection in each isolated microsomal fraction except for the negative control (Figure 4.7). Each protein, to which a C-

terminal FLAG affinity tag (1012 Da) had been added for diagnostic purposes, has an expected molecular weight of 19 kDa. As shown in Figure 4.7, comparison of each VKOR band signal intensity normalized to the intensity of a loading control (Sf9 GAPDH), demonstrates that the level of VKOR expression per microgram of microsomal protein, varied greatly. L128Q, for example exhibited very low levels of expression relative to wild-type (lane 3 of Figure 4.7). Relative to wild-type (1.0), the expression level of L128Q, Y139F, and Y139V was 0.07, 1.58, and 1.51 –fold, respectively (Table 4.2).

4.3.2 Kinetics of VK_1 Production by Recombinant hVKOR Enzymes

Reduction of KO to VK_1 by FLAG-tagged wild-type VKOR, L128Q, Y139F, and Y139V followed Michaelis-Menten kinetics (Figure 4.8). As derived from curve fittings, the kinetic parameters, K_m, V_{max}, and V_{max}/K_m are reported in Table 4.3 for the wild-type VKOR enzyme and the mutants, Y139F, Y139V, and L128Q. Maximal rates of enzymatic VK_1 production (normalized to the total protein content of the microsomes) were ~10- fold or greater than non-enzymatic reaction of DTT with KO (negative control microsomes). Values of K_m fell within a narrow range (4.64 ± 0.96 μM-5.61 ± 0.85 μM), similar to that seen previously for human liver microsomal VKOR catalysis (Chapter 2). The V_{max} of L128Q and Y139F (normalized to level of expression of each enzyme relative to wild-type), was 1.7-fold higher and 1.1- fold lower than the V_{max} of wild-type VKOR, respectively. Unlike the other mutants, Y139V exhibited a very low rate of basal activity (14-fold less than wild-type).

4.3.3 Kinetics of 3-OHVK$_1$ Production by Recombinant hVKOR Enzymes

Similarly, reduction of KO to 3-OH VK$_1$ by FLAG-tagged wild-type VKOR, L128Q, Y139F, and Y139V followed Michaelis-Menten kinetics (Figure 4.9). The kinetic parameters, K_m, V_{max} (normalized to level of expression of each enzyme relative to wild-type), and V_{max}/K_m are reported in Table 4.3 for the wild-type VKOR enzyme and Y139F mutant. The rate of non-enzymatic 3-OHVK$_1$ production (normalized to the total protein content of the microsomes) was below the limit of detection. With respect to the production of 3-OH VK$_1$, the affinity of these enzymes for KO, which also fell within a narrow range, were 4.25 ± 0.69 μM (wild-type), 6.49 ± 1.43 μM (Y139F), and 1.05 ± 0.37 μM (Y139V). The value of V_{max}/K_m of Y139F for VK$_1$ and 3-OH VK$_1$ production respectively were slightly lower than those for the wild-type enzyme (Table 4.3).

The ratio of 3-OH VK$_1$ to VK$_1$ rates of production at a saturating concentration of KO for wild-type and all of the Y139 mutants is reported in Table 4.4. Depending on the enzyme, the ratio was calculated from the V_{max} or the rate at 60 uM KO for the formation of each product. The ratio corresponding to wild-type, Y139F, Y139S, Y139C, and Y139V, were 0.032 ± 0.002, 0.036 ± 0.002, 0.065 ± 0.032, 0.051 ± 0.006, and 0.110 ± 0.009, respectively, indicative of no dramatic effect of the mutations on this partition ratio.

4.3.4 Warfarin-susceptibility of Recombinant hVKOR Enzymes in Vitro

All of the VKOR variants examined in this study were inhibited by racemic warfarin. Dose-response curves acquired by racemic warfarin inhibition of wild-type, Y139F, and L128Q are shown in Figure 4.10. The associated IC_{50} value for each curve is reported in Table 4.5. Relative

to wild-type VKOR, Y139F was ~ 270-fold and L128Q was ~ 42-fold less potently inhibited by warfarin. Like Y139F, Y139C and Y139S also exhibited normal basal (uninhibited) activity in the presence of 100 μM warfarin (Figure 4.11). Furthermore, as illustrated by panel A of Figure 4.12, racemic warfarin is a non-competitive inhibitor of wild-type VKOR with respect to KO. The value of K_i was derived from the Dixon plot x-intercepts (panel B of Figure 4.12) and is reported in Table 4.5.

4.4 Discussion

In the current study, we investigated potential roles of Y139 in the catalytic cycle and inhibitor-binding site of human VKOR. Wild-type VKOR and several mutants were recombinantly expressed and characterized with respect to KO turnover and warfarin inhibition. As an internal check on our data, we first evaluated the kinetic parameters, K_m (for KO) and $IC_{50,}$ and K_i, (for racemic warfarin) of the wild-type recombinant VKOR enzyme in comparison with the endogenous enzyme present in human liver microsomes (Table 4.6). Recombinant wild-type VKOR exhibited low micromolar K_m values for KO reduction (evaluated by the generation of VK_1) that was comparable to those we observed in genotyped human liver microsomes (1.6-2.9 μM) as described in Chapter 2. Moreover, the binding affinity of recombinant wild-type VKOR for warfarin, as evaluated by a K_i measurement of 2.0 ± 0.8 μM was close to the value obtained using human liver microsomes, as the enzyme source (0.71± 0.06 μM [data not shown]). Lastly, as was the case for the human liver microsomal enzyme, the recombinant enzyme is inhibited by warfarin in a non-competitive manner with respect to substrate. Based on these observations, we conclude that recombinantly expressed VKOR in insect cell microsomes adequately recapitulates the kinetic behavior of the endogenous enzyme, and so we feel confident that conclusions drawn

for the study of the recombinant mutant forms of the enzyme would be valid with respect to the situation in vivo.

As described in the Introduction, we hypothesized that Y139, could have a role in the catalytic reaction of VKOR by acting as either a catalytic base to initiate attack of the cysteine on the epoxide, or as a proton donor, either to stabilize the epoxide or facilitate elimination of water to generate vitamin K quinone. Because a Tyr→Phe change provides the most relevant site-directed mutant with which to evaluate acid/base catalysis in VKOR, we will formulate most conclusions around the data obtained with this mutant.

When Y139 was mutated to a phenylalanine, thereby eliminating its ability to act as either a base or as a proton donor, Y139F was only slightly less catalytically active than the wild-type enzyme and had a similar affinity for KO. This suggests that Y139 is not directly involved in substrate binding or the catalytic reduction of KO to VK_1, by VKOR. For the purpose of comparing the impact of mutations with different degrees of structural conservation, Y139 was also replaced by a valine thereby replacing the hydroxyl group of tyrosine with a smaller, hydrophobic, and non-ionizable side group. As was observed with Y139F, Y139V mutant also exhibited no difference in affinity for KO from wild-type. Since Y139V differs from Y139F only by having a smaller non-aromatic side chain, the more dramatically reduced V_{max} for VK_1 production demonstrated by Y139V is most likely a consequence of losing an essential hydrophobic interaction that can be achieved by a residue that has an aromatic or larger group. Thus, the kinetic behavior of Y139V for the reduction of KO to VK_1 further confirms our conclusion that Y139 does not participate in substrate turnover either as a base to initiate the attack on the epoxide or as a proton donor.

To assess the role of Y139 as a proton donor in the final water elimination step we also observed the effect of the Y139 mutation on the formation of 3-OH VK_1, a side-product of KO metabolism that was originally observed at higher levels in warfarin-resistant rats that normal rats [76]. Fasco proposed that, as a consequence of changes in the VKOR enzyme that confer warfarin-resistant phenotype in rats, misprotonation of the substrate at carbon-2, instead of the hydroxyl group on carbon-3, occurs to yield 3-OH VK_1 instead of VK_1 (Figure 4.13). (Another suggested pathway to 3-OH VK_1 from KO was tautomerism of the enol intermediate in solution due to a lower substrate affinity VKOR enzyme in warfarin-resistant rats). It would therefore be expected that if Y139 fulfills the role of proton donor in the normal enzyme, turnover of KO by Y139F would lead to a higher level of 3-OH VK_1 than turnover by wild-type VKOR, due to compromised elimination of water. (In warfarin-resistant rats, 3-OH VK_1 comprised 20% of the total product mixture). However, data obtained with the Y139F mutant argue against either of the above scenarios because of the minimal changes observed, relative to wild-type enzyme, in V_{max} and K_m for KO turnover and in the amount of 3-OH VK_1 generated during turnover. In comparison with the wild-type enzyme, a lower V_{max} was observed for the Y139V mutant, but this may reflect a loss of catalytic activity due to changes in substrate positioning within the active site following loss of a critical aromatic interaction that is maintained with the Y139F mutant. When calculated from V_{max} and K_m with respect to 3-OH VK_1 formation by Y139V, the catalytic efficiency was higher than expected on the basis of the low level of 3-OH VK_1 produced. This can be explained by the unusually low K_m that was measured for the Y139V mutant. Unfortunately, limited availability of expressed Y139V prevented us from performing a replicate kinetic experiment in order to confirm or dismiss the original K_m.

To compare the effect of different warfarin-resistant coding mutations on VKOR activity and warfarin inhibition, we also characterized L128Q, which unlike Y139, is located on the N-terminal side of the CXXC redox site. Like Y139F, L128Q was similar to wild-type VKOR with respect to both K_m and V_{max} for the formation of VK_1, suggesting that L128 also is not involved in substrate turnover or substrate binding, despite its predicted proximity to the active site. This result is consistent with a previous report that microsomal VKOR harvested from warfarin-resistant rats carrying the L128Q mutation exhibited turnover kinetics that were similar to that observed of normal rat microsomes [140].

L128, however, appears to have a significant role in warfarin inhibition, as it was observed that a Leu → Gln change had a sizable impact on warfarin susceptibility. Even more critical to the mechanism of warfarin binding or inhibition is Y139, as demonstrated by the resistance to inhibition exhibited by any mutant of Y139, even in the presence of 100 μM warfarin. Comparison of IC_{50} values further suggested that, between the two 'hotspot' mutants of VKOR [1], Y139 was the more influential residue on warfarin inhibition.

In the current study, we have investigated possible roles of human and rat VKOR mutational hot-spots, Y139 and L128, in catalysis and warfarin inhibition, by evaluating the kinetic behavior of strategically designed mutants of human VKOR in a validated recombinant expression system. In addition to determining that Y139 (and L128) are not directly involved in the reduction of substrate, we discovered that they are both strong determinants of warfarin binding/inhibition, especially Y139. This supports the likelihood that Y139 provides a critical electrostatic

interaction with warfarin during therapeutic inhibition of the vitamin K cycle by this oral anticoagulant.

TABLE 4.1: **^{1}H-NMR proton assignments for the chemically synthesized 3-hydroxyvitamin K standard.**

Position	δ (ppm)	Splitting
2-CH_3	1.45	d
2-H	3.10	q
3-OH	4.00	s
1'-CH_2	2.00, 2.50	dd
2'-H (vinyl)	4.80	t
R-alkyl	< 1.20	Overlapped
Aromatic Hs	8.05	Multiplet
Aromatic Hs	7.75	Multiplet

TABLE 4.2**: Relative V_{max} values for VK_1 and 3-OH VK_1 formation by recombinant human VKOR enzymes expressed in Sf9 microsomes** **The band density of each VKOR band was divided by density of the corresponding GAPDH band. *The value of V_{max} , which had been normalized by the band density relative to wild-type VKOR, was divided by V_{max} of the wild-type enzyme.

Recombinant Human VKOR Enzyme	**Band Density Ratio	Band Density Relative to Wild-type	*Fold over V_{max} of Wild-type VK_1	3-$OHVK_1$
Wild-type	1526	1.00	1.00	1.00
Y139F	2404	1.58	0.88	1.00
Y139V	2298	1.51	0.07	0.25
L128Q	110	0.07	1.68	-

TABLE 4.3: **Kinetic parameters of VK_1 and 3-OH VK_1 formation from KO in Sf9 microsomes containing recombinant human wild-type VKOR or mutants.** Saturation kinetic curves were best fit using a one-site binding model. Values represent the mean ± SEM from 2 experiments performed with each enzyme. *V_{max}/K_m for Y139V is not reported because of the unusually low K_m.

Recombinant Human VKOR Enzyme	VK_1			3-OH VK_1		
	Relative V_{max} (pmol/unit of wild-type/min)	K_m (μM)	Relative V_{max}/K_m	Relative V_{max} (pmol/unit of wild-type/min)	K_m (μM)	Relative V_{max}/K_m
Wild-type	100 ± 4.96	4.64 ± 0.96	21.6	3.20 ± 0.15	4.25 ± 0.69	0.75
Y139F	95.9 ± 3.07	5.61 ± 0.85	17.0	3.38 ± 0.15	6.49 ± 1.43	0.52
Y139V	7.15 ± 0.33	5.30 ± 1.17	1.35	0.72 ± 0.03	1.05 ± 0.37	0.68
L128Q	213 ± 5.21	5.20 ± 0.66	41.0	-	-	-

TABLE 4.4: **Formation of 3-OHVK$_1$ relative to VK$_1$ by recombinant human wild-type VKOR or mutants in Sf9 microsomes at saturating KO concentrations.**

Recombinant Human VKOR Enzyme	3-OHVK$_1$/VK$_1$ at V_{max} or *rate at 60 μM KO
Wild-type	0.032 ± 0.002
Y139F	0.036 ± 0.002
Y139S	0.065 ± 0.032*
Y139C	0.051 ± 0.006*
Y139V	0.110 ± 0.009

TABLE 4.5: **Calculated parameters describing the inhibition of human recombinant wild-type VKOR and mutants.**

Recombinant Human VKOR Enzyme	IC_{50} (μM)	SEM	K_i (μM)	SD
Wild-type	1.50	0.09	1.99	0.80
Y139F	406	5.45	-	
L128Q	71.3	8.13	-	

TABLE 4.6**: Comparison of kinetic parameters describing the production of VK_1 by human liver microsomal and recombinant wild-type VKOR.**

Human VKOR	V_{max} (pmol/mg/min)	K_m (μM)	(R,S)-Warfarin IC_{50} (μM)	(R,S)-Warfarin K_i (μM)
HLM	11.5 ± 0.21	2.6 ± 0.23	0.51 ± 0.03	0.71 ± 0.09
Wild-type Recombinant	-	4.25 ± 0.69	1.50 ± 0.09	1.99 ± 0.8

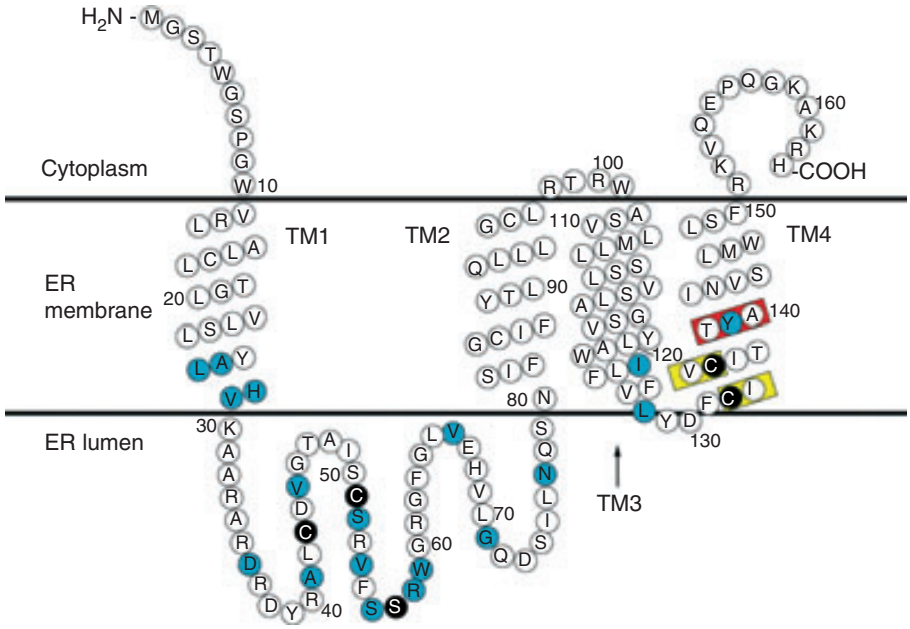

FIGURE 4.1: **The topological model of VKOR predicted by the bioinformatic analysis of 327 *VKORC1* ortholog sequences.** The yellow boxed amino acids represent the CXXC active site and the red-boxed amino acids represent the TYA sequence motif containing Y139 [134].

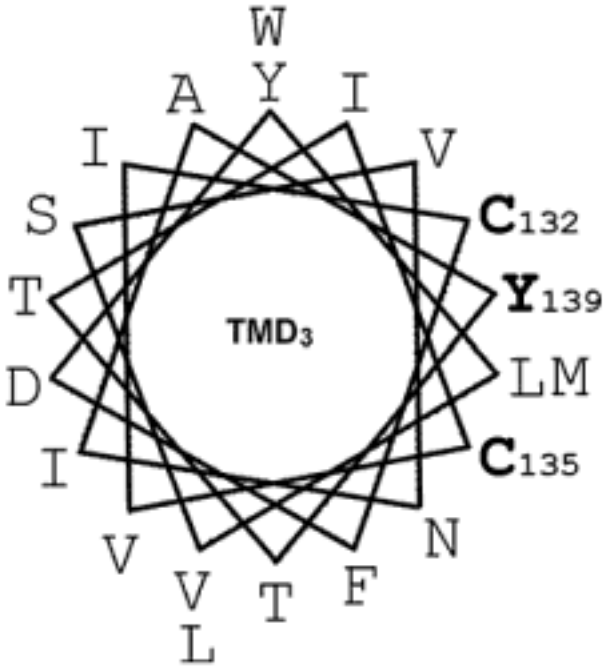

FIGURE 4.2: **α-helix wheel representation of the transmembrane domain containing the active site cysteines and Y139 of VKOR** [13]**.** Y139 is positioned on the same side of the α-helix as the active cysteines, 132 and 135 and only one turn away from the CXXC active site.

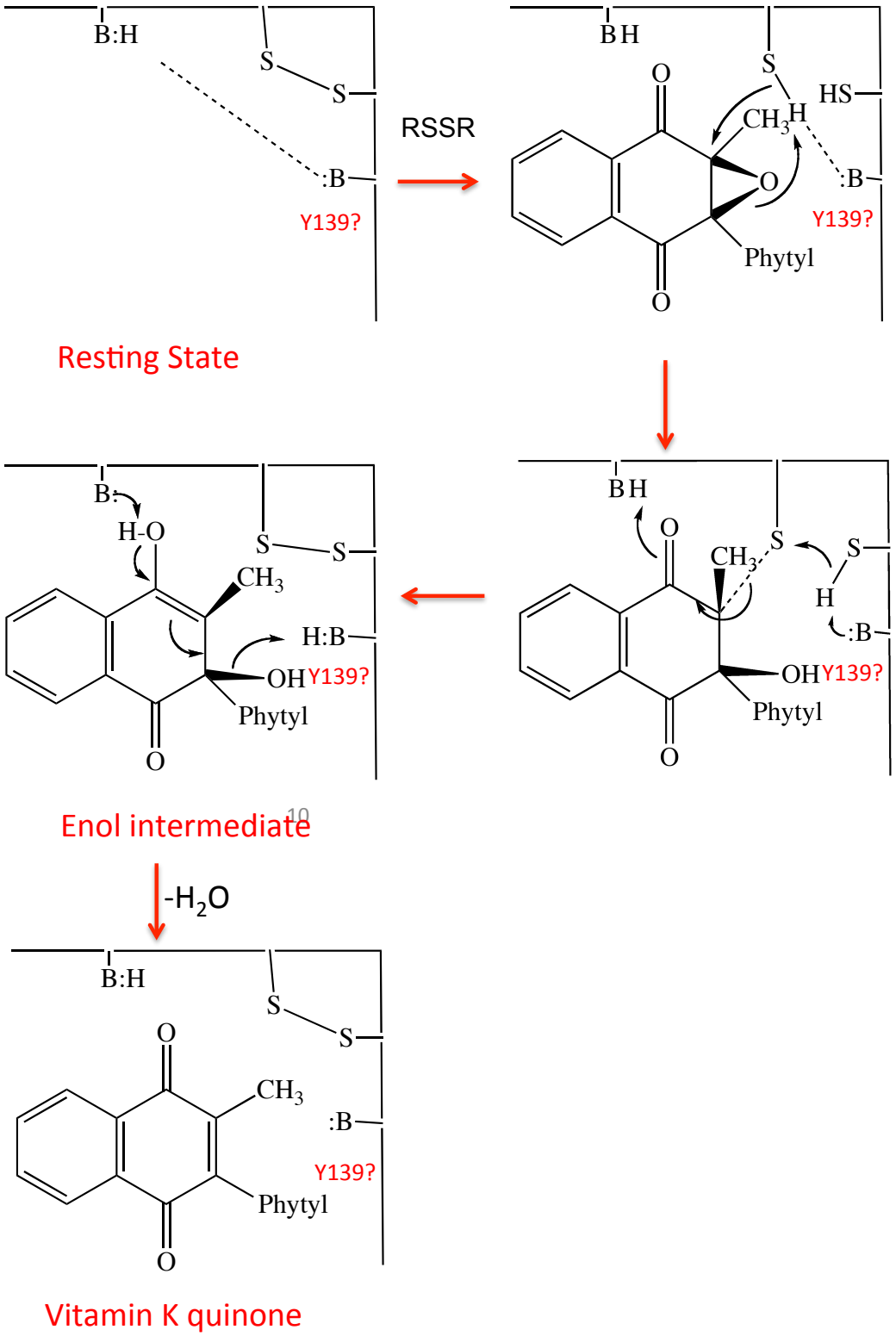

FIGURE 4.3**: Proposed mechanism of VKOR-(base)catalyzed vitamin K epoxide reduction to vitamin K_1** [76]**.** Y139 is labeled as a putative active site residue that participates in the catalytic reaction.

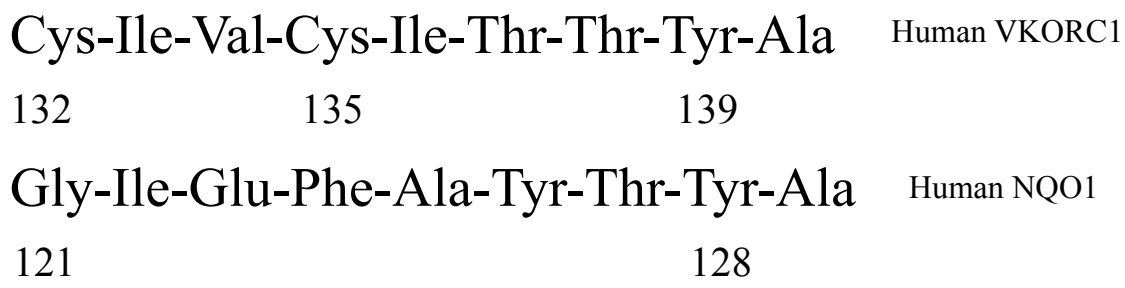

FIGURE 4.4: **Partial primary sequences of human VKOR and NQO1 demonstrating the shared presence of a TYA sequence motif.**

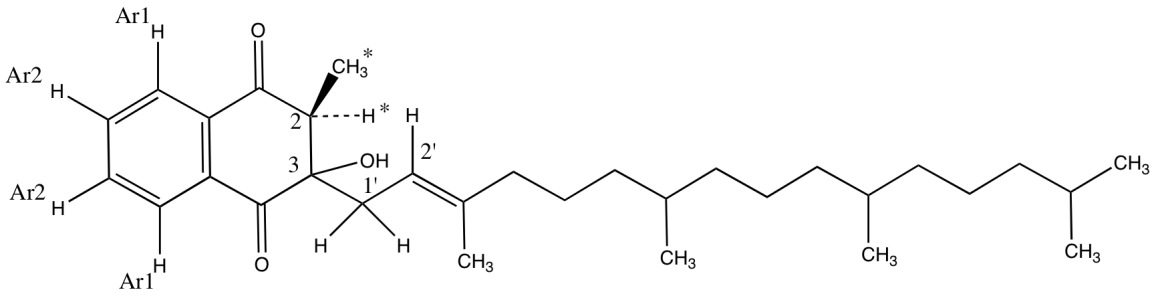

FIGURE 4.5: **Chemical structure of 3-Hydroxyvitamin K standard.** ^{1}H-NMR proton assignments are listed in **Table 4.1**.

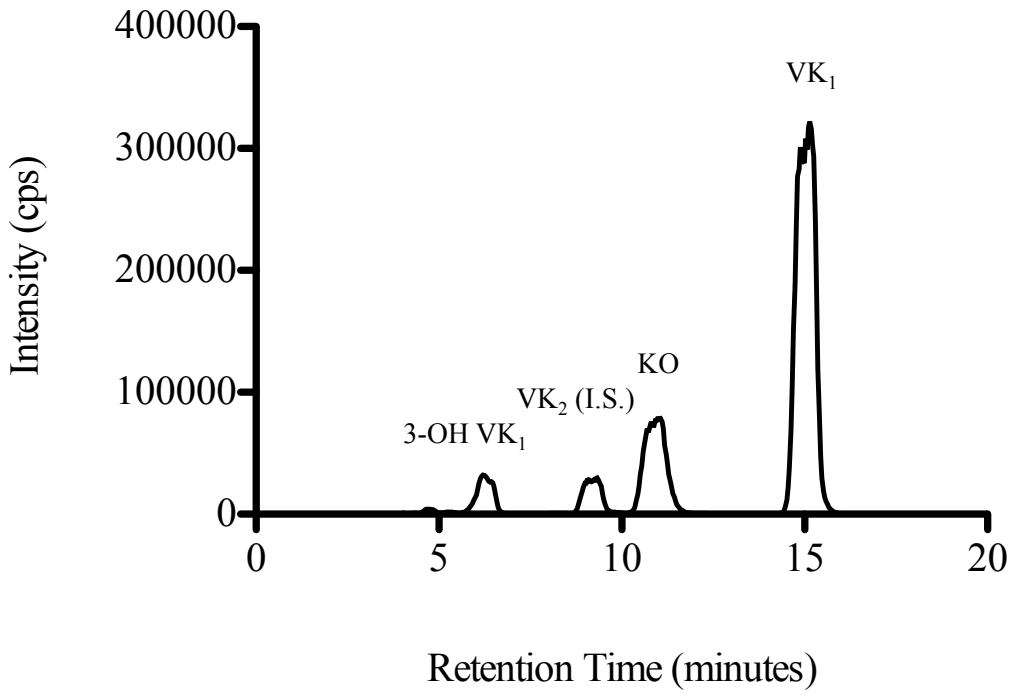

Figure 4.6: **Chromatographic separation of vitamin K analytes by HPLC with APCI-MS-MS detection**. 3-OH VK_1, VK_2, KO, and VK_1 peaks were resolved under the conditions described in **Section 4.2.9**.

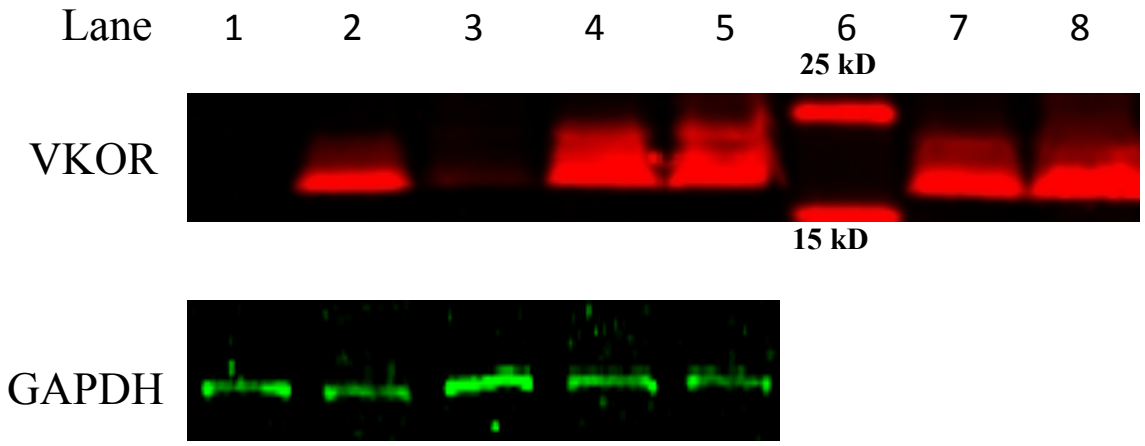

FIGURE 4.7**: Expression and relative quantitation of recombinant human wild-type VKOR and Y139 and L128 mutants in Sf9 microsomes.** Sf9 microsomes were immunoblotted with a VKOR-specific antibody as described in **Section 4.2.7**. Each lane contains 12 ug of protein. The exact preparations of microsomes in lanes 1-5 were characterized as described in **Section 4.2.10**. Lane 1 contains negative control microsomes. Lane 2 contains wild-type VKOR. Lane 3 contains L128Q. Lane 4 contains Y139F. Lane 5 contains Y139V. Lane 6 contains the molecular weight marker. Lane 7 contains Y139C. Lane 8 contains Y139S. In Sf9 microsomes, GAPDH appears as a green band while VKOR (FLAG-tagged) appears as a red band (19 kDa).

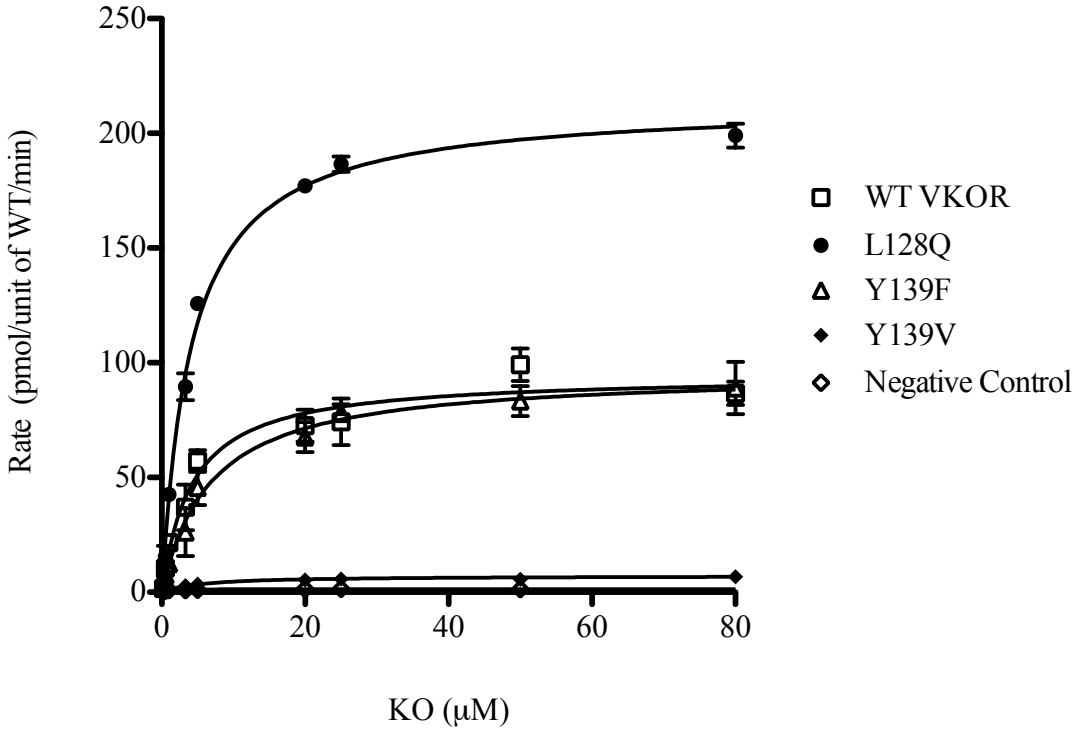

FIGURE 4.8: **Saturation kinetics of VK_1 formation from KO in Sf9 microsomes containing recombinant human wild-type VKOR or mutants.** Each data point represents the mean of duplicate measurements from a representative experiment (n = 2) and each error bar represents the standard error of the mean. Data presented on a substrate vs. rate plot was fit with the one-site binding model. Values for kinetic parameters that were derived from the curve-fittings for each experiment are reported in Table 4.3 as the mean ± standard error of the mean.

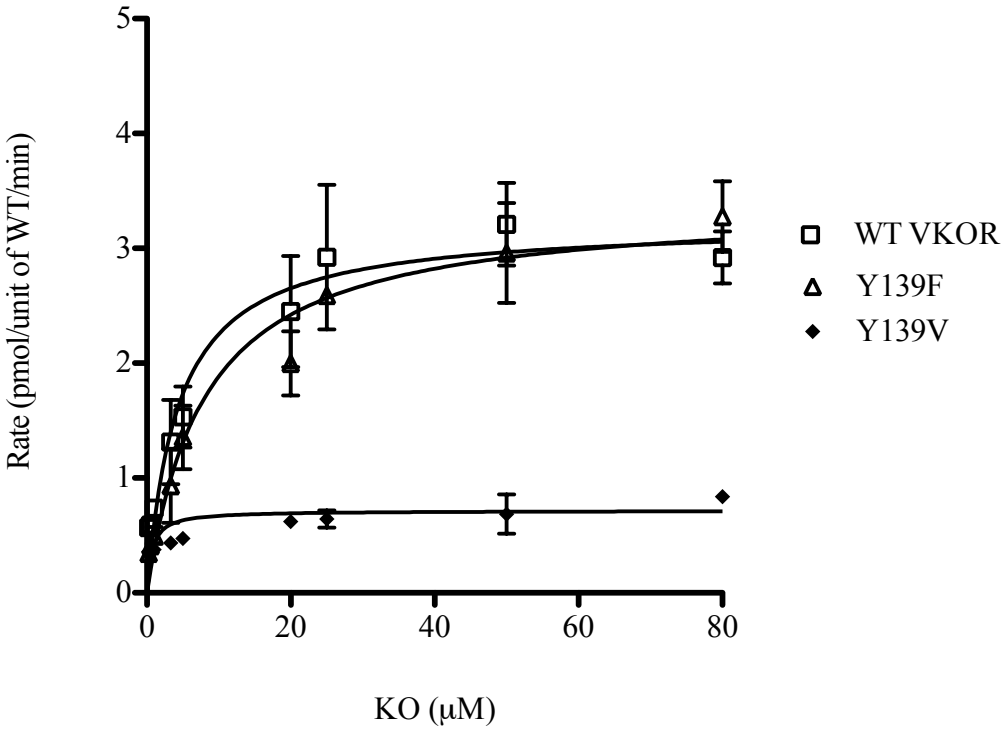

FIGURE 4.9: **Saturation kinetics of 3-OHVK$_1$ formation from KO in Sf9 microsomes containing recombinant wild-type VKOR or mutants.** Each data point represents the mean of duplicate measurements from a representative experiment (n = 2) and each error bar represents the standard error of the mean. Data presented on a substrate vs. rate plot was fit with the one-site binding model. Values for kinetic parameters that were derived from the curve-fittings for each experiment are reported in Table 4.4 as the mean ± standard error of the mean.

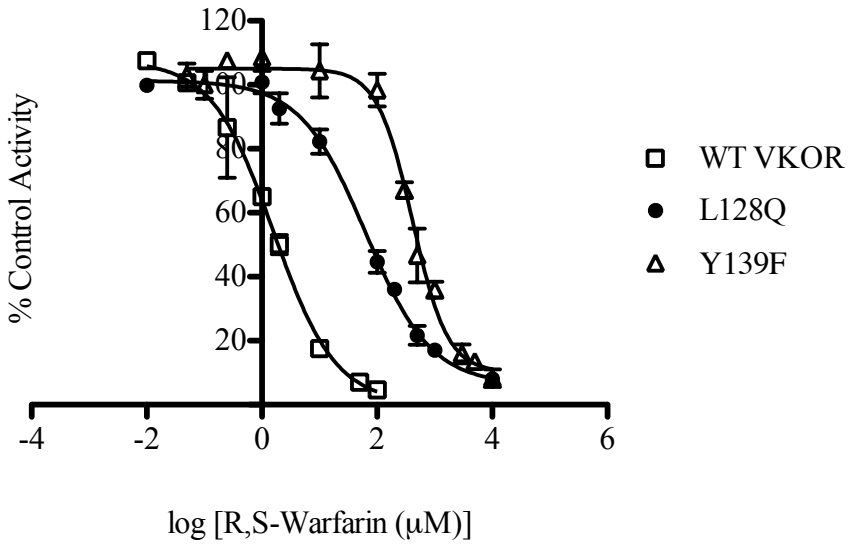

FIGURE 4.10: **Inhibition of recombinant human wild-type VKOR or mutants in Sf9 microsomes by racemic warfarin.** Data points represent the mean of triplicate measurements from a representative experiment and error bars represent standard deviations. IC_{50} values were calculated by fitting the data with a sigmoidal dose-response (variable slope) equation. The mean IC_{50} and the standard error of the mean of two experiments performed with each enzyme are listed in Table 4.7.

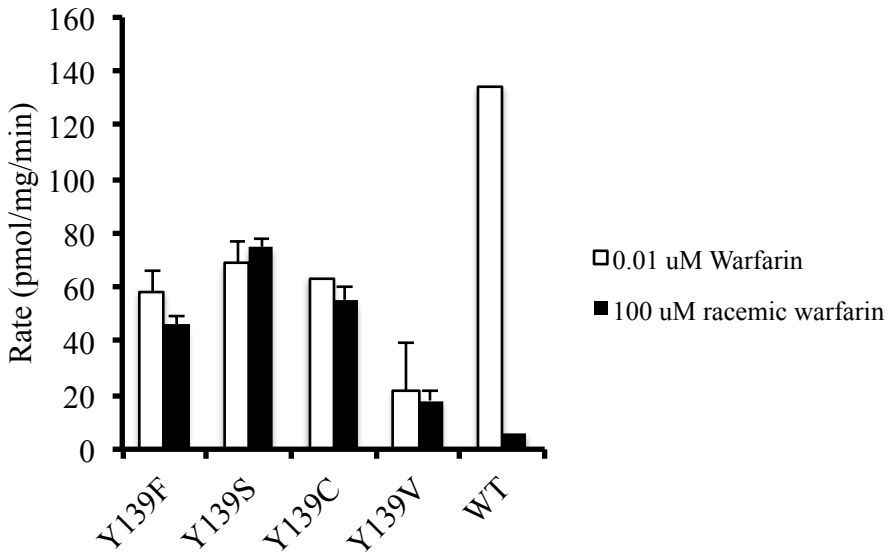

FIGURE 4.11: **VKOR activity of recombinant human VKOR Y139 mutants in Sf9 microsomes in the absence and presence of racemic warfarin.** Data points represent the mean of triplicate measurements from a representative experiment and error bars represent standard deviations.

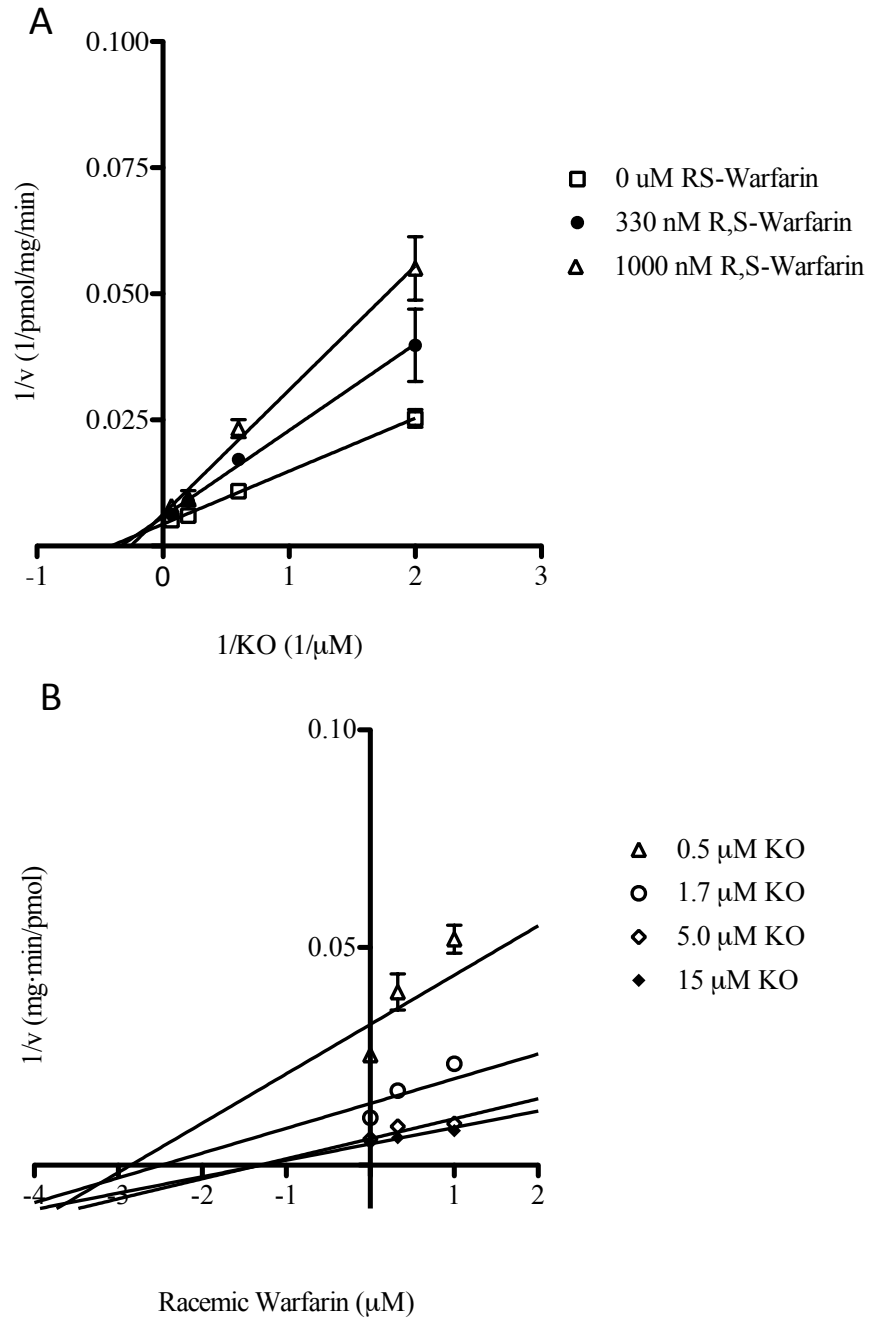

FIGURE 4.12: **(A)** Lineweaver-Burk plot illustrating VKOR activity at various concentrations of KO (0.5, 1.7, 5.0, and 15 μM) in the presence of 0, 0.33, 1.0, and 3.0 μM R-warfarin incubated with bovine liver microsomes (0.5 mg/mL). Data points represent the mean of triplicate measurements and error bars represent standard deviations. The data is also presented on a **(B)** Dixon plot, from which the value of K_i was deduced. The K_i for R-warfarin is listed in the Table 4.7.

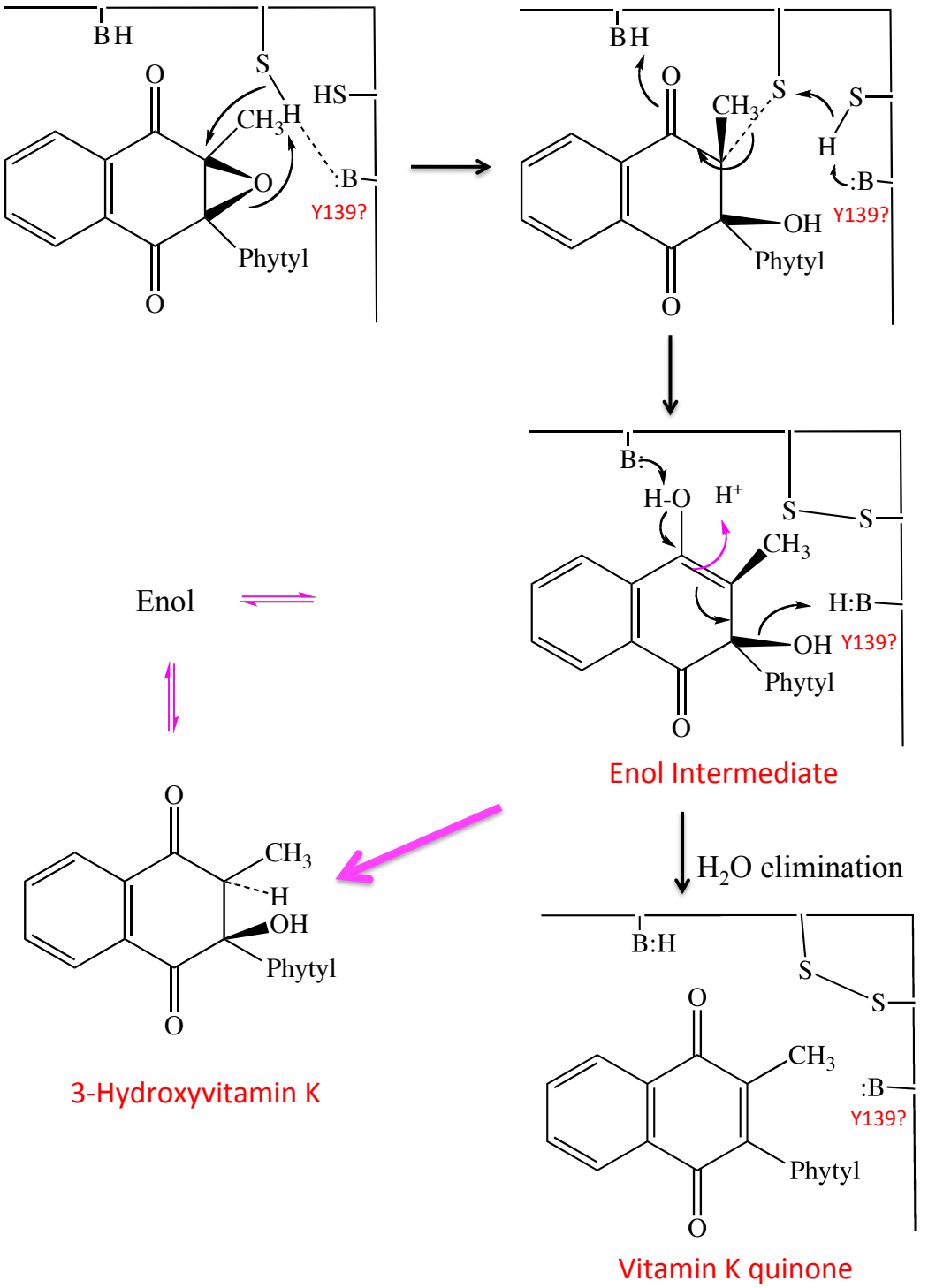

FIGURE 4.13**: Proposed mechanism of vitamin K_1 and 3-hydroxyvitamin K production from vitamin K epoxide.** Y139 is labeled as a putative residue that participates in the catalytic reaction. The magenta-colored arrows indicate the proposed pathway(s) for 3-hydroxy vitamin K formation in warfarin-resistant rats and the black arrows indicate the normal pathway for vitamin K formation by VKOR.

Chapter 5
General Conclusions and Future Directions

5.1 General Conclusions

The discovery of *VKORC1* has had a significant impact on the study of the interactions between vitamin K antagonists and VKOR, by confirming the results of past studies and enabling future ones. Taking advantage of this progress, we explored (in vitro) two important mechanistic questions about the warfarin-VKOR relationship: 1) the pharmacogenetic mechanism by which genetic polymorphisms of *VKORC1* genotype affect warfarin pharmacodynamics (Chapter 2) and 2) the molecular mechanism by which a vitamin K antagonist inhibits VKOR (Chapter 3 and Chapter 4).

An unfortunate complication of warfarin therapy is that a patient's dose response is influenced by genetic variability of the vitamin K cycle enzymes, in particular, VKOR. In pursuit of a mechanistic explanation for the dose variance observed for subjects carrying non-coding polymorphisms in *VKORC1*, Rieder et al. found that the levels of *VKORC1* mRNA expression were significantly correlated with haplotype groups that were used to stratify patients into low and high dose warfarin groups {[9,16,70]. Based on this result, we hypothesized that warfarin dose response is determined by human *VKORC1* transcriptional activity, which in turn is directed by *VKORC1* haplotype. By conducting an in vitro evaluation of the downstream effects of altered mRNA expression: VKOR activity and protein expression, we found that in genotyped human liver microsomes, both enzymatic parameters increase as a function of the high dose warfarin haplotype, and thus we concluded that our transcriptional hypothesis was correct.

A second goal of this project was to improve our understanding of vitamin K antagonist inhibition of VKOR at a molecular level. Our first aim was to resolve conflicting data that had been presented in the past regarding the irreversible nature of the warfarin VKOR interaction. We modified a dilution method that had been previously employed by Fasco et al. to demonstrate irreversible warfarin binding [2], by adding 20 mM DTT and/or 4% BSA to the dilution buffer. (Past studies suggested that these agents have properties that could be exploited to facilitate the removal of warfarin from microsomes). Not only did we observe that dilution of warfarin-inhibited bovine liver microsomes under the adjusted conditions could almost completely reverse the inhibitory effects of warfarin on VKOR, we also discovered that acenocoumarol and the structurally distinct, but pharmacologically identical, 1,3-indanedione oral anticoagulants also were not irreversiblely bound. Inhibitors representing both classes of vitamin K antagonists were kinetically categorized as non-competitive reversible inhibitors (with respect to vitamin K epoxide), providing additional confirmation of similar results previously obtained for warfarin. Taking into account all of the the above results, we concluded that vitamin K antagonists are not irreversible inhibitors of VKOR in the traditional sense (no in vitro covalent adducts formed), but bind to the target enzyme in an extremely tight, but reversible interaction.

Our second aim was to examine potential amino acid residues of VKOR involved in warfarin binding and inhibition, namely Y139 and L128, both of which are located near, but on opposite sides of the VKOR active site cysteines [134]. Since previous reports have suggested that Y139 could be part of the warfarin-binding site of VKOR [18,141], and its location relative to the active site cysteines make it a prime candidate for a role in catalysis, we compared the kinetic behavior of the recombinantly expressed human mutant, Y139F, with wild-type enzyme in

established in vitro assays designed to assess the fulfillment of either role. (The Y139F mutant differs from wild-type only by a loss of a hydroxyl group and, therefore, could be used to evaluate the behavior of Y139 as a base or proton donor in the mechanism of vitamin K epoxide reduction). We found that in addition to Y139F, several other mutants of Y139 resulted in a complete loss of warfarin inhibition. (L128 was similar to wild-type in activity, and partially resistant to warfarin by our analysis). Based on the observation that neither vitamin K_i production (to assess Y139 as a catalytic base and 3-hydroxyvitamin production (to assess Y139 as a proton donor) were affected as a result of the tyrosine→phenylalanine mutation, we concluded that tyrosine 139 is not a residue that directly promotes the mechanism of vitamin K epoxide reduction, but greatly impacts warfarin binding and inhibition.

5.2 Future Directions

Chapter 2

The results presented in Chapter 2 suggest that the mechanism underlying *VKORC1* haplotype effects on warfarin response is transcriptional. VKOR, however is just one of the known (genetic) contributors to variance in warfarin dose. Naturally, the next step would be to identify and investigate the factors that make up the unknown 40% of the 'warfarin pie' Factors to consider from a pharmacogenetic perspective include the endogenous reductant, the biomolecules that are involved in vitamin K metabolism, absorption, and transport in the body, and proteins that transport warfarin out of the liver [142]. A non-genetic factor that may be investigated in vitro is the biochemical basis of warfarin-drug or food interactions, which are prevalent in elderly patients as a result of multi-drug regimens.

Chapter 3

Establishing an in vitro system in which VKOR and its redox partner are present would be beneficial to confirming our in vitro findings regarding warfarin inhibition under conditions that more closely resemble in vivo conditions. The results described in Chapter 3 regarding the reversibility of inhibition under stringent removal conditions may explain the discrepancy between the in vitro irreversible nature of the warfarin-VKOR interaction under standard in vitro conditions (2 mM DTT), and reversible nature in vivo as a difference in reducing efficiency of the in vitro substitute and the in vivo reductant. A model that includes both VKOR and the endogenous reductor would help to determine in vivo mode of inhibition by warfarin and other vitamin K antagonists. To identify the reductant, two frequently used methods to discover protein-protein interactions to consider are yeast 2 hybrid screening of specific cDNA libraries or arrays (as an in vivo approach), although this is very challenging for membrane-bound sytstems, and affinity purification-MS to identify proteins by proteolytic fragments of complexes with VKOR (as an in vitro approach). Validation by both experiments would be highly desirable, due to inherent limitations (false positives) associated with both methods [143].

Chapter 4

To extend our studies of the warfarin binding site, site-directed mutagenesis; 1) at the 2 other amino acids of the TYA motif on the inhibitory effects of warfarin and 2) at L128 and Y139 to observe the inhibitory effects 1,3-indanedione inhibition would complement the studies in Chapter 2, since our SAR studies were unable to distinguish structural properties that render 1,3-indanediones more potent than 4-hydroxycoumarins. To develop a more detailed SAR for warfarin binding, comprehensive alanine scanning mutagenesis around the catalytic pocket

tentatively identified from homology modeling studies (Watzka et al., 2010) could be implemented to determine the effect of residue side chains on warfarin inhibition, with the advantage of assuming the mutation would only affect secondary structure locally and maintain the backbone of the protein. Photoaffinity labeling using radiolabeled 4'-azidowarfarin to adduct the over-expressed and purified VKOR enzyme and further evolution of current enzyme homology models might also provide useful information to guide strategic mutagenesis and interpretation of results from those experiments.

List of References

[1] E. Valente, E. Lingafelter, W. Porter, Structure of warfarin in solution - Journal of Medicinal Chemistry (ACS Publications), … Of Medicinal Chemistry. (1977).

[2] M.J. Fasco, L.M. Principe, R- and S-Warfarin inhibition of vitamin K and vitamin K 2,3-epoxide reductase activities in the rat, J. Biol. Chem. 257 (1982) 4894–4901.

[3] H. Dam, The antihaemorrhagic vitamin of the chick, Biochemical Journal. 29 (1935) 1273.

[4] R. Wallin, J.W. Suttie, Vitamin K-dependent carboxylation and vitamin K epoxidation. Evidence that the warfarin-sensitive microsomal NAD(P)H dehydrogenase reduces vitamin K1 in these reactions, Biochem. J. 194 (1981) 983–988.

[5] A.J. Quick, M. Stefanini, Effect of dicumarol on concentration of the labile factor, Proc. Soc. Exp. Biol. Med. 72 (1949) 232–234.

[6] J. Stenflo, P. Fernlund, W. Egan, P. Roepstorff, Vitamin K dependent modifications of glutamic acid residues in prothrombin, Proc. Natl. Acad. Sci. U.S.a. 71 (2006) 2730–2733.

[7] G.L. Nelsestuen, T.H. Zytkovicz, J.B. Howard, The mode of action of vitamin K. Identification of gamma-carboxyglutamic acid as a component of prothrombin, J. Biol. Chem. 249 (1974) 6347–6350.

[8] C.A. Owen, T.B. Magath, J.L. Bollman, Prothrombin conversion factors in blood coagulation, Am. J. Physiol. 166 (1951) 1–11.

[9] C. Hougie, E.M. Barrow, J.B. Graham, Stuart clotting defect. I. Segregation of an hereditary hemorrhagic state from the heterogeneous group heretofore called stable factor (SPCA, proconvertin, factor VII) deficiency, J. Clin. Invest. 36 (1957) 485–496.

[10] P.M. Aggeler, S.G. White M.B. Glendening, E.W. Page, T.B. Leake, G. Bates, Plasma thromboplastin component (PTC) deficiency; a new disease resembling hemophilia, Proc. Soc. Exp. Biol. Med. 79 (1952) 692–694.

[11] R. Biggs, A.S. Douglas, R.G. Macfarlane, J.V. Dacie, W.R. Pitney, Merskey, Christmas disease: a condition previously mistaken for haemophilia, Br Med J. 2 (1952) 1378–1382.

[12] R. Lasseur, C. Longin-Sauvageon, B. Videmann, M. Billeret, P. Berny, E. Benoit, Warfarin resistance in a French strain of rats, J. Biochem. Mol. Toxicol. 19 (2006) 379–385.

[13] G. Litwack, Vitamin K, Academic Press, 2008.

[14] R. Silverman, Chemical model studies for the mechanism of vitamin K epoxide reductase - Journal of the American Chemical Society (ACS Publications), J. Am. Chem. Soc. (2001) 1–3.

[15] N.M. McKeown, P.F. Jacques, C.M. Gundberg, J.W. Peterson, K.L. Tucker, D.P. Kiel, et al., Dietary and nondietary determinants of vitamin K biochemical measures in men and women, J. Nutr. 132 (2002) 1329–1334.

[16] H.H.W. Thijssen, L.M.T. Vervoort, L.J. Schurgers, M.J. Shearer, Menadione is a metabolite of oral vitamin K, Br J Nutr. 95 (2007) 260–266.

[17] S.J. Elder, D.B. Haytowitz, J. Howe, J.W. Peterson, S.L. Booth, Vitamin k contents of meat, dairy, and fast food in the u.s. Diet, J. Agric. Food Chem. 54 (2006) 463–467.

[18] G. Asher, O. Dym, P. Tsvetkov, J. Adler, Y. Shaul, The Crystal Structure of NAD(P)H Quinone Oxidoreductase 1 in Complex with Its Potent Inhibitor Dicoumarol †, Biochemistry. 45 (2006) 6372–6378.

[19] H.H.H. Thijssen, M.J.M. Drittij-Reijnders, Vitamin K status in human tissues: tissue-specific accumulation of phylloquinone and menaquinone-4, Br J Nutr. 75 (1996) 121–127.

[20] H.J. Pelz, The Genetic Basis of Resistance to Anticoagulants in Rodents, Genetics. 170 (2005) 1839–1847.

[21] K.L. Berkner, THE VITAMIN K–DEPENDENT CARBOXYLASE, Http://Dx.Doi.org.Offcampus.Lib.Washington.Edu/10.1146/Annurev.Nutr.25.050304.092713. (2005).

[22] C. Vermeer, Gamma-carboxyglutamate-containing proteins and the vitamin K-dependent carboxylase, Biochem. J. 266 (1990) 625–636.

[23] B. Furie, B.C. Furie, Molecular and cellular biology of blood coagulation, N. Engl. J. Med. 326 (1992) 800–806.

[24] R.G. Bell, J.T. Matschiner, Warfarin and the inhibition of vitamin K activity by an oxide metabolite, Nature. 237 (1972) 32–33.

[25] M.A. Stahmann, C.F. Huebner, K.P. Link, Studies on the hemorrhagic sweet clover disease, J. Biol. Chem. 138 (1941) 513–527.

[26] W.R. Porter, Warfarin: history, tautomerism and activity, J Comput Aided Mol Des. 24 (2010) 553–573.

[27] K.P. Link, The discovery of dicumarol and its sequels, Circulation. 19 (1959) 97–107.

[28] J.T. Matschiner, R.G. Bell, J.M. Amelotti, T.E. Knauer, Isolation and characterization of a new metabolite of phylloquinone in the rat, Biochimica Et Biophysica Acta (BBA) - General Subjects. 201 (1970) 309–315.

[29] R.G. Bell, J.T. Matschiner, Vitamin K activity of phylloquinone oxide, Archives of Biochemistry and Biophysics. 141 (1970) 473–476.

[30] J.T. Matschiner, R.G. Bell, Metabolism and vitamin K activity of cis phylloquinone in rats, J. Nutr. 102 (1972) 625–629.

[31] A. Zimmermann, J.T. Matschiner, Biochemical basis of hereditary resistance to warfarin in the rat, Biochem. Pharmacol. 23 (1974) 1033–1040.

[32] J.J. Lee, M.J. Fasco, Metabolism of vitamin K and vitamin K 2,3-epoxide via interaction with a common disulfide, Biochemistry. 23 (1984) 2246–2252.

[33] H. Thijssen, Y. Janssen, L. Vervoort, Microsomal lipoamide reductase provides vitamin K epoxide reductase with reducing equivalents, Biochemical Journal. 297 (1994) 277.

[34] B. Soute, M. Groenen-van Dooren, A. Holmgren, J. Lundström, C. Vermeer, Stimulation of the dithiol-dependent reductases in the vitamin K cycle by the thioredoxin system. Strong synergistic effects with protein disulphide-isomerase, Biochemical Journal. 281 (1992) 255.

[35] S.L. Gardill, J.W. Suttie, Vitamin K epoxide and quinone reductase activities. Evidence for reduction by a common enzyme, Biochem. Pharmacol. 40 (1990) 1055–1061.

[36] R. Silverman, Reduced thioredoxin: a possible physiological cofactor for vitamin K epoxide reductase. Further support for an active site disulfide, Biochemical and Biophysical Research …. (1988).

[37] P. Preusch, Is thioredoxin the physiological vitamin K epoxide reducing agent? FEBS Letters. (2001) 1–3.

[38] R. Wallin, D.C. Sane, S.M. Hutson, ScienceDirect.com - Thrombosis Research - Vitamin K 2,3-epoxide reductase and the vitamin K-dependent γ-carboxylation system, 108 (2002) 221–226.

[39] N. Wajih, S.M. Hutson, R. Wallin, Disulfide-dependent protein folding is linked to operation of the vitamin K cycle in the endoplasmic reticulum. A protein disulfide isomerase-VKORC1 redox enzyme complex appears to be responsible for vitamin K1

2,3-epoxide reduction, J. Biol. Chem. 282 (2007) 2626–2635.

[40] J.J. Lee, L.M. Principe, M.J. Fasco, Identification of a warfarin-sensitive protein component in a 200S rat liver microsomal fraction catalyzing vitamin K and vitamin K 2,3-epoxide reduction, Biochemistry. 24 (1985) 7063–7070.

[41] D. Cain, S.M. Hutson, R. Wallin, Assembly of the warfarin-sensitive vitamin K 2,3-epoxide reductase enzyme complex in the endoplasmic reticulum membrane, J. Biol. Chem. 272 (1997) 29068–29075.

[42] P.H. Chu, T.Y. Huang, J. Williams, D.W. Stafford, Purified vitamin K epoxide reductase alone is sufficient for conversion of vitamin K epoxide to vitamin K and vitamin K to vitamin KH2, Proceedings of the National Academy of Sciences. 103 (2006) 19308–19313.

[43] J. Patterson, P. Preusch, Patterson: Purification and Stereospecificity of... - Google Scholar, Fed. Proc, 1981.

[44] P.C. Preusch, J.W. Suttie, Stereospecificity of vitamin K-epoxide reductase, J. Biol. Chem. 258 (1983) 714–716.

[45] S. Rost, A. Fregin, V. Ivaskevicius, E. Conzelmann, K. Hörtnagel, H.-J. Pelz, et al., Mutations in VKORC1 cause warfarin resistance and multiple coagulation factor deficiency type 2, Nature. 427 (2004) 537–541.

[46] T. Li, C.-Y. Chang, D.-Y. Jin, P.-J. Lin, A. Khvorova, D.W. Stafford, Identification of the gene for vitamin K epoxide reductase, Nature. 427 (2004) 541–544.

[47] A. Fregin, S. Rost, W. Wolz, A. Krebsova, C.R. Muller, J. Oldenburg, Homozygosity mapping of a second gene locus for hereditary combined deficiency of vitamin K-dependent clotting factors to the centromeric region of chromosome 16, Blood. 100 (2002) 3229–3232.

[48] J.K. Tie, Membrane Topology Mapping of Vitamin K Epoxide Reductase by in Vitro Translation/Cotranslocation, Journal of Biological Chemistry. 280 (2005) 16410–16416.

[49] P. Ren, P. Stark, R. Johnson, Mechanism of action of anticoagulants: correlation between the inhibition of prothrombin synthesis and the regeneration of vitamin K1 from vitamin K1 epoxide, Journal of Pharmacology and …. (1977).

[50] J. Ansell, J. Hirsh, L. Poller, H. Bussey, A. Jacobson, E. Hylek, The pharmacology and management of the vitamin K antagonists: the Seventh ACCP Conference on Antithrombotic and Thrombolytic Therapy, Chest. 126 (2004) 204S–233S.

[51] L.G. Jacobs, Warfarin pharmacology, clinical management, and evaluation of hemorrhagic risk for the elderly, Clin. Geriatr. Med. 22 (2006) 17–32– vii–viii.

[52] R.A. O'Reilly, Studies on the optical enantiomorphs of warfarin in man, Clinical Pharmacology & Therapeutics. 16 (1974) 348–354.

[53] E. Jähnchen, T. Meinertz, H.J. Gilfrich, U. Groth, A. Martini, The enantiomers of phenprocoumon: pharmacodynamic and pharmacokinetic studies, Clinical Pharmacology & Therapeutics. 20 (1976) 342–349.

[54] M.A. de Boer-van den Berg, H.H. Thijssen, C. Vermeer, The in vivo effects of acenocoumarol, phenprocoumon and warfarin on vitamin K epoxide reductase and vitamin K-dependent carboxylase in various tissues of the rat, Biochim. Biophys. Acta. 884 (1986) 150–157.

[55] S. Toon, K.J. Hopkins, F.M. Garstang, B. Diquet, T.S. Gill, M. Rowland, The warfarin-cimetidine interaction: stereochemical considerations, Br J Clin Pharmacol. 21 (1986) 245–246.

[56] A.E. Rettie, K.R. Korzekwa, K.L. Kunze, R.F. Lawrence, A.C. Eddy, T. Aoyama, et al., Hydroxylation of warfarin by human cDNA-expressed cytochrome P-450: a role for P-4502C9 in the etiology of (S)-warfarin-drug interactions, Chem. Res. Toxicol. 5 (1992) 54–59.

[57] A.E. Rettie, G. Tai, The pharmocogenomics of warfarin: closing in on personalized medicine, Mol. Interv. 6 (2006) 223–227.

[58] J.J. Hermans, H.H. Thijssen, Stereoselective acetonyl side chain reduction of warfarin and analogs. Partial characterization of two cytosolic carbonyl reductases, Drug Metab. Dispos. 20 (1992) 268–274.

[59] S.M. Bratton, C.M. Mosher, F. Khallouki, M. Finel, M.H. Court, J.H. Moran, et al., Analysis of R- and S-Hydroxywarfarin Glucuronidation Catalyzed by Human Liver Microsomes and Recombinant UDP-Glucuronosyltransferases, Journal of Pharmacology and Experimental Therapeutics. 340 (2011) 46–55.

[60] P.M.M. Kuijer, B.A. Hutten, M.H. Prins, H.R. Büller, Prediction of the Risk of Bleeding During Anticoagulant Treatment for Venous Thromboembolism, Arch. Intern. Med. 159 (1999) 457–460.

[61] G. Palareti, N. Leali, S. Coccheri, M. Poggi, [Hemorrhagic complications of oral anticoagul... [G Ital Cardiol. 1997] - PubMed - NCBI, Giornale Italiano Di …. (1997).

[62] F. Kamali, T.I. Khan, B.P. King, R. Frearson, P. Kesteven, P. Wood, et al., Contribution of age, body size, and CYP2C9 genotype to anticoagulant response to

warfarin, Clinical Pharmacology & Therapeutics. 75 (2004) 204–212.

[63] T.J. Wilkinson, R. Sainsbury, Evaluation of a warfarin initiation protocol for older people, Intern Med J. 33 (2003) 465–467.

[64] E.A. Sconce, The impact of CYP2C9 and VKORC1 genetic polymorphism and patient characteristics upon warfarin dose requirements: proposal for a new dosing regimen, Blood. 106 (2005) 2329–2333.

[65] D. Voora, C. Eby, M.W. Linder, P.E. Milligan, B.L. Bukaveckas, H.L. McLeod, et al., Prospective dosing of warfarin based on cytochrome P-450 2C9 genotype, Thromb Haemost. 93 (2005) 700–705.

[66] F. Takeuchi, R. McGinnis, S. Bourgeois, C. Barnes, N. Eriksson, N. Soranzo, et al., A Genome-Wide Association Study Confirms VKORC1, CYP2C9, and CYP4F2 as Principal Genetic Determinants of Warfarin Dose, PLoS Genet. 5 (2009).

[67] M.G. McDonald, M.J. Rieder, M. Nakano, C.K. Hsia, A.E. Rettie, CYP4F2 Is a Vitamin K1 Oxidase: An Explanation for Altered Warfarin Dose in Carriers of the V433M Variant, Molecular Pharmacology. 75 (2009) 1337–1346.

[68] U.I. Schwarz, C.M. Stein, Genetic determinants of dose and clinical outcomes in patients receiving oral anticoagulants, Clinical Pharmacology & Therapeutics. 80 (2006) 7–12.

[69] H. Sagreiya, C. Berube, A. Wen, R. Ramakrishnan, A. Mir, A. Hamilton, et al., Extending and evaluating a warfarin dosing algorithm that includes CYP4F2 and pooled rare variants of CYP2C9, Pharmacogenetics and Genomics. 20 (2010) 1.

[70] M.J. Rieder, A.P. Reiner, B.F. Gage, D.A. Nickerson, C.S. Eby, H.L. McLeod, et al., Effect of VKORC1 haplotypes on transcriptional regulation and warfarin dose, N. Engl. J. Med. 352 (2005) 2285–2293.

[71] E.E. Schadt, C. Molony, E. Chudin, K. Hao, X. Yang, P.Y. Lum, et al., Mapping the genetic architecture of gene expression in human liver, PLoS Biol. 6 (2008).

[72] D. Wang, H. Chen, K.M. Momary, L.H. Cavallari, J.A. Johnson, W. Sadee, Regulatory polymorphism in vitamin K epoxide reductase complex subunit 1 (VKORC1) affects gene expression and warfarin dose requirement, Blood. 112 (2008) 1013–1021.

[73] A. Rettie, R. Haining, M. Bajpai, UW NetID Weblogin, Epilepsy Research. (1999).

[74] M.D. Caldwell, T. Awad, J.A. Johnson, B.F. Gage, M. Falkowski, P. Gardina, et al., CYP4F2 genetic variant alters required warfarin dose, Blood. 111 (2008) 4106–4112.

[75] P.C. Preusch, J. Suttie, A chemical model for the mechanism of vitamin K epoxide reductase, The Journal of Organic Chemistry. 48 (1983) 3301–3305.

[76] M.J. Fasco, P.C. Preusch, E. Hildebrandt, J.W. Suttie, Formation of hydroxyvitamin K by vitamin K epoxide reductase of warfarin-resistant rats, J. Biol. Chem. 258 (1983) 4372–4380.

[77] L. Goodstadt, Vitamin K epoxide reductase: homology, active site and catalytic mechanism, Trends in Biochemical Sciences. 29 (2004) 289–292.

[78] N. Wajih, Engineering of a Recombinant Vitamin K-dependent -Carboxylation System with Enhanced -Carboxyglutamic Acid Forming Capacity: EVIDENCE FOR A FUNCTIONAL CXXC REDOX CENTER IN THE SYSTEM, Journal of Biological Chemistry. 280 (2005) 10540–10547.

[79] S. Rost, A. Fregin, M. Hunerberg, C.G. Bevans, C.R. Muller, J. Oldenburg, Site-directed mutagenesis of coumarin-type anticoagulant-sensitive VKORC1: evidence that highly conserved amino acids define structural requirements for enzymatic activity and inhibition by warfarin, Thromb Haemost. 94 (2005) 780–786.

[80] J.J. Lee, M.J. Fasco, Metabolism of vitamin K and vitamin K 2,3-epoxide via interaction with a common disulfide, Biochemistry. 23 (1984) 2246–2252.

[81] D.-Y. Jin, J.-K. Tie, D.W. Stafford, The conversion of vitamin K epoxide to vitamin K quinone and vitamin K quinone to vitamin K hydroquinone uses the same active site cysteines, Biochemistry. 46 (2007) 7279–7283.

[82] A.K. Wittkowsky, Warfarin and other coumarin derivatives: pharmacokinetics, pharmacodynamics, and drug interactions, Semin Vasc Med. 3 (2003) 221–230.

[83] M. Gebauer, Synthesis and structure–activity relationships of novel warfarin derivatives, Bioorganic & Medicinal Chemistry. (2007).

[84] J. Gueguen, CR Soc, Biol, 1947.

[85] C. Boyle, Case of Apparent Resistance of Rattus norvegicus Berkenhout to Anticoagulant Poisons, (1960).

[86] R.B. Silverman, A model for a molecular mechanism of anticoagulant activity of 3-substituted 4-hydroxycoumarins, J. Am. Chem. Soc. 102 (1980) 5421–5423.

[87] R.B. Silverman, Model studies for a molecular mechanism of action of oral anticoagulants, J. Am. Chem. Soc. 103 (2001) 3910–3915.

[88] M.J. Fasco, L.M. Principe, R- and S-Warfarin inhibition of vitamin K and vitamin K

2,3-epoxide reductase activities in the rat, J. Biol. Chem. 257 (1982) 4894–4901.

[89] D.J. Lorusso, J.W. Suttie, Warfarin binding to microsomes isolated from normal and warfarin-resistant rat liver, Molecular Pharmacology. 8 (1972) 197–203.

[90] M.J. Fasco, L.M. Principe, W.A. Walsh, P.A. Friedman, Warfarin inhibition of vitamin K 2, 3-epoxide reductase in rat liver microsomes, Biochemistry. 22 (1983) 5655–5660.

[91] A. Garner, C. Pallister, M. Watson, Haematology, Second Edition, Scion Pub Ltd, 2010.

[92] A.E. Rettie, G. Tai, The pharmocogenomics of warfarin: closing in on personalized medicine, Mol. Interv. 6 (2006) 223–227.

[93] E.F. Hildebrandt, J.W. Suttie, Mechanism of coumarin action: sensitivity of vitamin K metabolizing enzymes of normal and warfarin-resistant rat liver, Biochemistry. 21 (1982) 2406–2411.

[94] J.W.J. Suttie, P.C.P. Preusch, Studies of the vitamin K-dependent carboxylase and vitamin K epoxide reductase in rat liver, Haemostasis. 16 (1986) 193–215.

[95] I. Mukharji, R.B. Silverman, Purification of a vitamin K epoxide reductase that catalyzes conversion of vitamin K 2,3-epoxide to 3-hydroxy-2-methyl-3-phytyl-2,3-dihydronaphthoquinone, Proc. Natl. Acad. Sci. U.S.a. 82 (1985) 2713–2717.

[96] R. Wallin, L.F. Martin, Vitamin K-dependent carboxylation and vitamin K metabolism in liver. Effects of warfarin, J. Clin. Invest. 76 (2007) 1879–1884.

[97] Y. Haroon, D.S. Bacon, J.A. Sadowski, Liquid-chromatographic determination of vitamin K1 in plasma, with fluorometric detection, Clin. Chem. 32 (1986) 1925–1929.

[98] P. Dowd, S. Ham, A. Marchand, Mechanism of epoxidation of vitamin K with basic hydrogen peroxide. - The Journal of Organic Chemistry (ACS Publications), The Journal of Organic …. (1992).

[99] K.W. Davidson, J.A. Sadowski, Determination of vitamin K compounds in plasma or serum by high-performance liquid chromatography using postcolumn chemical reduction and fluorimetric detection, Meth. Enzymol. 282 (1997) 408–421.

[100] L.Y. Wang, C.J. Bates, L. Yan, D.J. Harrington, M.J. Shearer, A. Prentice, Determination of phylloquinone (vitamin K1) in plasma and serum by HPLC with fluorescence detection, Clin. Chim. Acta. 347 (2004) 199–207.

[101] K.J. Livak, T.D. Schmittgen, Analysis of Relative Gene Expression Data Using Real-Time Quantitative PCR and the $2^{-\Delta\Delta CT}$ Method, Methods. 25 (2001) 402–408.

[102] S.M. Wu, V.P. Mutucumarana, D.W. Stafford, Purification of gamma-glutamyl carboxylase from bovine liver, Meth. Enzymol. 282 (1997) 346–357.

[103] C.R. Wilson, J.-M. Sauer, G.P. Carlson, R. Wallin, M.P. Ward, S.B. Hooser, Species comparison of vitamin K1 2,3-epoxide reductase activity in vitro: kinetics and warfarin inhibition, Toxicology. 189 (2003) 191–198.

[104] R.E. Pearce, C.J. McIntyre, A. Madan, U. Sanzgiri, A.J. Draper, P.L. Bullock, et al., Effects of freezing, thawing, and storing human liver microsomes on cytochrome P450 activity, Archives of Biochemistry and Biophysics. 331 (1996) 145–169.

[105] P.C. Preusch, D.M. Smalley, Vitamin K, 2,3-Epoxide And Quinone Reduction: Mechanism And Inhibition, (1990).

[106] R.G. Bell, J.A. Sadowski, J.T. Matschiner, Mechanism of action of warfarin. Warfarin and metabolism of vitamin K 1 , Biochemistry. 11 (1972) 1959–1961.

[107] M.J. Fasco, L.M. Principe, W.A. Walsh, P.A. Friedman, Warfarin inhibition of vitamin K 2,3-epoxide reductase in rat liver microsomes, Biochemistry. 22 (1983) 5655–5660.

[108] R.B. Silverman, D.L. Nandi, Effect of N-ethylmaleimide on beef and rat liver vitamin K1 epoxide reductase, J. Enzym. Inhib. 3 (1990) 289–294.

[109] R. Wallin, S.D. Patrick, L.F. Martin, Rat and human liver vitamin K epoxide reductase: inhibition by thiol blockers and vitamin K1, Int. J. Biochem. 19 (1987) 1063–1068.

[110] A.E. Rettie, A.C. Eddy, L.D. Heimark, M. Gibaldi, W.F. Trager, Characteristics of warfarin hydroxylation catalyzed by human liver microsomes, Drug Metab. Dispos. 17 (1989) 265–270.

[111] Y. Lin, A. Dowling, S. Quigley, F. Farin, Co-Regulation of CYP3A4 and CYP3A5 and Contribution to Hepatic and Intestinal Midazolam Metabolism, Molecular …. (2002).

[112] A. Choppin, I. Irwin, L. Lach, M.G. McDonald, A.E. Rettie, L. Shao, et al., Effect of tecarfarin, a novel vitamin K epoxide reductase inhibitor, on coagulation in beagle dogs, Br. J. Pharmacol. 158 (2009) 1536–1547.

[113] R. Meech, P.I. Mackenzie, Structure and function of uridine diphosphate glucuronosyltransferases, Clin Exp Pharmacol Physiol. 24 (1997) 907–915.

[114] J.H. Lin, B.K. Wong, Complexities of glucuronidation affecting in vitro in vivo extrapolation, Curr. Drug Metab. 3 (2002) 623–646.

[115] W. Li, S. Schulman, R.J. Dutton, D. Boyd, J. Beckwith, T.A. Rapoport, Structure of a

bacterial homologue of vitamin K epoxide reductase, Nature. 463 (2010) 507–512.

[116] E. Hildebrandt, P. Preusch, J. Patterson, Solubilization and characterization of vitamin K epoxide reductase from normal and warfarin-resistant rat liver microsomes, Archives of Biochemistry …. (1984).

[117] R. Wallin, T.M. Guenthner, Purification of warfarin-sensitive vitamin K epoxide reductase, Meth. Enzymol. 282 (1997) 395–408.

[118] R. Wallin, A molecular mechanism for genetic warfarin resistance in the rat, The FASEB Journal. (2001).

[119] S.L. Gardill, J.W. Suttie, Vitamin K epoxide and quinone reductase activities. Evidence for reduction by a common enzyme, Biochem. Pharmacol. 40 (1990) 1055–1061.

[120] M.J. See, S.E. Staggs, J.P. Dubey, E.N. Villegas, Evaluation of four RNA extraction methods for gene expression analyses of Cryptosporidium parvum and Toxoplasma gondii oocysts, J. Microbiol. Methods. 89 (2012) 185–192.

[121] W. Levine, Levine: Heavy-metal antagonists - Google Scholar, The Pharmacological Basis of Therapeutics, 1975.

[122] H.H. Thijssen, L.G. Baars, H.T. Vervoort-Peters, Vitamin K 2,3-epoxide reductase: the basis for stereoselectivity of 4-hydroxycoumarin anticoagulant activity, Br. J. Pharmacol. 95 (1988) 675–682.

[123] R. Lasseur, A. Grandemange, C. Longin-Sauvageon, P. Berny, E. Benoit, Comparison of the inhibition effect of different anticoagulants on vitamin K epoxide reductase activity from warfarin-susceptible and resistant rat, Pesticide Biochemistry and Physiology. 88 (2007) 203–208.

[124] P.C. Preusch, J.W. Suttie, Lapachol inhibition of vitamin K epoxide reductase and vitamin K quinone reductase, Archives of Biochemistry and Biophysics. 234 (1984) 405–412.

[125] D. Woolley, Some biological effects produced by α-tocopherol quinone, J. Biol. Chem. 159 (1945) 59–66.

[126] P. Dowd, On the mechanism of the anticlotting action of vitamin E quinone, … Of the National Academy of Sciences. (1995).

[127] H.H. Thijssen, L.G. Baars, Hepatic uptake and storage of warfarin. The relation with the target enzyme vitamin K 2,3-epoxide reductase, J. Pharmacol. Exp. Ther. 243 (1987) 1082–1088.

[128] H.H.W. Thijssen, C.A.T. Janssen, M.J. Drittij-Reijnders, The effect of S-warfarin administration on vitamin K 2,3-epoxide reductase activity in liver, kidney and testis of the rat, Biochem. Pharmacol. 35 (1986) 3277–3282.

[129] R.S. Overman, M.A. Stahmann, C.F. Huebner, W.R. Sullivan, L. Spero, D.G. Doherty, et al., STUDIES ON THE HEMORRHAGIC SWEET CLOVER DISEASE, J. Biol. Chem. 153 (1944) 5.

[130] P.C. Preusch, S.E. Hazelett, K.K. Lemasters, Sulfaquinoxaline inhibition of vitamin K epoxide and quinone reductase, Archives of Biochemistry and Biophysics. 269 (1989) 18–24.

[131] W. Sawyer, D. Lowenthal, Porter: Warfarin - Google Scholar, Applied Pharmacokinetics Principles of …, 1992.

[132] H.D. Christensen, Pharmacology, Springer, 1995.

[133] T.M. Misenheimer, J.W. Suttie, Warfarin resistance in a Chicago strain of rats, Biochem. Pharmacol. 40 (1990) 2079–2084.

[134] M. Watzka, C. Geisen, C.G. BEVANS, K. SITTINGER, G. SPOHN, S. ROST, et al., Thirteen novel VKORC1 mutations associated with oral anticoagulant resistance: insights into improved patient diagnosis and treatment, Journal of Thrombosis and Haemostasis. 9 (2011) 109–118.

[135] H.O. Hallak, P.J. Wedlund, M.W. Modi, I.H. Patel, G.L. Lewis, B. Woodruff, et al., High clearance of (S)-warfarin in a warfarin-resistant subject, Br J Clin Pharmacol. 35 (1993) 327–330.

[136] M. Ishizuka, F. Okajima, T. Tanikawa, H. Min, K.D. Tanaka, K.Q. Sakamoto, et al., Elevated warfarin metabolism in warfarin-resistant roof rats (Rattus rattus) in Tokyo, Drug Metab. Dispos. 35 (2007) 62–66.

[137] R. Wallin, S.M. Hutson, D. Cain, A. Sweatt, D.C. Sane, A molecular mechanism for genetic warfarin resistance in the rat, The FASEB Journal. 15 (2001) 2542–2544.

[138] C. Morisseau, Epoxide hydrolases: mechanisms, inhibitor designs, and biological roles, Annu. Rev. Pharmacol. Toxicol. (2005).

[139] Y. Suhara, M. Kamao, N. Tsugawa, Method for the Determination of Vitamin K Homologues in Human Plasma Using High-Performance Liquid Chromatography-Tandem Mass Spectrometry - Analytical Chemistry (ACS Publications), Anal. Chem. (2005).

[140] A. MacNicoll, A comparison of warfarin resistance and liver microsomal vitamin K epoxide reductase activity in rats, Biochimica Et Biophysica Acta (BBA) - General Subjects. (1985).

[141] S. Chen, J. Hwang, P. Deng, Inhibition of NAD (P) H: quinone acceptor oxidoreductase by flavones: A structure-activity study, Archives of Biochemistry and Biophysics. 302 (1993) 72–77.

[142] M. Wadelius, L.Y. Chen, N. Eriksson, S. Bumpstead, J. Ghori, C. Wadelius, et al., Association of warfarin dose with genes involved in its action and metabolism, Hum Genet. 121 (2006) 23–34.

[143] A. Brückner, C. Polge, N. Lentze, D. Auerbach, U. Schlattner, Yeast Two-Hybrid, a Powerful Tool for Systems Biology, Ijms. 10 (2009) 2763–2788.

CURRICULUM VITAE

Clara K. Hsia

EDUCATION

2002-2012 University of Washington, Seattle, WA.
Ph.D., Medicinal Chemistry
Advisor: Professor Allan E. Rettie

1998-2002 Harvey Mudd College, Claremont, CA.
B.S., Chemistry

RESEARCH EXPERIENCE

2002-2010 Research Assistant, University of Washington, Seattle, WA.
HPLC-Fluorescence, LC-MS/MS, recombinant protein expression, real-time PCR, site-directed mutagenesis, western blot analysis, organic synthesis

2007 Eli Lilly Student Intern, Drug Disposition, Eli Lilly and Company, Indianapolis, IN. *Myeloperoxidase-mediated reactive metabolism*

2001-2002 Research assistant, Department of Chemistry, Harvey Mudd College, Claremont, CA. *Aqueous Organometallic Chemistry*

2000 Student Research Intern, Department of Chemistry, Lewis and Clark College, Portland, OR. *Aqueous Organometallic Chemistry*

1999 Student Research Intern, School of Nursing, Oregon Health Sciences University, Portland, OR. *Oxygen saturation monitoring in neonates*

PUBLICATIONS

L.Y. Kuo, T.J.R. Weakley, K. Awana, C. Hsia, Aqueous "Green" Organometallic Chemistry: Structure of the Molybdocene Monohydride Used for Carbonyl Reduction in Water, Organometallics, 20 (2001) 4969–4972.